

Morphological model of the river Rhine

Partially calibrated (v0.5) model of the Waal branch



Morphological model of the river Rhine
Partially calibrated (v0.5) model of the Waal branch

Author(s)

Anna Kusters

Anke Becker

Willem Ottevanger

Victor Chavarrias

Ana Luisa Nunes de Alencar Osorio

Morphological model of the river Rhine

Partially calibrated (v0.5) model of the Waal branch

Client	-
Contact	Arjan Sieben, Michiel Reneerkens, Dénes Beyer
Reference	-
Keywords	Morphological model, Rhine, DVR

Document control

Version	1.0
Date	21-11-2024
Project nr.	11210364-003
Document ID	11210364-003-ZWS-0007
Pages	116
Classification	
Status	final

Author(s)

	Anna Kusters Anke Becker Willem Ottevanger Victor Chavarrias Ana Luisa Nunes de Alencar Osorio	

Summary

The riverbed (main channel and flood plains) of the Rhine branches is dynamic and changes over time under the influence of morphological processes and human intervention. Currently, morphodynamics in the Rhine branches can be predicted and assessed with the so-called DVR model. For three reasons, this model is however outdated:

- The calibration is based on periods before realization of several important interventions (Room for the River, Water Framework Directive).
- RWS is moving to a new model generation in new software (the 6th generation models in the D-HYDRO Suite software package).
- There are new data and insights regarding morphological developments.

Therefore, a new model and set of tools is being developed to replace the old one.

The model developments take place over the course of several years and started in 2023. The work carried out in 2023 is reported in Becker et al. (2023) and led to model version v0 (uncalibrated). The current report is a progress report that describes only changes or additions that were made in 2024 and resulted in model version v0.5 (partially 1D calibrated). Choices made in 2023 and 2024 may be changed in the following years to further improve model performance. Once the model of the entire Rhine branches is ready, a final report will be made that contains a full description of all data, methods and results used for the final version v1 of the model.

The first morphological Waal model version (v0) developed in 2023 was set-up based on existing 6th generation hydrodynamic models. In 2024, several improvements have been made to the initial model set-up, resulting in model version v0.5. With these changes, the numerical stability has been improved significantly, and simulation times have decreased through optimization of the morphological factor and the number of sediment fractions. Furthermore, significant attention has been paid to the implementation of fairway maintenance (dredging and dumping) and sediment extraction in the model. For this, information on the current practice and data on dredging volumes has been collected. Through several discussions with Rijkswaterstaat, it was decided how the practice of fairway maintenance and sediment extraction could best be schematized in the model. The modelled dredging, dumping and extraction volumes resulting from this implementation were subsequently analysed and compared to reported volumes. Furthermore, the computation of dune heights in the model was validated. By taking into account dune heights, the dredging and dumping routine can be improved further.

This report also presents the results of several analyses of the model results, regarding the accuracy of the downstream boundary condition, the roughness of the fixed layers and the sensitivity of model results to the parameters of the sediment transport formula. Based on the latter, a set of sediment transport parameters has been selected as starting point for the 1D calibration.

With the selected sediment transport parameters, modelled sediment transport is significantly lower than the estimate based on bed level changes by Sloff (2019), and than the results of model version v0 in 2023 (which used a different transport formula, which was abandoned in discussion with RWS). In the final model, sediment transport on the Waal should match the incoming sediment transport from Boven-Rijn. That model will be set up in 2025.

First model results need to show if the parameter settings in the transport formula for the Waal need to be changed to achieve a better match.

The modelled transport gradients are somewhat too high, resulting in faster bed level changes than observed in reality. It is recommended to analyse if this can be improved by a different initial sediment composition, by a more appropriate schematization of sand mining, and possibly by changes in the downstream boundary condition in 2025. Once the model is sufficiently calibrated for the long-term and on the larger scale, we can proceed to a detailed 2D calibration.

In calibration runs for the IJssel, it turned out that the model is very close to ill-posed near the upstream boundary, which means that it easily becomes unstable. Due to this, a large sedimentation wave enters the model. Similar behaviour has been observed in some of the Waal model runs of 2023 (v0), without making the connection to ill-posedness yet. It is recommended to check whether also the Waal model is close to ill-posedness. Also, the possibility to add extra diffusion to the model in case of ill-posedness should be added in the software.

Contents

	Summary	4
	Contents	6
1	Introduction	9
1.1	Background and motivation	9
1.2	Objective	9
1.3	This report	9
1.4	Software	11
2	Approach for model set-up	12
2.1	General approach of the long-term model development	12
2.2	Overview of the activities carried out in 2024	13
3	Data	16
3.1	Fairway maintenance and sediment extraction	16
3.1.1	Fairway maintenance	16
3.1.1.1	Dredging rules	16
3.1.1.2	Dumping rules	17
3.1.1.3	Data	17
3.1.2	Sediment extraction	17
4	Hydrodynamic model schematization and validation	19
4.1	Improvement of model stability	19
4.2	Choice of downstream boundary condition	19
4.3	Yearly discharge hydrographs for the calibration and validation periods	24
4.3.1.1	Method	25
4.3.1.2	Discharge regimes	26
4.3.1.3	Hydrographs for Lobith	26
5	Morphological model schematization	30
5.1	Optimization of simulation times by means of the morphological factor	30
5.1.1	Using a morphological scale factor	30
5.1.2	Set-up of test simulations	31
5.1.2.1	Trench simulations with constant discharge	31
5.1.2.2	Hydrograph simulations	32
5.1.3	Influence of the morphological factor on trench propagation	33
5.1.4	Influence of the morphological factor on bed level and sediment composition development in hydrograph simulations	34
5.1.5	Simulation times	34
5.1.6	Conclusion	35
5.2	Number of sediment fractions in the implementation of graded sediment	35
5.3	Sediment transport formula	39

5.4	Fixed layers, constructions and morphologically active area	39
5.4.1	Fixed layer roughness	39
5.5	Upstream boundary condition (morphology)	44
5.6	Dredging and dumping	45
5.6.1	Updating of the reference plane	45
5.6.2	Required water depth below OLR/OLW	45
5.6.3	Clearance	46
5.6.4	Dredging at OLR	46
5.6.5	Depth after dumping	46
5.6.6	Dump locations	46
5.6.7	Sequence of dredging and dumping	47
5.6.8	Sand mining	48
5.6.9	Dune height computation	48
6	Offline calibration	50
6.1	Methodology	50
6.2	Results	51
6.2.1	Offline sediment transport	51
6.2.2	Gradient analysis	59
7	First steps in 1D calibration	62
7.1	Calibration procedure	62
7.2	1D calibration results	62
7.2.1	Yearly sediment transport rates and transport gradients	62
7.2.2	Bed level development	63
7.2.3	Grain size distribution changes	66
7.2.4	Fairway maintenance and sediment extraction	68
7.2.4.1	Effect of dredge depth and clearance	68
7.2.4.2	Effect of parameter TriggerAll	71
7.2.4.3	Comparison between modelled and reported dredging volumes	72
8	Conclusions and recommendations	74
9	Literature	78
A	Results analysis of morphological factor	80
A.1	Trench movement	80
A.1.1	$Q_{Lobith} = 1.635 \text{ m}^3/\text{s}$	80
A.1.1.1.	Morfac = 2, 10 and 50	80
A.1.1.2.	Morfac = 2, 100 and 200	82
A.1.1.3.	Morfac = 2 and 400	83
A.1.2	$Q_{Lobith} = 3.824 \text{ m}^3/\text{s}$	85
A.1.2.1.	Morfac = 2, 10 and 50	85
A.1.2.2.	Morfac = 2, 100 and 200	86
A.1.2.3.	Morfac = 2 and 400	88
A.1.3	$Q_{Lobith} = 8.592 \text{ m}^3/\text{s}$	89
A.1.3.1.	Morfac = 2, 10 and 50	89
A.1.3.2.	Morfac = 2, 100 and 200	91
A.1.3.3.	Morfac = 2 and 400	92
A.2	Sediment composition in trench simulations	94

A.2.1	$Q_{\text{Lobith}} = 1.635 \text{ m}^3/\text{s}$	94
A.2.2	$Q_{\text{Lobith}} = 3.824 \text{ m}^3/\text{s}$	95
A.2.3	$Q_{\text{Lobith}} = 8.592 \text{ m}^3/\text{s}$	96
A.3	Bed level differences for hydrograph simulations	96
A.3.1	r068-r066	96
A.3.2	r067-r066	98
A.3.3	r070-r066	100
A.3.4	r072-r066	101
A.3.5	r071-r066	103
A.4	Differences in D_{50} for hydrograph simulations	104
A.4.1	r068-r066	104
A.4.2	r067-r066	106
A.4.3	r070-r066	108
A.4.4	r072-r066	111
A.4.5	r071-r066	113

1 Introduction

1.1 Background and motivation

The riverbed (main channel and flood plains) of the Rhine branches is dynamic and changes over time under the influence of morphological processes and human intervention. Currently, morphodynamics in the Rhine branches can be predicted and assessed with the so-called DVR model (Duurzame Vaardiepte Rijndelta – sustainable fairway Rhine delta). For three reasons, this model will be outdated in the foreseeable future:

- The calibration is based on periods before realization of several important interventions (Room for the River, Water Framework Directive).
- RWS is moving to a new model generation in new software (the 6th generation models in the D-HYDRO Suite software package).
- There are new data and insights regarding morphological developments.

An up-to-date and reliable model is however needed for river management issues such as:

- project design of interventions in/along the summer bed (normalisation, sediment management),
- impact assessment for evaluation of measures (river engineering assessment framework / licensing),
- analyses of/after monitoring in pilots (sediment management, eroding banks, river widening such as by longitudinal dams, etc.),
- system analyses for long-term scenarios with management variants, e.g. for IRM (Integraal RivierManagement – Integrated River Management) so that estimates can be made of the morphological development on the different river functions.

These are reasons to replace the current modelling instrument for the Rhine branches with a new set of models and tools.

1.2 Objective

The objective of this project is the development of a new modelling instrument that simulates the complex spatial riverbed dynamics in the Rhine branches, enabling us to predict developments and effects of interventions in the riverbed, examine options for long-term (2050-2100) management and policy decisions, and thus shape the river management of the future.

1.3 This report

The development of such a modelling instrument for the entire Rhine branches will take several years and started in 2023. The work carried out in 2023 is reported in Becker et al. (2023) and led to model version v0 (uncalibrated). The current report is a progress report that describes only changes or additions that were made in 2024 and resulted in model version v0.5 (partially 1D calibrated). Choices made in 2023 and 2024 may be changed in the following years to further improve model performance. Once the model of the entire Rhine branches is ready, a final report will be made that contains a full description of all data, methods and results used for the final version v1 of the model (see end of this paragraph for more detail).

In 2023, a start was made with model developments (v0) for the Waal river branch. In 2024 the model set up for the IJssel was initiated (v0.5) and the Waal model was refined and calibrated further (v0.5). This report presents the developments for the Waal realized in 2024. Chapter 2 summarizes the steps taken in 2024. Chapter 3 presents the data used in addition to what has already been reported in Becker et al. (2023). Chapters 4 to 8 describe the model set-up and present validation results. Chapter 8 shows conclusions and recommendations for the following steps to be taken in the model development.

Once the models for all branches are finished completely, a series of final reports will be made as follows:

- 1 main report for all Rhine branches together, summarizing the definitive choices and results
- 2 calibration reports per branch
- 3 brief synthesis report, which summarizes, per Rhine branch, the information used in the model and what the model can be used for. This report needs to be easy to read, also by non-experts on morphological modelling.
- 4 manual, with sections on
 - a tutorial for setting up a new model
 - i. how to change model input, if needed specified per branch or river section
 - ii. which input is the user allowed to modify, and which not
 - iii. how to use the available scripts for modifying input and for visualizing model output
 - b how to apply the model in applications for permits (“vergunningaanvragen”) according to the “Rivierkundig Beoordelingskader (RBK)”
 - i. which hydrograph to use
 - ii. how many years to simulate
 - iii. which standard figures to produce and analyse
 - iv. etc.
 - c how to apply the model for policy studies, such as “Integrated River Management (IRM)”
 - i. which hydrograph to use
 - ii. how many years to simulate
 - iii. which standard figures to produce and analyse
 - iv. etc.
- 5 factsheets, for use on the IPLO website, via which model schematizations can be requested. These need to support the choice of model for a specific question.
- 6 Transfer protocol – “Protocol van Overdracht (PvO)” - the questionnaire to be answered before the model can formally become part of the official set of RWS models

1.4 Software

Within this project, the following software is used:

Software package	Version	Used for
D-HYDRO Suite	2.21.17.76916 (2023.01)	Hydrodynamic simulations
	2.26.15.78894	
	2.26.01.78771	Morphological simulations
	2.26.15.78894	
	2.27.03.79079	
Baseline	6.3.2	Schematization of model geometry
ArcGIS	10.6	In combination with Baseline

2 Approach for model set-up

2.1 General approach of the long-term model development

Spruyt (2023) has made an inventory of the intended use of the new modelling instrument and its required functionality. Based on this, she presents a general approach, which foresees a model development in several steps. These steps are extended as follows for this project:

- v0 This version is a basic model that contains the most important functionality, with the main goal to have a running but not yet too complex model. Within this step, we further distinguish the following sub-steps:
 - v0.5: after offline calibration
 - v0.8: after 1D calibration
 - v1: after 2D-calibration, so fully calibrated
- v1 Building on v0, the first model version replaces the existing DVR model. It covers the same functionality, but is based on the latest available data and insights.
- v2 The second model version is based on v1 but extended with new functionality to make the model suitable for more types of applications (e.g. finer grids, exchange of sediment between main channel and flood plains, bank erosion processes, etc.).
- v3 The third model version is used to develop new insights and functionality.

To give structure to this long-term development, several activity areas are defined as presented in Table 2.1 and linked to the stages of model development (v0-v3). The starting point is formed by the existing hydrodynamic model schematizations of RWS (the so-called 6th generation hydrodynamic models).

To effectively carry out the model set-up and associated calibration, we start by setting up submodels for different river branches, which can then relatively easily be merged into an overall model. The intended coverage of the final model is presented in Figure 2.1.

In each year of the model development, specific activities are identified for the different areas of activity per submodel.



Figure 2.1 Coverage of the sixth-generation hydrodynamic Rhine branches model (orange) and the current DVR instrument (purple areas, the different purple colours indicate the subdomains of which that model consists). Light and dark blue areas are water bodies that are not part of aforementioned models.

2.2 Overview of the activities carried out in 2024

In 2023, a start was made with the development of the first basic models (v0) of the Waal and IJssel branches. The Waal model was used as example to test methodologies and develop the necessary scripts. Both the Waal and IJssel models helped to identify issues in the existing tools and software used as well as in the model schematizations. In 2024, the following steps were carried out for the Waal, leading to model version v0.5:

- The stability issue detected in 2023 was solved,
- simulation times were decreased to acceptable values by an optimization of the morphological factor,
- the model schematization for the validation period (j16) was set-up,
- data on fairway maintenance and sand mining was collected, and a dredging and dumping module was added to the model,
- modelled dune heights were validated,
- the number of sediment fractions in the model was reduced in order to reduce computation time and the size of output files, while still getting results that are accurate enough,
- the downstream hydrodynamic boundary condition was analyzed in more detail in order to improve the long-term large-scale bed development on the Lower Waal and Upper Merwede,
- yearly discharge hydrographs were derived for the calibration and validation periods,
- the upstream morphological boundary condition was improved,
- an “offline” calibration was carried out to visualize the sensitivity of modelled sediment transport to the parameters of the transport formula, and appropriate parameter values were chosen,
- the spin-up procedure was refined for branches (like the Waal) that contain fixed layers, and
- the functionality of the SMT tool, required to run the model, was extended (enable running simulations on an arbitrary number of partitions; update of the reference plane for dredging and dumping). These new functionalities were tested and found to need some improvements, which will be implemented in 2025.

Furthermore, the IJssel model was set-up and calibration was started, leading to model version v0.5 (see Castañon et al., 2024), and decisions on the calibration and validation periods for the next model extension – with Boven-Rijn, Pannerdensch Kanaal and Neder-Rijn-Lek – were taken.

Table 2.1 Steps in model development.

activity areas	associated activities	model version	done in 2024
data collection	<ul style="list-style-type: none"> Collection of all data needed to set-up a model, e.g. boundary conditions, calibration data hydrodynamics and sediment transport and morphology, bed composition, etc. 	v0 v1	specifications of fairway maintenance
morphodynamic model schematization: towards a well-working basic model (v0)	<ul style="list-style-type: none"> set-up of a first running model including: <ol style="list-style-type: none"> dynamic river bed representative initial bed elevation (e.g. smoothing of bed forms) suitable roughness formulation for morphology sediment (grain sizes and sediment layers, with focus on active/upper layer) secondary flow first choice of transport formula and parameters (uncalibrated) non-erodible and less erodible layers suitable grid resolution testing phase v0 model, identification of problems and modification of the schematization accordingly 	v0	Waal v0: stability issue solved; set-up of the validation schematization j16; reduction of no. of sediment fractions; improvement of upstream morphological boundary condition
extending the basic model to a v1 model	<ul style="list-style-type: none"> more sophisticated description of <ol style="list-style-type: none"> main channel roughness composition and thickness of underlayers, including non-erodible layers set-up of a dredging and dumping module testing phase v1 model, and iterative modification of model schematization if necessary 	v1	Waal v0.8: Set-up and validation of dredging and dumping module; validation of simulated dune heights
development of methodologies and tools for running the model	<ul style="list-style-type: none"> approach and tools for model simulation (i.e. Simulation Management Tool) strategy for model spin-up strategy and tools for model evaluation and presentation of results strategy and tools for simplification of model set-up and improving reproducibility 	v0 v1	Waal v0: Choice of appropriate morphological factors; extension of SMT functionality
model calibration and validation	<ul style="list-style-type: none"> calibration and validation strategy adapting the hydrodynamic model to make it suitable for morphodynamic simulations hydrodynamic validation "offline" calibration giving a first estimate of morphological response based on the flow field in the hydrodynamic simulations 1D morphodynamic calibration and validation (focusing on width-averaged, large-scale and long-term trends) 2D morphodynamic calibration and validation (focusing on 2D patterns in the river bed, such as bank patterns and bend profiles) validation of dredging and dumping module 	v1	Waal v0.8: Analysis of influence of downstream boundary condition and sand mining; preparation of discharge hydrographs for calibration and validation periods;

activity areas	associated activities	model version	done in 2024
			"offline" calibration
exploring model uncertainties	<ul style="list-style-type: none"> influence of unknown physical variables (e.g. roughness in transport, bed composition, active layer thickness) influence of model settings (e.g. initial geometry/composition and boundary conditions) or modelling concepts (e.g. Hirano model) influence of simulation strategy and approaches (e.g. methods for optimizing simulation time, schematization of the hydrograph, choice of simulation period) 	v1-v3	-
development of modeling strategies and development for future use of the model	<ul style="list-style-type: none"> identifying types of application and requirements development of strategies for application of the model (e.g. choice of scenarios, choices for model settings and geometry, type of interventions) identifying needs for further development of the model schematization (including needs for knowledge development and data requirements) implementation and testing 	v1-v3	-
verification of model application	<ul style="list-style-type: none"> testing the model application in test cases of <ul style="list-style-type: none"> a. effect of interventions b. planning study ("planstudie") c. (long-term) forecast of system behaviour improvement of the model schematization, modelling strategies, methodologies and tools based on the outcomes of the test cases 	v1-v3	-
Implementation of new functionality in D-HYDRO	<ul style="list-style-type: none"> Identifying requirements of new functionality functional design of needs design of implementation implementation and testing updating user manuals 	v2-v3	-

3 Data

3.1 Fairway maintenance and sediment extraction

Dredging and dumping activities play an important role in the morphological development of the Rhine branches. This section describes the practice of dredging and dumping in the Rhine branches, as well as the available data on dredging and sediment extraction volumes.

3.1.1 Fairway maintenance

3.1.1.1 Dredging rules

Within the Central Commission for the Navigation of the Rhine (CCNR), the member states have agreed on requirements regarding the width and depth of the navigation channel. The required width and depth are defined for a certain reference discharge. This reference discharge, the 'Overeengekomen Lage Afvoer' (OLA), is the discharge that is exceeded 345 days per year – i.e. about 95% of the time. For the Dutch part of the Rhine, the OLA is defined at Lobith. The water level plane connected to this reference discharge is called the 'Overeengekomen Lage Rivierwaterstand' (OLR). From Tiel (Waal) and Hagestein-beneden (Lek) onward, tidal influence is taken into account through a smooth transition between OLR and the Lowest Astronomical Tide (LAT) at the river mouth. The resulting plane is called the 'Overeengekomen Lage Waterstand' (OLW). Because both OLA and OLR (and thus OLW) change over time (the OLA due to changes upstream of Lobith, and the OLR due to changes in river geometry downstream of Lobith), they are updated every 10 years.

For Boven-Rijn, Waal, Pannerdens Kanaal, Neder-Rijn and Lek, the required water depth is 2.80 m at OLA. For the IJssel, which is not part of the CCNR agreements, the Dutch government requires a water depth of 2.50 m at OLA. Hence, the bed level to be maintained by dredging is defined by the OLR plane minus the required water depth. The resulting plane is called the Dredging Reference Plane (Dutch: Baggerreferentievlak, BRV). In practice, a margin ('beheersruimte') of 0.50 m below the BRV is allowed to be dredged. Only for Boven-Rijn and Waal, it is since 2021 no longer allowed to dredge below the BRV. Instead of subtracting 0.50 m, a margin of 0.40 m was added to the BRV to define the minimally required bed level. This was done to minimize the risk of exposing objects present below the river bed (e.g. pipes, cables, archeological objects and unexploded ordnances).

Another exception for the Boven-Rijn and Waal yields when the water level at Lobith exceeds 9.5 m +NAP (roughly at $Q_{\text{Lobith}} = 2400 \text{ m}^3/\text{s}$). In this case, the bed level to be maintained by dredging increases with the water level and is thus no longer defined by the BRV, but by the Water Level Reference Plane (Dutch: Waterstandsreferentievlak, WSRV). This means for example that when the water level at Lobith is 9.8 m +NAP, the WSRV is 30 cm (9.8 – 9.5) higher than the BRV. In these situations, the same margins (either -0.50 or +0.40 m) apply as when the water level at Lobith is lower than 9.5 m +NAP.

For $H_{\text{Lobith}} > 10.5 \text{ m +NAP}$, dredging activities are increasingly hampered by the conditions and for $H_{\text{Lobith}} > 12 \text{ m +NAP}$, dredging activities cease altogether.

3.1.1.2 Dumping rules

Rijkswaterstaat Oost-Nederland defined a set of rules for relocation of dredged sediment in the Rhine branches (Treurniet and Tönis, 2019), that can be summarized as follows:

- 1 If it meets the environmental requirements, dredged sediment needs to be relocated within the main channel of the river (between the 'normaallijnen').
- 2 In principle, sediment needs to be dumped within a radius of 1.5 km around the location where it was removed. For some locations the radius is extended to 5 km, but in these cases the preferred dumping location is upstream of the dredging location.
- 3 After dumping, the channel width and depth requirements (see Section 3.1.1.1) need to be met.
- 4 Dredged sediment must be relocated within the same branch. Only for the section between IJsselkop and Driel on the Neder-Rijn, dredged sediment may be relocated on the Pannerdens Kanaal. In this case, rule number 2 (dumping within a 5 km radius) may be violated as well.
- 5 Ploughing of sediment within the fairway is allowed if environmental requirements are met.
- 6 Dumping in groyne fields is allowed under certain conditions.
- 7 The dredger reports activities.
- 8 Main channel lowering in the IJssel is maintained.
- 9 Sediment nourishments are supported in order to mitigate river bed erosion.

3.1.1.3 Data

In 2024, RWS-ON made an overview of dredging and dumping volumes for the Rhine branches for the period 1900 – 2024 (Krabbendam, 2024). The data contains total volumes per branch per year, but where possible the numbers have been broken down per river kilometer and even per 500 m as well.

For Boven-Rijn and Waal, dredging volumes per rkm are not available for the period 1997 – 2004 and 2020 – 2024. Total volumes are not available for 2022 – 2024. Also for 2003 and 2004, no reliable data on total dredging volumes could be obtained, possibly because no dredging activities took place in this period.

3.1.2 Sediment extraction

On the Beneden-Waal (rkm 916-952) and the Boven-Merwede (rkm 953-961) sand is being extracted through maintenance contracts (concessions) and for construction projects.

On the Beneden-Waal, 90.000 m³ of sediment could be extracted each year through the concession, until 2019 (RWS-WVL, 2017; RWS-ON, 2010). The actual amounts reported were similar (Arjan Sieben, personal communication, May 27, 2024). After 2019, there was no sediment extraction through the maintenance contract.

For the Boven-Merwede, 300.000 m³/y was conceded before 2008; after 2008 this was decreased to 125.000 m³/y (RWS-WVL, 2017). Reported quantities (Arjan Sieben, personal communication, May 27, 2024) show that on average, only about 75% of the conceded volume was actually dredged (Table 3.1).

Table 3.1 Reported sediment volumes extracted from the Boven-Merwede.

year	concession [m ³]	extracted volume [m ³]
2000	300.000	257.320
2001	300.000	329.305
2002	300.000	252.266
2003	300.000	196.796
2004	300.000	226.271
2005	300.000	178.814
2006	300.000	225.587
2007	300.000	114.062
2008	125.000	118.451
2009	125.000	119.078

4 Hydrodynamic model schematization and validation

4.1 Improvement of model stability

In 2023, Waal model results (with version v0) became instable after a few years of simulation, so simulating long-term trends was impossible. A thorough analysis of the instabilities revealed that they were caused by drying and flooding of cells at the edge of the main channel, in the hydrodynamic part of the simulation. Changing the value of parameter *epshu*, which defines the minimum water level above which a cell is considered wet, from a very low value of 0.0001 m to 0.1 m solved this problem. Figure 4.1 shows that this results in only very little difference in simulated water levels for the steady state simulations.

In light of the objective to, in the future, use the same model for both hydrodynamic and morphodynamic simulations, it should be analysed how a change of *epshu* influences the results of the unsteady standard simulations for hydrodynamic analyses. The value of *epshu* needs to be optimized for the quality of results of both hydrodynamic and morphological models as well as stability of the morphological model.

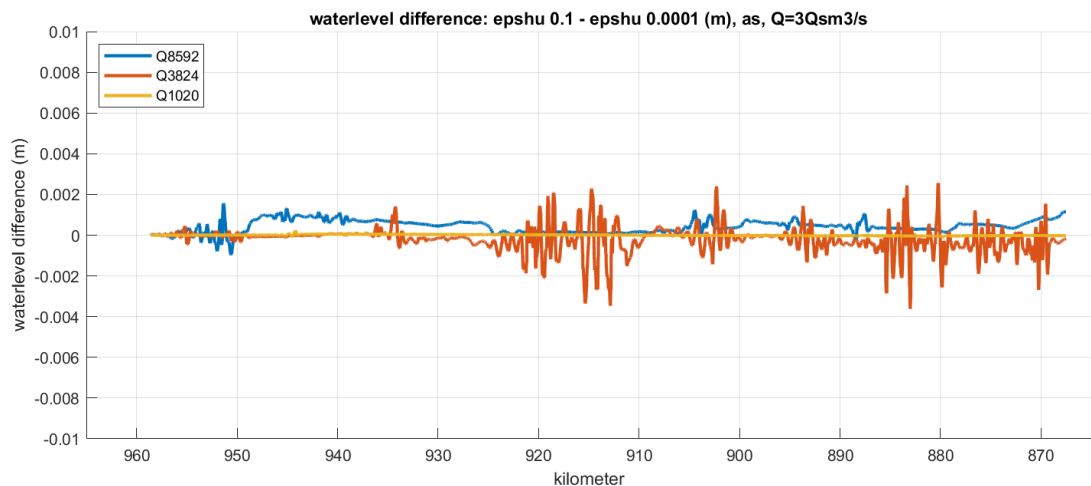


Figure 4.1 Water level difference caused by increasing the threshold water depth for considering cells as being wet (*epshu*) to 0.1 m for three discharge levels.

4.2 Choice of downstream boundary condition

At the downstream boundary of the model, which is located at Hardinxveld, a Qh relation is used as boundary condition (see Table 4.1). In reality, the conditions at this location are influenced by tide, which cannot be represented with a Qh relation. The effect of this simplification needs to be investigated. Furthermore, in the report of 2023 (Section 4.4 of Becker et al., 2023), it was explained that the Qh relation used for j16 and j19 gives higher water levels than would be obtained from averaging the tidal signal at this location. This leads to a deviation in the modelled velocities and sediment transport rates.

The difference between using the Qh relation by Van der Wijk (2022) and a water level signal which represents the tidal motion was investigated with a set of hydrodynamic simulations with the j19 pilot model. The model was run for two stationary discharge levels, corresponding to $Q_{\text{Lobith}} = 3824$ and $8592 \text{ m}^3/\text{s}$.

For each discharge level two simulations were carried out: one with the Qh relation as applied in Becker et al. (2023), and one with an average tidal signal (representative for the full tidal motion at this location) as downstream boundary condition. The tidal signal was derived from standard simulations carried out with the j19 model of the Rhine-Meuse estuary, dflowfm2d-rmm_vzm-j19_6-v2d (Gradussen, 2024). These standard simulations contain different combinations of extremes in river discharge, downstream water levels and wind speed. While the river discharge is constant during the simulation, downstream water levels and wind speed increase gradually from average to extreme values towards the end of the simulation. By extracting the water level at Hardinxveld for the first 12 days of the simulations, an average tidal signal for different river discharges can be obtained. We made use of the standard simulations tbc and tbb, corresponding to $Q_{\text{Lobith}} = 3000$ and $9000 \text{ m}^3/\text{s}$. This was considered close enough to the discharge levels within the pilot model ($Q_{\text{Lobith}} = 3824$ and $8592 \text{ m}^3/\text{s}$) for a first estimate of the effect of using a Qh relation instead of a tidal signal. The extracted tidal signal at Hardinxveld is shown in Figure 4.2 for both discharges. For $Q_{\text{Lobith}} = 3824 \text{ m}^3/\text{s}$ the tidal influence is still significant, while it hardly plays a role for $Q_{\text{Lobith}} = 8592 \text{ m}^3/\text{s}$.

Figure 4.3 shows the resulting water levels and flow velocities along the river axis for the 4 simulations with the j19 pilot model. Note that these values are not width-averaged, but taken directly from model output at the river axis. The top panel confirms that the Qh relation leads to overestimation of water levels during average tidal conditions in the downstream part of the Waal. For the 3824 discharge level the deviation seems to be larger, but this is due to the difference between the modelled discharge and the discharge for which the downstream boundary condition is representative ($3000 \text{ m}^3/\text{s}$ at Lobith). For a discharge of $3824 \text{ m}^3/\text{s}$ at Lobith, the tidal range would be somewhat smaller and the average water level somewhat higher, therefore corresponding better to the Qh relation. However, for the 8592 discharge level we also see that water levels are overestimated by the Qh relation, even though the tidal signal corresponds to a higher discharge ($9000 \text{ m}^3/\text{s}$).

An overestimation of water levels, and thus water depths, leads to an underestimation of average flow velocities, as shown by the bottom panel of Figure 4.3. The difference between the velocities from the stationary simulations and the maximum tidal velocities is in the order of 0.1 m/s for the 3824 case, and smaller for the 8592 case.

An estimate of the influence of this underestimation of the flow velocity on sediment transport can be made by supposing a difference in flow velocity of 0.1 m/s for all discharge conditions, and using the following sediment transport relation (Meyer-Peter-Müller):

$$S_{MPM} = aD\sqrt{\Delta gD}(\mu\theta - \xi\theta_c)^b$$

$$\theta = \left(\frac{u}{C}\right)^2 \frac{1}{\Delta D}$$

With Δ the relative density of the sediment [-], D the characteristic grain size of the sediment fraction considered [m], μ the ripple factor, θ_c the critical Shields parameter, ξ the hiding and exposure factor for the sediment fraction considered, a and b calibration parameters and u the magnitude of the flow velocity [m/s].

Following the 1D calibration simulations (Chapter 7), we use $\Delta = 1.65$, $\mu = 1$, $\theta_c = 0.047$, $a = 2$, $b = 1.6$ and $C = 45 \text{ m}^{1/2}\text{s}^{-1}$. For simplicity, we use $\xi = 1$ (no hiding and exposure).

Using $u = 0.8$ and 0.9 m/s, $D_{50} = 7 \cdot 10^{-4}$ m and a main channel width of 300 m (characteristic values near the downstream end of the Waal), we get a difference in sediment transport of around $7 \cdot 10^4$ m³/y. This is a significant percentage (ca. 35 %) of the transport at this location, which is in the order of $2 \cdot 10^5$ m³/y (with $u = 0.9$ m/s). Improving the downstream boundary condition should therefore be considered, for example by constructing a Qh relation that better approximates the tidal signal in terms of resulting sediment transport.

Furthermore, anticipating the setup of a morphological model for all Rhine branches together, it must be considered that the tidal influence at the downstream boundary of the Neder-Rijn – Lek is much larger than at the Waal boundary. If for the Neder-Rijn – Lek the use of a Qh relation leads to unacceptable errors, the type of downstream boundary condition on the other branches needs to be changed as well.

Table 4.1 Qh-relation at Hardinxveld for j16 and j19, excluding the effect of sea level rise (Van der Wijk, 2022).

Q [m ³ /s]	H [m +NAP]
380.0	0.50
473.9	0.58
1483.7	0.91
2709.5	1.19
4050.7	1.74
5404.0	2.30
6614.6	2.66
8456.3	3.21
10185.1	3.71
10735.9	3.85
11266.9	3.99
12257.9	4.25
14219.3	4.75
18200.0	5.70

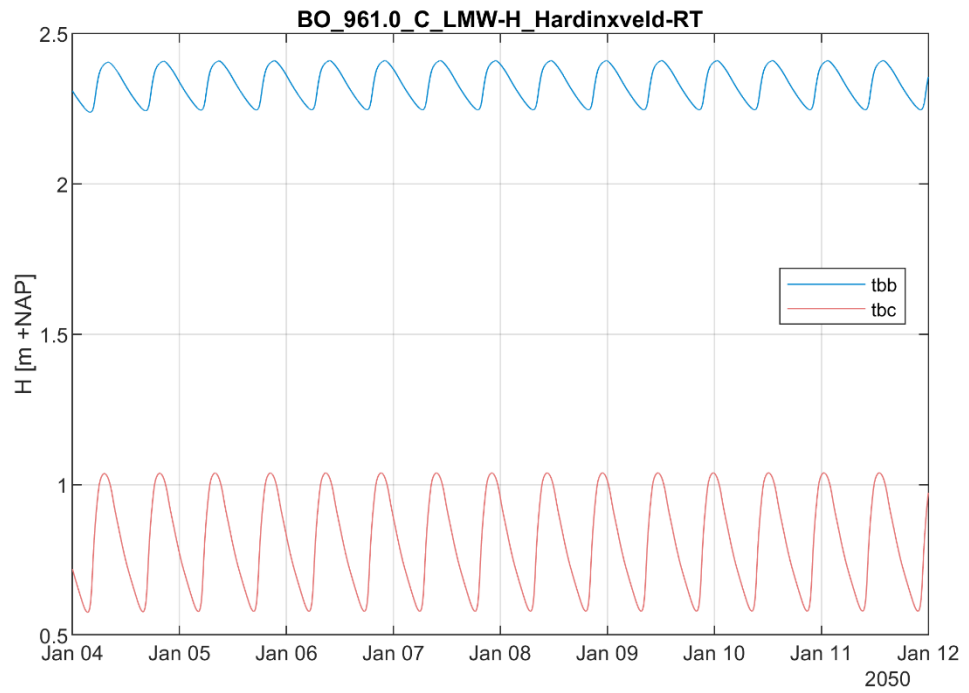


Figure 4.2 Water levels at Hardinxveld as computed with *dflowfm2d-rmm_vzm-j19_6-v2d* for a discharge corresponding to $Q_{Lobith} = 3000$ (red) and $9000 \text{ m}^3/\text{s}$ (blue).

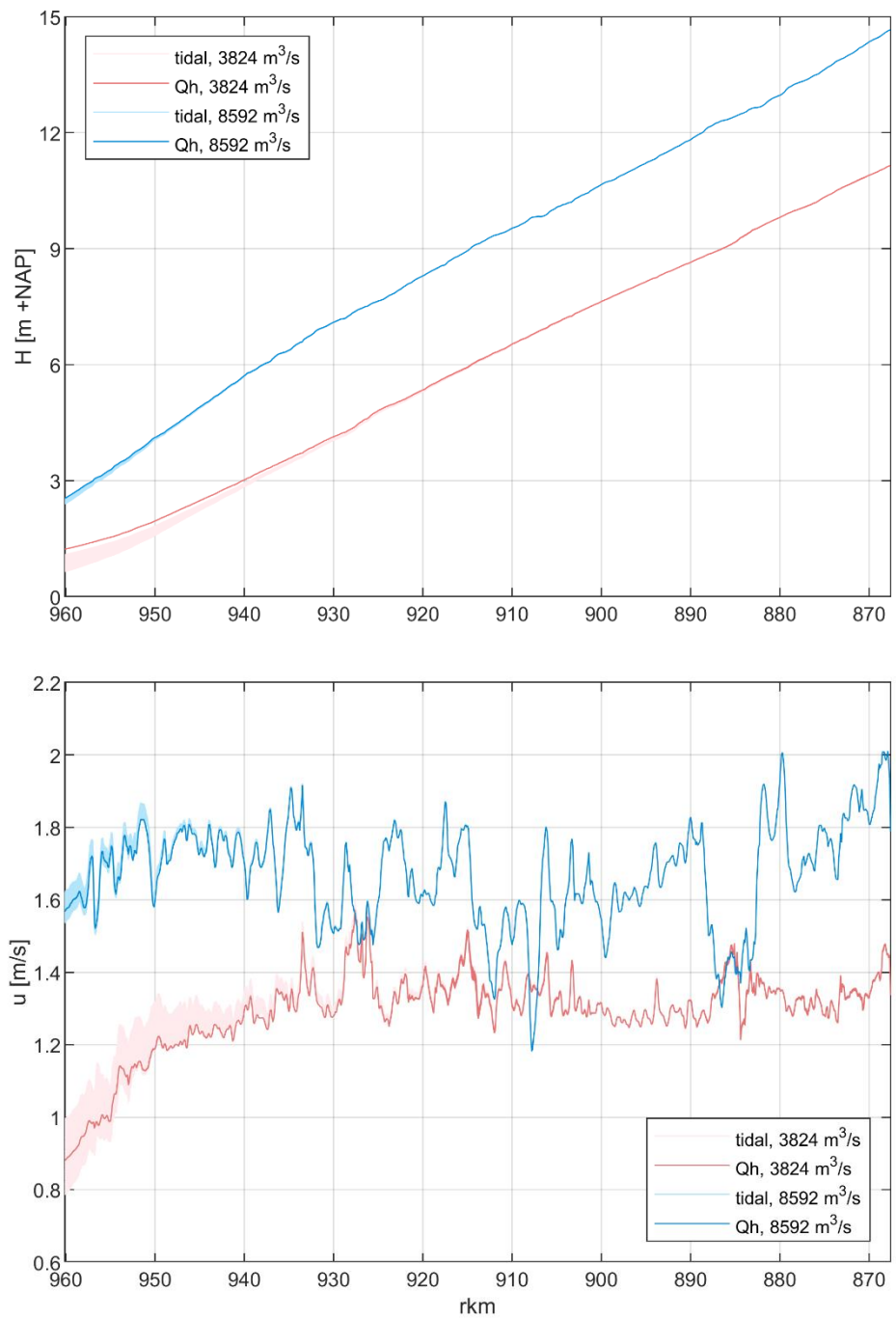


Figure 4.3 Water level (top) and velocity magnitude (bottom) along the main channel axis in the j19 model for $Q_{Lobith} = 3824$ and 8592 m³/s, with the Qh relation (see Table 4.1) and a tidal signal (see Figure 4.2) at the downstream boundary.

4.3 Yearly discharge hydrographs for the calibration and validation periods

The initial version (v0 till v1) of the new morphodynamic model of the Waal still makes use of approaches that were derived for its predecessor, the “DVR model” in Delft3D 4. This also applies for the hydrodynamic upstream boundary condition, which is a standardized yearly hydrograph consisting of several stages with constant discharges (see details in Becker et al., 2023). The same hydrograph was used in the first test simulations (v0) of the new model. For calibration and validation, similar hydrographs have been derived that are representative for these periods (1999-2012 for calibration, 2016-2022 for validation). Figure 4.4 shows the resulting hydrographs.

Using these hydrographs ensures that the calibration is valid for future simulations that are supposed to produce a long term trend in bed development. At a later stage, it can be decided to use a different type of upstream model boundary (e.g. a “normal” hydrograph), or to extend the methodology with different ways of forcing for different applications.

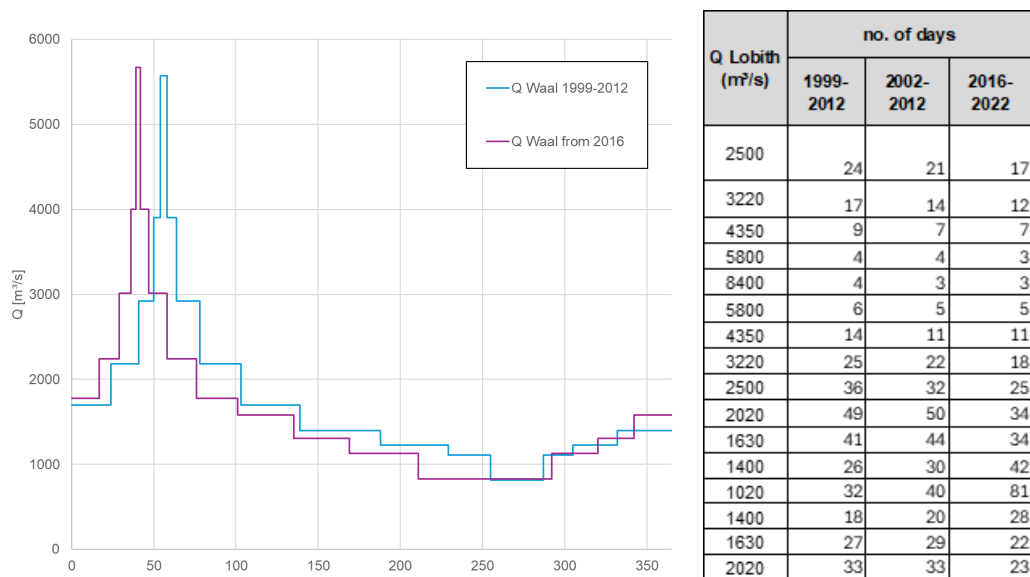


Figure 4.4 Standardized yearly hydrograph for calibration and validation converted to the Waal (left) and at Lobith (table on the right).

Average yearly discharge hydrographs were derived for the calibration and validation periods for the Waal and IJssel models, to be used in the 1D and 2D calibration of the models:

- 1999 – 2012: calibration Waal
- 2002 – 2012: calibration IJssel
- 2016 – 2022: validation Waal and IJssel

The following sections describe how the hydrographs were derived for Lobith on the Boven-Rijn and present the resulting hydrographs (discharge levels and durations). The discharges were translated from Lobith to the Waal by means of the QQ relation 2000.1 (1999-2012) and Qf18 (2016-2022) as explained in Becker et al. (2023).

4.3.1.1 Method

The approach to derive the discharge hydrographs is as follows:

- Observed discharges at Lobith for the respective calibration or validation period are used as input.
- These are ordered from small to high to obtain a probability density function (pdf, blue line in Figure 4.5).
- To keep the necessary modeling steps as limited as possible (e.g. hydrodynamic spin-up), it was decided to use the same discharge levels for all hydrographs. Nine suitable discharge levels have been determined in previous studies (“Uitwerking systeemmaatregelen beleidskeuze rivierbodemplugging IRM” and “vaarweg Rijn grensregio”, both not yet published) based on relevant discharge regimes in the Rhine branches. The nine levels are presented in Table 4.2. Paragraph 4.3.1.2 discusses the discharge regimes.
- The moment of intersection of the levels with the pdf were determined (black points in Figure 4.5). The moment at which the hydrograph changes from one discharge level to the next was defined as halfway between these intersection points ($d_i/2$).
- In cases with relatively low high discharges, a minimum duration of the highest discharge level of 3 days was enforced at the cost of the duration of the level below. This was needed for the periods 2002-2012 and 2016-2022, which based on the procedure above received only 2 days of the highest discharge each.
- The nine levels and durations were then split into a hydrograph with 16 steps, as presented in Figure 4.4, that resembles a typical year with a flood event in winter and a low flow period during summer. Following the same procedure as for the DVR model, it is assumed that 40% of the higher discharges (levels 5-8) occur before the flood (100% of level 9), and 60% occur after the flood and before low flow season. Of the lower discharges (levels 2-4), 60% occur before the lowest discharge (level 1) and 40% after it. The resulting durations are rounded to full days.

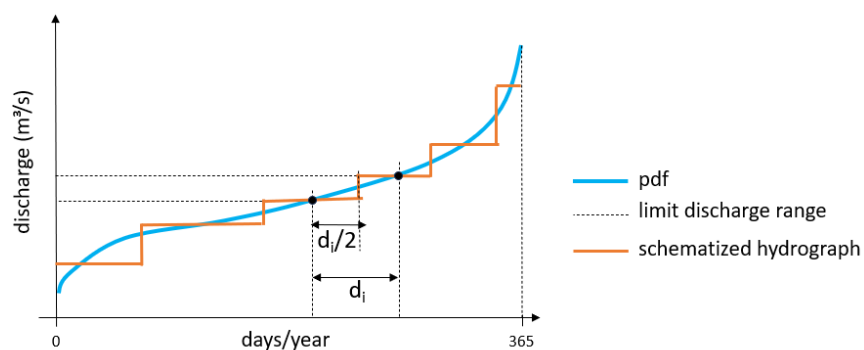


Figure 4.5 Approach to derive a schematized hydrograph from a pdf.

Table 4.2 Discharge levels and total duration for the three calibration and validation periods.

Discharge level (m ³ /s)	1999-2012 (d)	2002-2012 (d)	2016-2022 (d)
1020	32	40	81
1400	44	50	70
1630	68	73	56
2020	82	83	57
2500	60	53	42
3220	42	36	30
4350	23	18	18
5800	10	9	8
8400	4	3	3

4.3.1.2 Discharge regimes

The following discharge regimes have been identified as relevant regimes for the morphological development of the Rhine branches (based on the discharge at Lobith):

Table 4.3 Relevant discharge regimes in the Rhine branches based on the discharge at Lobith.

Q (from) (m ³ /s)	Q (to) (m ³ /s)	description discharge regime	Discharge levels (m ³ /s)
0	1770	weirs Nederrijn closed (impounded)	1020 1400 1630
1770	2740	weirs Nederrijn in transition from closed to open (impounded)	2020 2500
2740	3870	free flowing, discharge within main channel	3220
3870	ca. 5000	flow through flood plains starts to develop	4350
ca. 5000	18000	fully developed flow through flood plains	5800 8400

4.3.1.3 Hydrographs for Lobith

Figure 4.6 shows the resulting yearly hydrographs. Figure 4.7 presents the difference in volume under the pdfs compared to the schematized hydrographs. Note that the difference in volume is not a good indicator for the difference in yearly sediment transport due to the non-linearity in the transport relation. The final check on the suitability of these hydrographs will be made by using them for calibration and validation. If it is possible to reproduce the desired river bed dynamics (long-term and large-scale effects) using these boundary conditions, they are suitable.

Table 4.4 shows how the nine discharge levels were discretized further into hydrographs of 16 steps. Figure 4.4 shows the resulting hydrograph for the Waal (i.e. with Waal discharges).

In the next step, these discharges at Lobith are translated into discharges at the upstream end of Waal and IJssel, so that they can be used as boundary conditions for the separate branch models. We used the Q-Q-relations 2000.1 (calibration periods) and 2018 (*Qf18*, validation period) for this.

Table 4.4 Discretization into 16-step-hydrographs for the three different periods.

step	Q (Lobith) (m ³ /s)	duration (d)		
		1999-2012	2002-2012	2016-2022
1	2500	24	21	17
2	3220	17	14	12
3	4350	9	7	7
4	5800	4	4	3
5	8400	4	3	3
6	5800	6	5	5
7	4350	14	11	11
8	3220	25	22	18
9	2500	36	32	25
10	2020	49	50	34
11	1630	41	44	34
12	1400	26	30	42
13	1020	32	40	81
14	1400	18	20	28
15	1630	27	29	22
16	2020	33	33	23
		365	365	365

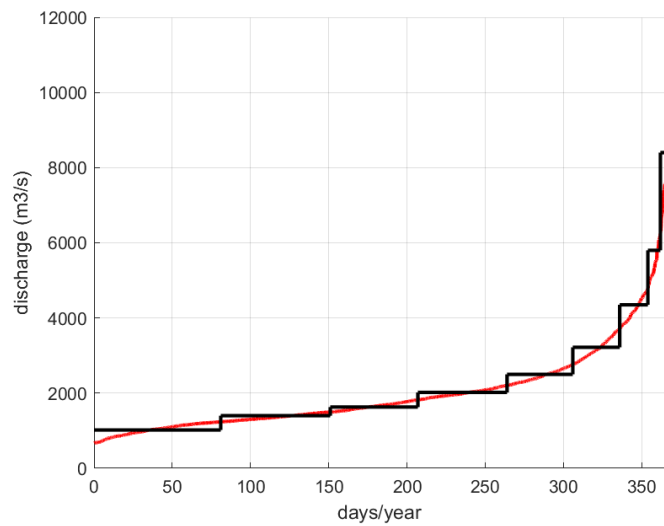
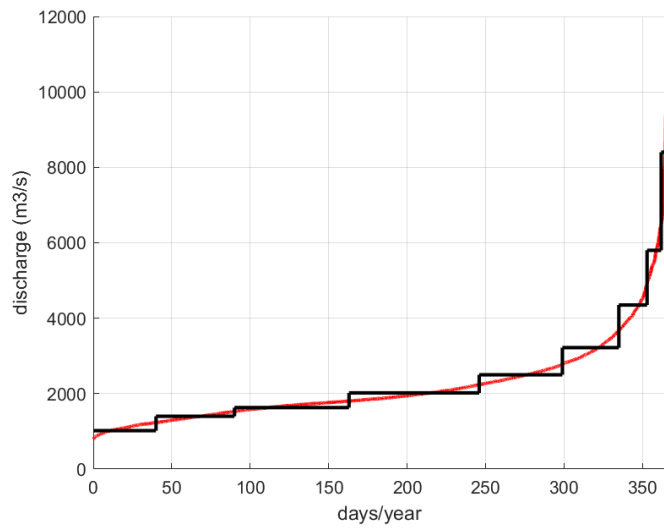
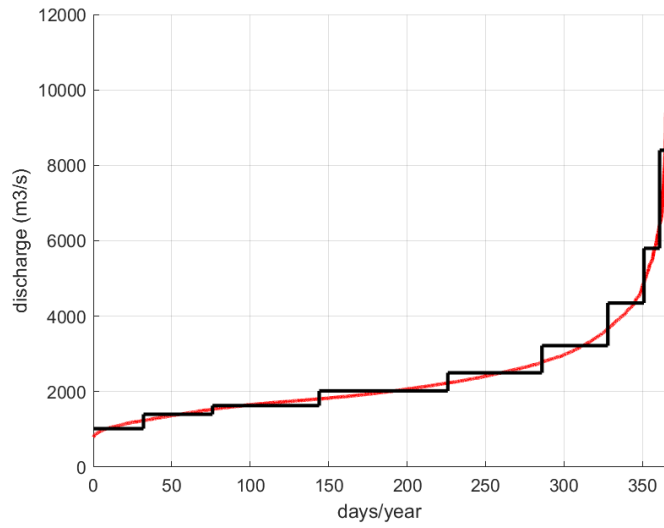


Figure 4.6 Pdfs (red lines) and duration of the discharge levels in the schematized hydrographs (black lines) for the calibration and validation periods 1999-2012 (top), 2002-2012 (centre), and 2026-2022 (bottom).

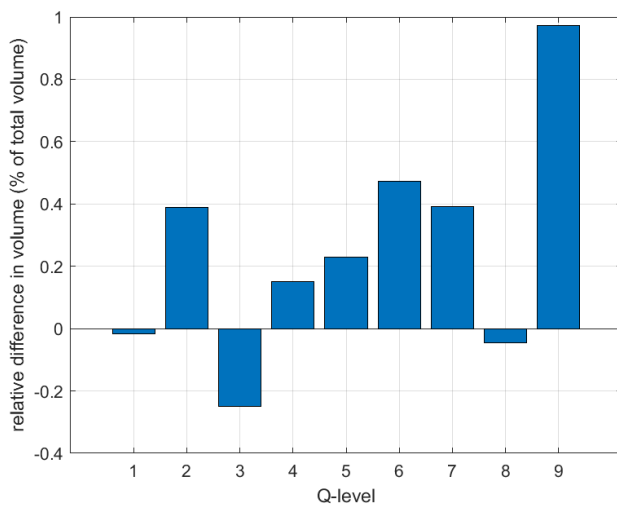
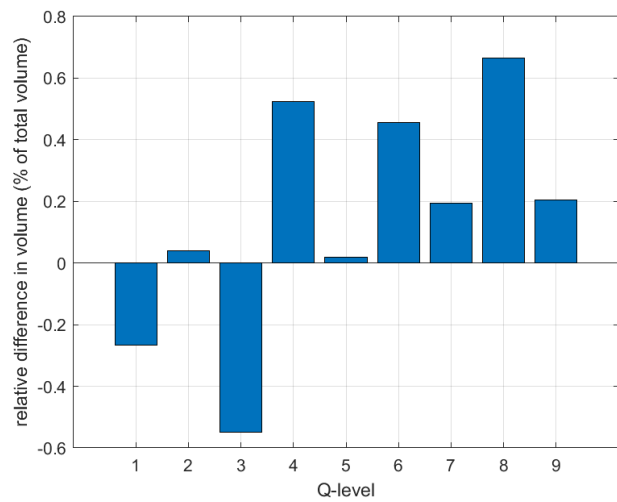
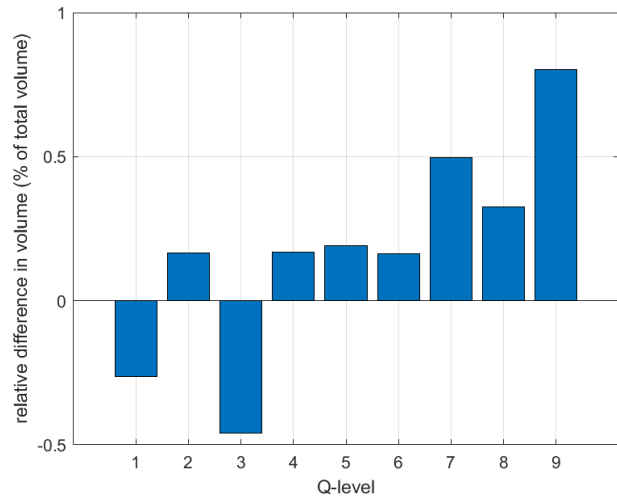


Figure 4.7 Relative difference in volume (% of the total year volume) between the pdf and the schematized hydrographs for the calibration and validation periods 1999-2012 (top), 2002-2012 (centre), and 2026-2022 (bottom).

5 Morphological model schematization

The morphological model schematization of model version v0 is described in the report of 2023 (Becker et al., 2023). This chapter describes changes that were made in 2024 to the original set-up and led to model version v0.5.

5.1 Optimization of simulation times by means of the morphological factor

5.1.1 Using a morphological scale factor

Long-term (in the order of years) two-dimensional morphodynamic simulation of long river stretches (tens of kilometres) require a significant computational time. Parallelization reduces the computational time, but it has a limit above which more computational power does not decrease the computational time. Considering that the changes in the bed level occur on time scales which are much larger than hydrodynamic time scales this allows the introduction of a morphological acceleration factor as alternative (e.g. Lesser et al., 2004). The essence is that the bed level changes in one hydrodynamic time step are multiplied by a factor larger than one. As a consequence, the modelled changes in bed level are larger than the hydrodynamic time modelled. As an example, a morphological factor of 100 means that the effect of 1 minute of flow upon morphology (both bed level and sediment composition) is multiplied by 100 before morphological updates are performed. Effectively, the use of a morphological factor means that a much shorter flow time can be used to simulate a certain morphological time, and thus simulation times can be reduced significantly.

The physical set of equations solved using a morphodynamic acceleration factor is different from the original set of equations and only for “small” factors the differences are acceptable. The larger the Froude number and the sediment transport, the smaller the factor can be. While some analytical approximations can be derived for the upper bound of the morphodynamic acceleration factor under some idealized conditions, a comparison with a case with no morphodynamic acceleration factor is required to provide evidence that the negative effects are small. The results of these tests for the Waal are described in this section.

For long-term river-morphological simulations with varying discharges it is important to understand that in the reduced flow time still all the regular variations in discharge (in the correct sequence) are introduced: this means that the time-scale of the flow hydrograph is ‘squeezed’ to the short flow time.

Looking at the flow time scale, it is clear that this squeezing causes the flood waves to become much steeper (shorter duration), which leads to a different propagation of these waves (more attenuation, different celerity) than without squeezing. For instance, for morphological factors higher than 10, and model lengths over 100 km, this effect can noticeably affect the morphological results.

To prevent this, we apply the quasi-steady approach that was used in the DVR model as well (Yossef et. al. 2008). With this approach (which is explained in more detail in last year’s report by Becker et al., 2023), morphological factors can be chosen much higher without losing accuracy.

Apart from this flow-unsteadiness problem, the morphological factor is also constrained to ensure numerical stability.

Note that in our D-HYDRO simulations, a restriction of morphological changes per time step is used (by using the keyword MorCFL and setting the maximum bed level change to 10 cm per time step). If this bed level change is exceeded, the time step is reduced, similar to the CFL stability criterium for hydrodynamics. This provides additional safety for the accuracy in simulations with high morphological factors. This option was not available in the old DVR model in Delft3D 4.

5.1.2 Set-up of test simulations

5.1.2.1 Trench simulations with constant discharge

To evaluate the stability and accuracy of bed level development, simulations were run with increasing morphological factor and the j19_6 schematization for constant discharges (all 9 levels that are used in the v0 yearly discharge hydrograph, i.e. the one that was already used in the DVR model). Sloff et al. (2009) tested morphological factors for the graded sediment domains (Boven-Rijn, Waal, Pannerdensch Kanaal) of the DVR model in Delft3D 4. They used factors between 1440 (for discharges of up to approximately 1400 m³/s at Lobith) and 120 (for discharges of 3800 m³/s at Lobith and higher). Up to this speed-up, bed level development in the model remained approximately the same as in simulations without morphological acceleration. For D-HYDRO, new tests need to be made, as it uses a different numerical scheme. Van Dongeren et al. (2018) found that simulations for a test case in the Western Scheldt could become unstable at morphological factors of 25. These simulations used fixed time steps, though, which did not fulfil the stability criterion of a Courant number below 0.7 that is applied in our simulations. Furthermore, this was a tidal test case that is expected to behave differently than the Rhine branches. Therefore, tests for the Waal are now being made using morphological factors of 2, 10, 50, 100, 200 and 400. The simulation with a morphological factor of 2 is regarded as the reference case, in which morphological development is not significantly distorted by the acceleration factor. Ideally, a simulation with morphological factor of 1 should have been used, but that would have taken too much simulation time.

To assess the influence of the morphological factor on bed level development, three trenches were added to the initial bed level of the j19_6 model of the Waal. Simulations were then run with and without trenches in order to compare the movement of the trenches for different morphological factors. The trenches are approximately 1 m deep and are introduced across the entire width of the morphologically active part of the main channel. They are located in the Boven-Waal (km 879.5), the Midden-Waal (km 900), and the Beneden-Waal (km 942), see Figure 5.1. Results for these simulations are shown in section 5.1.3.

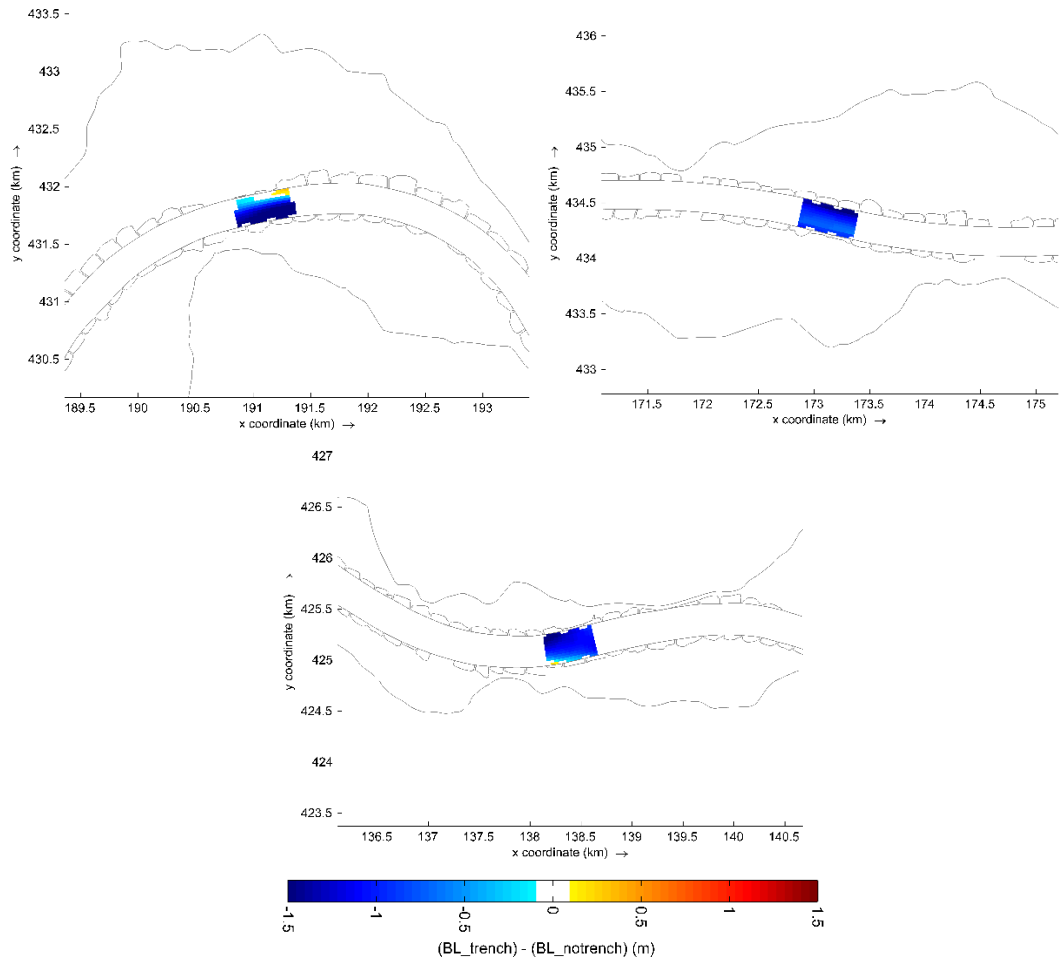


Figure 5.1 Initial location and depth of the trenches. Top left: Boven-Waal around km 880, top right: Midden-Waal around km 902, bottom: Beneden-Waal around km 942.

As morphological changes are larger at higher discharges, the maximum value for the morphological factor is expected to be discharge dependent. Therefore, simulations with constant discharges in combination with the different morphological factors were run. Trench movement was assessed separately for each discharge. This resulted in a first idea about accuracy of model results for different morphological factors.

5.1.2.2 Hydrograph simulations

As a next step, bed level development was then compared for simulations using the average yearly discharge hydrograph and appropriate morphological factors per discharge level and the j99_6 model of the Waal (= the calibration model). Table 5.1 presents the combinations of morphological factors used in the different simulations. The simulation using a factor of 10 for all discharge levels is regarded as reference, because simulations with a factor of 1 would have taken too long, and a factor of 10 has shown to be very acceptable compared to simulations using a factor of 1 or 2 for all discharge levels in the simulations with trenches, see section 5.1.3.

Table 5.1 List of hydrograph simulations carried out with different choices for the morphological factors per discharge level.

Q (m ³ /s)	mor-time (yearly hydrograph) (days)	r066	r068	r067	r070	r072	r071
		morfac	morfac	morfac	morfac	morfac	morfac
3053	16	10	100	100	100	200	400
3824	8	10	10	100	10	200	400
4717	4	10	10	100	10	200	400
6151	2	10	10	100	10	200	400
8592	2	10	10	100	10	200	400
6151	4	10	10	100	10	200	400
4717	7	10	10	100	10	200	400
3824	12	10	10	100	10	200	400
3053	25	10	100	100	100	200	400
2250	53	10	100	100	100	200	400
1635	70	10	100	100	400	200	400
1203	35	10	100	100	400	200	400
1020	21	10	100	100	400	200	400
1203	23	10	100	100	400	200	400
1635	47	10	100	100	400	200	400
2250	36	10	100	100	100	200	400
simulation time¹ (h):		179.72	120.15	22.80	37.73	25.20	9.68
simulation time¹ (d):		7.49	5.01	0.95	1.57	1.05	0.40

5.1.3 Influence of the morphological factor on trench propagation

The bed level development around the three trenches for different morphological factors compared to the results for a factor of 2 is given in Appendix A.1. For a discharge of 1.635 m³/s at Lobith, for morphological factors of up to 200, bed level development and trench movement remain very similar to the reference with a morphological factor of 2. The bed level differences are mostly lower than 1 cm. For a factor of 400, the differences get slightly bigger, especially for the most upstream trench in the Waal bends. But the general shape and celerity of the trench still remain the same. Therefore, a factor of 400 is acceptable for discharges of at least up to 1.635 m³/s. In the discharge hydrograph, a morphological factor of 400 for all discharges of 1.635 m³/s and lower leads to simulation times of about 10 min/yr for the entire block of those discharges (Section 5.1.4), so a further increase of the morphological factor would result in only a limited reduction of overall simulation times.

¹ For 10 years of simulation

For a discharge of 3.824 m³/s at Lobith, the results are similar, with slightly bigger deviations but still a very similar trench movement for the highest morphological factor of 400. Therefore a morphological factor of 400 still seems acceptable for this discharge level, but it is probably at the limit of the increase.

For a discharge of 8.592 m³/s at Lobith, a factor of 200 still seems acceptable, but for a factor of 400, trench movement starts to deviate in general, so a factor of maximum 200 is advised.

Outside of the zone of influence of the trenches, very local deviations in bed level development can be seen between the runs with different morphological factors. The number of these, as well as the amount of deviation, seems to increase with higher morphological factor.

In Appendix A.2, a comparison of sediment composition development (D_{50}) in the trench simulations is shown for different values of the morphological factor. Differences are mostly negligible. Only on top of and downstream of the fixed layer at Sint Andries some differences occur, but they are small. Note that the development of sediment composition is not necessarily realistic, because these are simulations with constant discharge for a full year with large discharges.

5.1.4 Influence of the morphological factor on bed level and sediment composition development in hydrograph simulations

Appendix A.3 compares the bed level development after 10 years of simulation for different combinations of morphological factors per discharge level to the reference simulation (which uses a factor of 10 for all discharge levels). Bed level differences mainly occur downstream of the fixed layers at Erlecom, Nijmegen and Sint Andries, and in the most downstream reach from approximately km 940. The simulations with very high factors (200 and 400 for all discharge levels, r072 and r071) show consistently lower bed levels in the Middle Waal and consistently higher bed levels in the lower Waal after 10 years, but the differences remain low (maximum of about +/- 3cm). Just downstream of the fixed layers, differences amount to up to +/-10 cm locally in these simulations. All simulations stayed stable during the entire 10 years. So all in all, morphological factors significantly higher than 10 can be used in future simulations. Results for high morphological factors might still be improved by improving hydrodynamic and morphodynamic spin-up.

Appendix A.4 presents the comparison for D_{50} . After 10 years of simulation, differences in D_{50} are still small compared to the absolute sediment diameter. For longer simulation periods, e.g. 20 or 30 years, differences might become too big when using large morphological factors.

5.1.5 Simulation times

The simulation times in Table 5.1 show that using a factor of 10 for the higher discharges significantly increases simulation times compared to simulations with factors of 100 or more for all discharges, even though the higher discharges run only for a few days per year. Strikingly, the simulation with a factor of 200 for all discharges (r072) took longer than the one with 100 (r067). Probably, this was caused by some problem on the computational cluster or with the connection between the cluster and the project drive, since all other simulations scale as can be expected from the morphological factors used. A simulation time of around 16 h would make more sense for this run.

Simulations with a factor of 400 would run over night, while simulations with a factor of 100 or 200 need up to a full day and night for 10 years. Both allow an efficient workflow in this project, in which the maximum length of simulations is around 10 years (length of the calibration periods). For much longer simulation periods, e.g. 20 or 30 years, it is recommended to check if differences introduced by the morphological factor don't become too large, especially differences in sediment composition.

5.1.6 Conclusion

Trench development and overall bed level development in all test simulations show that morphological factors of up to 100, or even 400 if one accepts slightly bigger differences, should be acceptable for all discharge levels. However, in the trench simulations there is still an issue with bed level differences developing outside the zone of influence of the trenches. Therefore, even though general trench development in the trench simulations and overall bed level development in the hydrograph simulations are not strongly influenced by factors of up to 200 or even 400, it is advised to – for the time being – continue with factors of 100 to be sure to keep simulations stable. Once more experience has been gained with model stability, the step towards even higher factors could be made. For much longer simulation periods, e.g. of 20 or 30 years, it is recommended to check if changes in D_{50} still remain acceptable.

Please note that this conclusion is valid for the current morphological settings, such as a constant active layer thickness of 1 m. The choice must be validated again once the model has been calibrated.

And please note that we also need to investigate if the hydrodynamic spin-up time used currently is enough. The hydrodynamic spin-up time is the time at the start of every stationary discharge computation in which no morphological changes take place yet. This spin-up is needed for the model to adapt to the boundary conditions. This part of the simulation also influences the overall simulation time significantly.

5.2 Number of sediment fractions in the implementation of graded sediment

The new morphodynamic model does not only need to assess local morphological developments of the navigation channel, but also the large-scale and long-term morphological development of the Rhine river system in the Netherlands. Therefore, it is important to account for the entire variety of processes that play a role in different reaches from upstream till downstream. Most relevant in this respect is the occurrence of grain-size variation and its relevance for sediment-transport processes. Characteristic for the Rhine River is a downstream fining of sediment when looking at it on the length-scale of the German Niederrhein and Dutch Rhine branches, see Figure 5.2. The Rhine in Germany (Niederrhein) can be considered as a gravel river, whereas it shows a transition towards a sand-bed river in the Dutch Rhine branches. In the transition zone between the German border and the upper-Waal, Pannerdensch Kanaal and upper-IJssel and Neder-Rijn, both gravel and sand play an important role in sediment transport and morphology. The river bed of the further downstream-located branches is composed of sand. In the tidal low-land part the interaction between sand, silt and mud becomes important.

Therefore, it was decided to apply graded sediment in the entire model. This means that different sediment fractions, from coarse to fine, and their interaction, are modelled separately. This is also important for a proper modelling of sediment management measures affecting sediment composition, such as sediment nourishment.

The boundaries of the fractions are based on the sieve sizes used in the 2020 measurement campaign (Onjira, 2023). Originally in the data there were 22 fractions available for sieves: 63 μm , 90 μm , 125 μm , 180 μm , 355 μm , 500 μm , 710 μm , 1 mm, 1.4 mm, 2 mm, 2.8 mm, 4 mm, 5.6 mm, 8 mm, 11.2 mm, 11.6 mm, 16 mm, 22.4 mm, 21.5 mm, 45 mm, 63 mm, 125 mm. In the simulations of 2023 (v0 model), 22 fractions were used, corresponding to the 22 sieve mesh sizes. In order to describe the sieve curves reasonably well, including the bimodal character in Boven-Rijn and Waal, at least approximately 10 fractions are expected to be needed. Since the final goal is to create one model of all upper Rhine branches, including a part of the German Niederrhein, together, all separate branch models should use the same fractions.

For model simplification and computation size reduction, in the v0.5 model version the data was combined into 11 fractions as follows (see also Table 5.2):

- The sediment diameters below 63 μm (clay and silt) are hardly present in the sediment samples of all branches and are not considered in the model. The smallest sediment fraction used in the model is very fine sand.
- The fifth sieve is the smallest that contains significant amounts of sediment on all branches. Therefore, sieves 2 to 5 are summarized in one fraction in the model. The (very small) amount of mud found in the samples is added to this fraction to make all fractions add up to a total of 100%.
- From the following sieves, each two are summarized in one fraction, apart from sieves 12 and 13, which are important for the sand-gravel transition and the bimodal sieve curves on Boven-Rijn and Waal, and sieve 22, which is present in important quantities on the Boven-Rijn.

Figure 5.2 shows that with this distribution, the general characteristics of the sediment mixture, expressed in percentiles D_{10} , D_{50} and D_{90} as well as the geometric mean D_g , are kept approximately the same as when using the information of all sieves, i.e. 22 fractions.

Table 5.2 Sediment fractions included in the first model schematization (v0).

Sieve	Minimum diameter [m]	Maximum diameter [m]	Fraction
Sieve01	0.000008	0.000063	Not considered
Sieve02	0.000063	0.000090	Fraction01
Sieve03	0.000090	0.000125	
Sieve04	0.000125	0.000180	
Sieve05	0.000180	0.000250	
Sieve06	0.000250	0.000355	Fraction02
Sieve07	0.000355	0.000500	
Sieve08	0.000500	0.000710	Fraction03
Sieve09	0.000710	0.001000	
Sieve10	0.001000	0.001400	Fraction04
Sieve11	0.001400	0.002000	
Sieve12	0.002000	0.002800	Fraction05
Sieve13	0.002800	0.004000	Fraction06
Sieve14	0.004000	0.005600	Fraction07
Sieve15	0.005600	0.008000	
Sieve16	0.008000	0.011200	Fraction08
Sieve17	0.011200	0.016000	
Sieve18	0.016000	0.022400	Fraction09
Sieve19	0.022400	0.031500	
Sieve20	0.031500	0.045000	Fraction10
Sieve21	0.045000	0.063000	
Sieve22	0.063000	0.125000	Fraction11

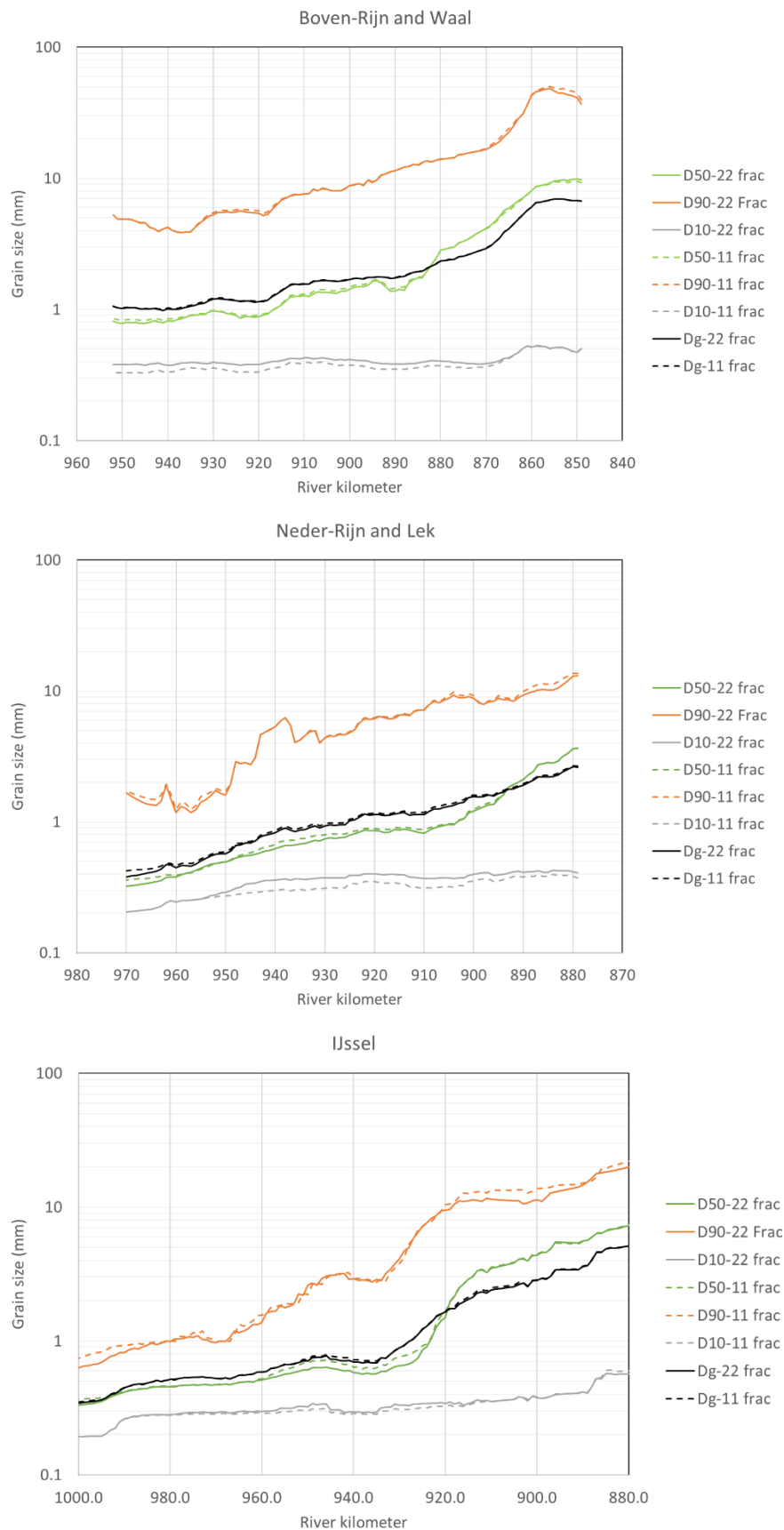


Figure 5.2 Characteristic diameters of the initial sediment composition for all Rhine branches (campaign of 2020).

5.3 Sediment transport formula

Based on the offline calibration presented in Chapter 6, the sediment transport relation of Meyer-Peter-Müller was selected for all fractions:

$$S_{MPM,i} = aD_i\sqrt{\Delta g D_i}(\mu\theta_i - \xi_i\theta_c)^b$$

$$\theta = \left(\frac{u}{C}\right)^2 \frac{1}{\Delta D_i}$$

with u the flow velocity magnitude [m/s], C the Chézy friction coefficient [$m^{1/2}/s$], Δ_i the relative density of the sediment fraction considered [-], D_i the characteristic grain size of the sediment fraction considered [m], μ the ripple factor, θ_c the critical Shields parameter, ξ_i the hiding and exposure factor for the sediment fraction considered, and a and b calibration parameters. Based on the offline calibration, we use the parameter set derived by Wong & Parker (2006), but with a lower calibration parameter a :

Parameter Sediment transport formula	Value
a	2
b	1.6
θ_c	0.047

For the effect of hiding and exposure, we use the power law (Parker, Klingeman & McLean or Soehngen, Kellerman & Loy):

$$\xi = \left(\frac{D_i}{D_m}\right)^\alpha$$

With D_m the arithmetic mean grain size [m]. For the calibration parameter α , we use the default:

Parameter Hiding/exposure	Value
α	-0.8

For the ripple factor μ , we use a constant value:

Parameter Ripple factor	Value
μ	1.0

5.4 Fixed layers, constructions and morphologically active area

5.4.1 Fixed layer roughness

In preliminary model simulations (without dredging and dumping), we observe large bed level changes in the inner bend next to fixed layers, as well as directly downstream of fixed layers. Figure 5.3 shows the modelled bed level after 2 years around the fixed layer of Nijmegen minus the original, unfiltered bed level from Baseline in a j99 simulation. Sediment transport is modelled with the parameter settings as mentioned in Section 5.3. We see significant lowering of the bed directly downstream of the fixed layer and at the upstream end of the inner bend, as well as deposition at the downstream end of the inner bend and upstream of the fixed layer. Over time, the patterns in the inner bend will grow further and propagate in downstream direction.

Keeping in mind that these changes are relative to the unfiltered bed level from Baseline, which already includes features such as the erosion pit downstream of the fixed layer, these patterns are artifacts that do not correspond to measurements.

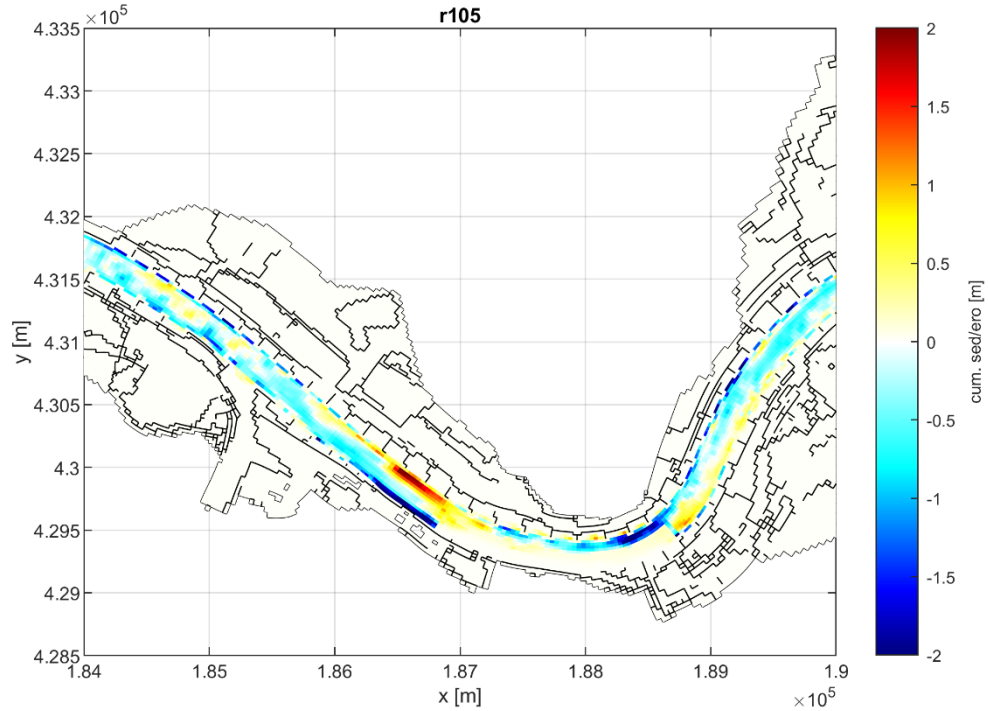


Figure 5.3 Difference between modelled bed level after 2 years (using the filtered initial bed level, see Becker et al., 2023) and the original, unfiltered bed level from Baseline around the fixed layer of Nijmegen in the j99 schematization.

The bed development around fixed layers is influenced by the discharge distribution over the fixed layer and the alluvial inner bend, which in turn depends on the channel geometry and the roughness ratio between fixed layer and inner bend. The uncertainty of the channel geometry as represented in the model is small compared to the uncertainty in the roughness ratio. The sensitivity of the morphological patterns around fixed layers to changes in the roughness ratio (in terms of Chézy coefficients) was therefore investigated by varying the fixed layer roughness.

In the morphological model, the roughness of the fixed layers in the Waal (at Erlecom, Nijmegen and Sint Andries) is defined by a constant White-Colebrook/Nikuradse value, following the hydrodynamic model (Kosters et al., 2022). These values were suggested by Sieben (2014). However, for the alluvial roughness of the main channel constant Chézy values are used (Becker et al., 2023). This means the Chézy roughness ratio between fixed layer and inner bend depends on the flow conditions. To avoid this dependency, the Nikuradse values for the fixed layers were first converted to Chézy coefficients, such that the Chézy roughness ratio is fixed. The original Nikuradse values are shown in the second column of Table 5.3. For the different discharge levels contained in the standard hydrograph (see Becker et al., 2023), these Nikuradse values result in Chézy values ranging from 34 to 42 $\text{m}^{1/2}\text{s}^{-1}$ for Erlecom and Nijmegen, and from 38 to 46 $\text{m}^{1/2}\text{s}^{-1}$ for St. Andries. Using the median of these values, the Chézy coefficient for Erlecom and Nijmegen was set at 38, while for St. Andries a value of 42 $\text{m}^{1/2}\text{s}^{-1}$ was used (see the third column of Table 5.3). With these roughness definitions, two years were simulated. Subsequently, the Chézy coefficients were increased to 42 for Erlecom/Nijmegen and 46 for St. Andries (fourth column of Table 5.3), resulting in smoother fixed layers, and the same 2 years were simulated again.

The resulting bed level changes (relative to the unfiltered bed level from Baseline) are shown in Figure 5.4 for both cases.

From the results, we can conclude that the bed level changes in the inner bend next to fixed layers can indeed be influenced by the roughness ratio between fixed layer and inner bend. Bed level differences between the two simulations are more than 1 m locally. However, although the erosion/deposition patterns in the inner bends are reduced somewhat when the fixed layer roughness is reduced, they remain present. Moreover, the erosion directly downstream of the fixed layers is hardly affected by the roughness changes. This suggests that the unrealistic erosion/deposition patterns are not (only) caused by a possibly inaccurate representation of the bed roughness, but (also) by limitations in the current modelling of sediment transport over fixed layers.

Firstly, in the model the fixed layer does not contain any sediment initially, while in reality some sediment is present here. In the model, sediment transport is reduced when the available sediment thickness drops below a user-defined threshold, 0.7 m in the current morphological simulations. This means hardly any sediment is transported across the fixed layer, while in reality some sediment will be transported onto the fixed layer and further downstream or towards the inner bend due to secondary flow.

Secondly, all sediment transport is represented as bed load in the model, while in reality part of the transport takes place in suspension. Hence, in reality part of the sediment may be transported across the fixed layer in suspension, after which it may deposit further downstream as the depth increases. Because this process is not included in the model, sediment transport across the fixed layers is limited further.

Because of these shortcomings, it is not meaningful to calibrate the fixed layer roughness based on observed and modelled patterns of bed level change. Such a calibration should rather be based on the velocity distribution over the cross-section, measured at the location of the fixed layers. Because this kind of measurements is currently not available², the roughness distribution remains highly uncertain. For version v0.5 of the model, it was therefore decided not to make changes in the fixed layer roughness as used in the original, hydrodynamic model. This means the Nikuradse values as reported in Table 5.3 will be used in the morphological model v0.5 until further information becomes available.

In general, current model results cannot be used to assess morphological development directly around the fixed layers (e.g. regarding the erosion and deposition patterns next to and directly downstream of the fixed layer). If more insight into the morphological effects of fixed layers is desired, changing the implementation of fixed layers within the model can be considered, see for example Chavarrías et al. (2022).

² In the period between draft and final version of this report, these measurements have been carried out and results have been made available. This information will be processed next year for the development towards v1.0 of the model.

Table 5.3 Fixed layer roughness. The second column includes the Nikuradse roughness heights as used in the morphological model. The third column shows the Chézy coefficients used in the reference simulation. The fourth column shows the Chézy coefficients used to assess the effect of changes in the fixed layer roughness compared to the reference simulation.

Fixed layer location	Nikuradse roughness height [m]	Chézy coefficient [$m^{1/2}s^{-1}$] (reference – r108)	Chézy coefficient [$m^{1/2}s^{-1}$] (variation – r109)
Erlecom	0.68	38	42
Nijmegen	0.63	38	42
St. Andries	0.34	42	46

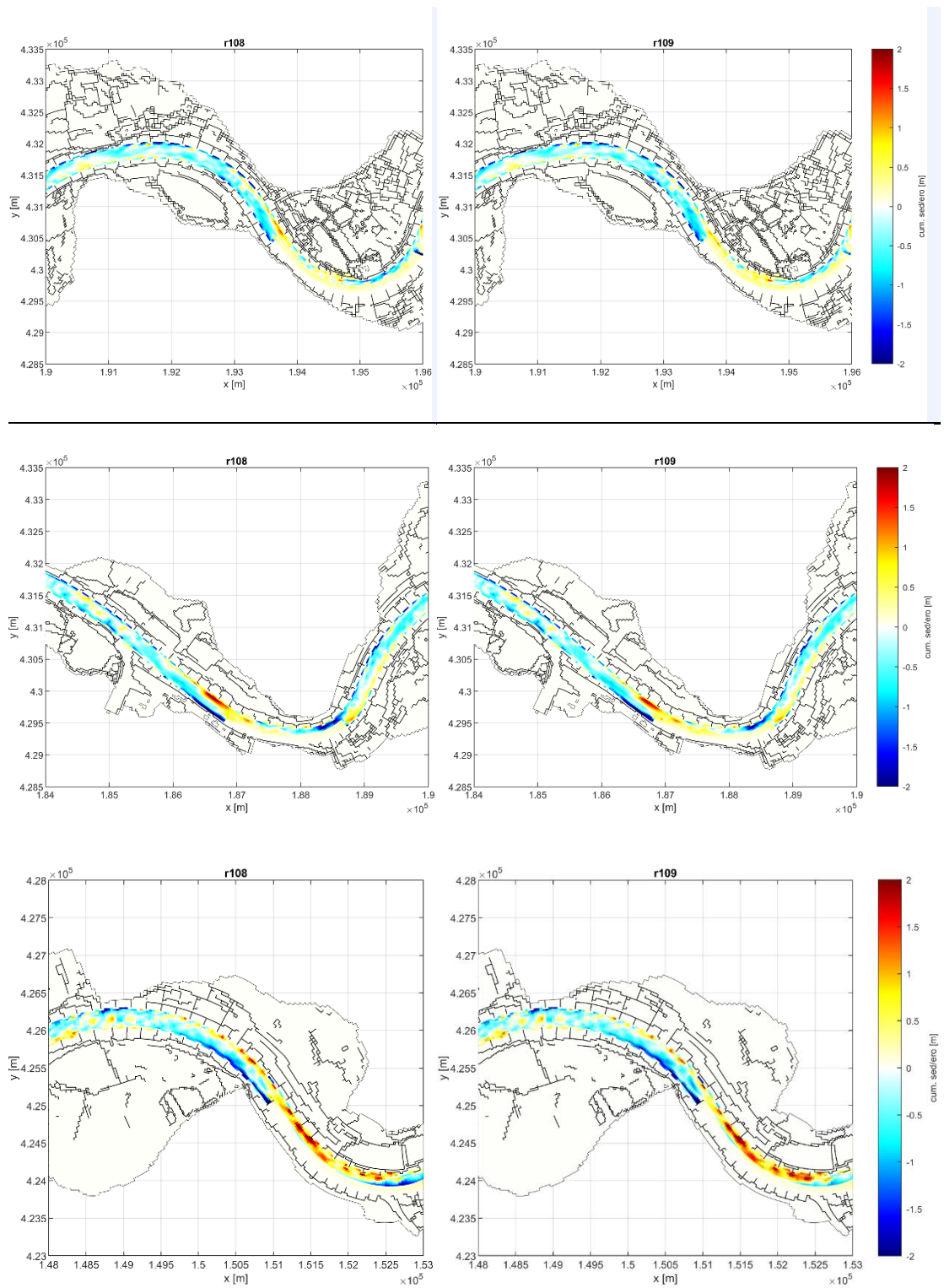


Figure 5.4 Difference between modelled bed level after 2 years (using the filtered initial bed level, see Becker et al., 2023) and the original, unfiltered bed level from Baseline around the fixed layer of Erlecom (top panel), Nijmegen (middle panel) and St. Andries (bottom panel) in the j99 schematization. The figures on the left show the results for the reference case (fixed layer roughness according to the third column in Table 5.3), the figures on the right show the results for the case with smoother fixed layers (fourth column in Table 5.3).

5.5 Upstream boundary condition (morphology)

In 2023 (model version v0), two boundary condition types were tested for morphology. The first type, for which a sediment influx is prescribed per fraction, led to unrealistic bed level changes within the first 400 m of the model domain. With the second type (a prescribed rate of bed level change), the sediment influx was too high and modelled changes in sediment composition were unrealistic (Becker et al., 2023).

To improve the upstream boundary condition for morphology, further testing with the second boundary condition type was done in 2024. The first type was not investigated further because the sediment influx per fraction cannot be derived from data, whereas a rate of bed level change (type 2) can be derived by trend analysis on bed level measurements.

To avoid unrealistic composition changes, a prescribed rate of bed level change was combined with fixing the bed composition at the boundary (ICmpBnd = 1). Furthermore, the keyword MorphoPol was used to make sure the prescribed rate of bed level change (-1.4 cm/y for the Waal) is only applied within the main channel (for which the trend was derived). With MorphoPol, a polygon can be defined in which the bed level is not updated (or vice versa, i.e. the bed level is only updated within the polygon). In this case, the polygon covers the first row of cells outside the morphologically active area³ (see Figure 5.5).

Results with this boundary type are reported in Section 7.2.



Figure 5.5 Boundary cells excluded from bed level updating (orange dots).

In general, the upstream boundary should be located at such a distance from the domain of interest that perturbations originating from the upstream boundary condition do not reach the domain of interest within the timespan of the simulation.

³ Using MorphoPol in this way requires setting the flag cstbnd to 1 when MaximumWaterdepth is true. MaximumWaterdepth = true means that the locally maximum water depth is used to compute the characteristic velocity for sediment transport at the cell center. Cstbnd = 1 means that advection terms containing gradients perpendicular to the boundary are switched off. By default, cstbnd is 0. Setting it to 1 has a small effect on the hydrodynamics at the upstream boundary, but this was deemed acceptable.

According to Sieben et al. (2005), perturbations migrate downstream with a speed of approximately 1 km/y on the Dutch Rhine branches. Hence, for a 20-year simulation (morphological time), the upstream boundary should be located at least 20 km away from the domain of interest. This means that if the morphological development of the Boven-Waal needs to be assessed over a period of 20 years, the Boven-Rijn should be included in the model domain. Furthermore, the development of the Boven-Waal influences the discharge distribution at the Pannerdensche Kop. This influence should be accounted for as well, for example by including (part of) the Pannerdens Kanaal in the model domain.

5.6 Dredging and dumping

The dredging and dumping routine as used in the DVR model (see the description by Becker, 2024) was modified according to the information on fairway maintenance and sediment extraction described in Section 3.1. In the following sections, the modifications are explained one by one. The dredging and dumping routine was developed in preparation for v1.0 of the model. The validation of the dredging and dumping volumes will be carried out as part of the 2D calibration. The final settings of the dredging and dumping routine will only be chosen after this validation.

The dredging and dumping rules as used in practice are now represented in the model in a relatively high amount of detail, compared to other model input such as initial composition of the bed, sediment transport relation, bed roughness, hydrograph, etc. Due to the high level of schematization of the sediment transport processes within the model, dredging and dumping volumes obtained from the model are highly uncertain. Hence, this uncertainty cannot be reduced by increasing the complexity of the dredging and dumping routine.

5.6.1 Updating of the reference plane

In reality, the OLR (Overeengekomen Lage Rivierwaterstand)/OLW (Overeengekomen Lage Waterstand) are updated every 10 years (see Section 3.1). Implementing the same frequency of updating in the model may lead to sudden changes in dredging/dumping volumes that do not occur in reality. For now, it was therefore decided to not update the reference plane within the duration of the simulations (10 years). The choice for reference plane update frequency will be discussed in preparation of v1.0 of the model.

5.6.2 Required water depth below OLR/OLW

In the DVR model, the required water depth was defined as a constant for each branch (2.80 m at Boven-Rijn, Waal, Pannerdensch Kanaal and Neder-Rijn/Lek, 4.50 m at the Boven-Merwede, 2.50 m at the IJssel). However, in the RBK (Rivierkundig Beoordelingskader), which describes the rules and procedures Rijkswaterstaat uses to grant or refuse permits within the river system, the required depth below OLR/OLW changes gradually along the branches (Van Doorn, 2023). These values were implemented in the new model. For the Boven-Merwede, the 'ingrijpdiepte' (intervention depth) as included in the RBK was used, because this is the minimum depth that should be maintained at all times. For the other branches, the RBK mentions only one type of value ('minimale waterdiepte onder OLR'). The 2.80 m for Boven-Rijn, Waal, Pannerdensch Kanaal and Neder-Rijn/Lek are valid since November 2006. So for the calibration (period: 1999-2012) it is probably better to use the previous requirement of 2.50 m. At this moment, the values apply to both dredging and sand mining. The resulting dredging and sand mining volumes can then be used to validate the model. Another approach is to force the volumes as model input (i.e. without depth restrictions). The approach will be further refined for v1.0.

5.6.3 Clearance

For practical reasons, the contractor is allowed to dredge up to 0.50 m below the reference plane. In the DVR model, this entire margin (referred to as 'clearance' in the software⁴) is dredged at the moment dredging is triggered. In reality, the contractor is most likely to dredge less to avoid exceeding the clearance. To better approximate this behaviour, the clearance was changed from 0.50 m to 0.30 m in the model.

For the Boven-Merwede, a separate clearance of 0.75 m is implemented. This is because next to the intervention depth, a maintenance depth ('onderhoudsdiepte') is defined for this branch in the RBK. The maintenance depth is 0.45 m larger than the intervention depth. Whenever the intervention depth is reached, dredging occurs at least up to the maintenance depth. On top of this, an additional clearance is defined for practical reasons. Assuming a clearance of 0.30 m (as for the other branches), a total of $0.45+0.30=0.75$ m is dredged below the intervention depth.

The approach will be further refined for v1.0.

5.6.4 Dredging at OLR

In the DVR model, dredging is switched on at discharge levels 1.203, 1.635 and 2.250 m³/s at Lobith. At higher discharges dredging is switched off. This makes sense because at higher discharges navigation is no longer hampered by limited water depths, which means there is less need for dredging. However, also at the lowest discharge within the hydrograph, 1.020 m³/s, dredging is switched off. This was done because this discharge level represents a prolonged period of low discharges that usually occurs in the summer months, in which morphological changes are minimal and very little dredging is needed. For the new model, it was decided to switch on dredging and dumping for this discharge level to be in accordance with reality. This change is however not expected to significantly influence results on time scales of years and longer.

5.6.5 Depth after dumping

After dumping, the bed level at that location should not be above the reference plane. In the DVR model additional, more stringent dumping requirements are used: the depth below OLR should be at least 4 m (instead of 2.80) on all branches except the Boven-Merwede (at least 5 m depth instead of 4.50) and IJssel (at least 3.50 m depth instead of 2.50). These requirements were implemented following earlier versions of the RBK (up to version 3.0), in which next to the minimally required depth also an average fairway depth was defined. With the dumping requirements, the resulting average depth was expected to better approximate the values defined in the RBK. However, since RBK version 4.0 (January 2017) average depth requirements are no longer mentioned.

For the new model, it was decided to define the dump depth as the required water depth below OLR (see Section 5.6.2) plus 50 cm. In this way, the dump depth varies gradually along the branches and is always larger than the dredge depth.

5.6.6 Dump locations

In principle, dumping is allowed within a radius of 1.5 km around the location where the material was removed. At some locations this distance is extended to 5 km. In these cases, sediment is dumped preferably upstream of the location where it was removed. In the DVR model, dredging/dumping polygons have a length of 1 km.

⁴ Note that here, clearance is not the same as the 'under keel clearance' (NL: kielspel) used for shipping.

Dumping locations are prioritized as follows:

- 1 Within the dredging polygon
- 2 First polygon downstream of the dredging polygon
- 3 Second polygon downstream of the dredging polygon
- 4 First polygon upstream of the dredging polygon

When dumping is not possible at any of these locations due to depth requirements, sediment is relocated to a polygon outside the active model domain, which means it is effectively removed from the system. To decrease the probability that this occurs, the number of locations eligible for dumping was increased in the new model. Furthermore, the dumping priority was modified to account for the preference of dumping upstream of the dredging location. These modifications lead to the following priority:

- 1 Within the dredging polygon
- 2 First polygon upstream
- 3 Second polygon upstream
- 4 Third polygon upstream
- 5 First polygon downstream
- 6 Second polygon downstream

In the DVR model, dumping is not allowed in the polygons just upstream or downstream of bifurcations. This additional requirement was based on the memo *Sedimentbeheer Rijntakken 2010-2015* (Tönis, 2010), in which the following rule is included: 'Dredged sediment should not be dumped back into the river close to a bifurcation, because of the negative impact on the distribution of water and sediment discharge.' However, in the rules defined by Treurniet and Tönis (2019), which replace the memo by Tönis (2010), this requirement is no longer included. It was therefore decided to remove it from the new model settings.

5.6.7 Sequence of dredging and dumping

In the DVR model, if dredging is triggered simultaneously at multiple locations within a polygon, the highest sediment deposits (with respect to NAP) are removed first. This is important when dredging or sand mining is limited by capacity. In the DVR model, a capacity limitation is only imposed for sand mining, and this only plays a role when sand mining volumes based on the depth requirements (see Section 5.6.2) are larger than the defined capacity.

In the new model, dredging/sand mining is prioritized based on the height with respect to the dredging reference plane instead of with respect to NAP. This means that not the highest deposits (which are on average located more towards the upstream end of the polygon) are dredged first, but those points that exceed the dredging reference plane the most. This is a more logical choice, but since it can only influence results when sand mining is actually limited by the defined capacity, the effect of this change is expected to be minor.

Similarly, for dumping, sediment is deposited at the deepest locations (i.e. with respect to the reference plane) first instead of at the lowest locations (i.e. with respect to NAP). As this only affects the distribution of sediment within dumping polygons, also this change is not expected to have a large influence.

Finally, the new model uses the keyword `TriggerAll = 1` to indicate that if one cell within a dredging polygon exceeds the dredging reference plane, all cells within that polygon are dredged up to the defined clearance.

This is expected to be in accordance with current practice, in which (for practical reasons) usually larger areas are dredged if the reference plane is exceeded within that area. Previously, dredging was triggered based on the average bed level within a polygon. However, a similar option has not been implemented in the dredging and dumping routine of D-HYDRO. This difference is expected to have some effect on sand mining, dredging and dumping volumes, but it will only have a minor influence on long-term bed level development.

The approach will be further refined for v1.0.

5.6.8 Sand mining

As explained in the previous sections, sediment extraction is in principle implemented in the same way as dredging, with the important difference that dredged sediment is not deposited back into the system. Another important difference is that for each sand mining polygon, a maximum sand mining capacity (in m^3 per morphological year) is imposed. This maximum capacity originates from the reported concessions, in this case $90.000 \text{ m}^3/\text{y}$ for the Beneden-Waal and $300.000 \text{ m}^3/\text{y}$ for the Boven-Merwede (see Section 3.1.2). The total yearly volume for each branch is divided among the sand mining polygons based on their area. The imposed numbers compensate for the fact that the dredging and dumping routine is not active during part of the discharge steps, so the maximum capacity imposed is higher than it would be if based on a full year. During the simulation, this maximum volume per year is translated to a maximum volume for each timestep. Hence, for an entire simulation, the maximum capacity is only reached when sand mining is never limited by sediment availability.

The approach will be further refined for v1.0.

5.6.9 Dune height computation

At this stage, the dredging and dumping routine as implemented in the new model does not take into account the presence of dunes when checking if the bed level exceeds the threshold for dredging to be triggered. It is possible to account for dunes by specifying the fraction of the dune height that should be added to the bed level before checking if the dredging threshold is exceeded. For this, the computation of dune heights should be switched on.

The functionality to compute dune heights was implemented by Van Vuren & Ottevanger (2006). They have also tested the implementation, but only for sediment of uniform size (specified by one fraction). As the current model uses multiple sediment fractions, we first investigated if the dune height computation gives plausible results in this case. The results of this analysis (see the separate memo by Chavarrías, 2024) indicate that the implemented functionality to compute dune heights can be used for mixed-size sediment as well. However, further testing and calibration of the input parameters is necessary to better approximate measured dune heights.

Subsequently, it should be determined which fraction of the dune height (defined as the difference between crest and trough) should be added to the bed level as used in the dredging and dumping routine to determine if dredging is triggered. The modelled bed level can be interpreted as the mean bed level averaged over several dunes (Ribberink, 1987). Assuming that dredging takes place on the scale of typical dune lengths in the Rhine branches (indicated in the model by the size of the dredging polygons), and that dredging of an area (i.e. a polygon within the model) occurs if the threshold is exceeded at one location within that area (typically the location of the dune crest), it would be logical to add 50% of the dune height to the bed level to determine if dredging should be triggered within a dredging polygon.

Furthermore, within SMT the dune height computed at the end of one discharge step should be used as initial condition for the following step.

The approach will be further refined for v1.0. Note that the dune height computation does not directly influence the roughness values currently used in the model, nor the sediment transport computed by the model.

6 Offline calibration

6.1 Methodology

Within the offline calibration, sediment transport is calculated based on hydrodynamic model simulations. This means that the computed sediment transports are not translated into bed level changes in the model, which in turn would influence hydrodynamics. Because this feedback mechanism is not included, we call this an offline calibration. The objective is to compute the expected sediment transport of an average year for varying sediment transport relations and parameters in order to be able to select suitable values for the start of the 1D calibration. To do so, the calculated sediment transport is compared to the estimates by Frings et al. (2019) and Sloff (2019) (“trend Pmap 20 yr”).⁵

For the offline calibration, use was made of the bed level schematization from Baseline without further modification, so bed level specified in corners and no averaging procedure. Given the uncertainty in sediment transport, the limited differences in water depth and velocity due to these adjustments are not expected to have any significant impact on the conclusions regarding yearly sediment transport rates.

The basis of the offline calibration is formed by the steady-state hydrodynamic results for nine different discharge levels as described in Becker et al. (2023). The final state of each hydrodynamic simulation (i.e., the steady-state for each discharge) is used to construct a schematized hydrograph. This step was carried out before the discharge hydrographs for calibration and validation were constructed (see section 4.3) and thus still used the hydrograph of the old DVR model.

As in the offline calibration there is no coupling between hydrodynamics and bed level changes, the order in which discharge levels occur does not influence the results. We can therefore simply take the total duration of each discharge level within the standard hydrograph, without dividing this duration over different periods through the year.

The hydrodynamic output is combined with morphodynamic input regarding the characteristic sediment sizes and the bed composition, defined as the available sediment volume per fraction in each grid cell. For the offline calibration, the rolling mean interpolation of the data from the 2020 measurement campaign was used (see Becker et al., 2023) in combination with 11 sediment fractions (Section 5.2).

For each flow field (i.e., for each discharge level), the sediment transport rate is computed given the morphodynamic input. The yearly sediment transport is obtained by multiplying each sediment transport rate by the duration of each discharge level.

The offline calibration of the Waal consisted of comparing the sediment transport results for variations of the parameters a , θ_c and b of the Meyer-Peter & Müller formula. Table 6.1 shows the parameters tested in the offline calibration.

⁵ Sloff (2019) derived sediment transport rates from the km- and width-averaged bed level changes of De Jong & Ottevanger (2020). De Jong & Ottevanger (2020) derived a trend in bed level change per river kilometer section based on all available multibeam measurements between 1999 to 2018. They first made a linear fit through all data per 1x1m raster cell, and then averaged the trend within each river kilometer section. In the end, they did not use the Pmap data (in which data gaps are filled with data from the previous year) but only the available data per year. So the name “Pmap trend” is a bit misleading.

The reasoning behind the choice of the MPM transport formula is included in Section 6.2 of the report for the morphological model of the IJssel (Castañon et al., 2024) and is mostly based on earlier experience with morphological modelling of the Rhine branches. In these tests, a ripple factor of $\mu = 1$ was used, and hiding & exposure was computed following the relation of Egiazaroff (see Table 6.2 in Castañon et al., 2024).

Table 6.1 Parameter list used in the offline calibration tests. *Reference MPM_a_8 in figures.

Abbreviation	Sediment transport formula	Parameters	Source
Sensitivity test	Meyer-Peter-Müller (all fractions)	a = [2, 4, 6] b = [1.1, 1.3, 1.7] θ_c = [0.015, 0.035, 0.055]	-
		a = 4.93 b = 1.6 θ_c = 0.047	Wong & Parker (2006)
		a = 8 b = 1.5 θ_c = 0.047	Meyer-Peter & Müller (1948)*
Final test	Meyer-Peter-Müller (all fractions)	a = 2 b = 1.6 θ_c = 0.047	-

6.2 Results

6.2.1 Offline sediment transport

Figure 6.1 to Figure 6.3 show the total (so including both sand and gravel) yearly sediment transport for all parameter variations. Comparing the parameter variations to the default MPM case the following conclusions can be drawn:

- Looking at the case in which all parameters are fixed except for the calibration parameter (a) (Figure 6.1), we see that sediment transport increases significantly by varying the parameter from 2 to 8 (default). The order of magnitude using a calibration parameter of 2 is the closest to the sediment transport estimates by Frings et al. (2019);
- Sediment transport is sensitive to small variations in parameter b, the exponent (Figure 6.2). The higher the parameter value, the smaller the sediment transport. This is because on average, the difference between actual and critical shear stress is smaller than 1.0 on the Waal.
- Downstream of rkm 930, sediment transport becomes less sensitive to variations of the critical Shields parameter θ_c (c in the legend) (Figure 6.3). Increasing θ_c by 0.02 decreases sediment transport by less than 250.000 m³/year. On the upper part of the Waal, the critical shear stress significantly influences the yearly sediment transport. This is because the sediment here is more graded, and the critical shear stress determines which fractions are mobile. For the same reason, the critical shear stress also influences the transport gradient on the upstream part of the Waal.
- Default parameters for MPM (light grey solid line) strongly overestimate the yearly sediment transport (Figure 6.1).
- Adopting the parameters suggested by Wong and Parker (2006) provides a better estimate of the sediment transport than the default parameters for MPM, because the calibration parameter is lower (4.93 instead of 8) and the exponent is higher (1.6 instead of 1.5).
- Changes in the calibration parameter (a) and the exponent (b) also affect the gradients upstream and downstream. The smaller (a)/higher (b) the parameter, the smaller the gradients.

- With all parameter sets, gradients in transport are overestimated compared to the Pmap analysis (Sloff, 2019).

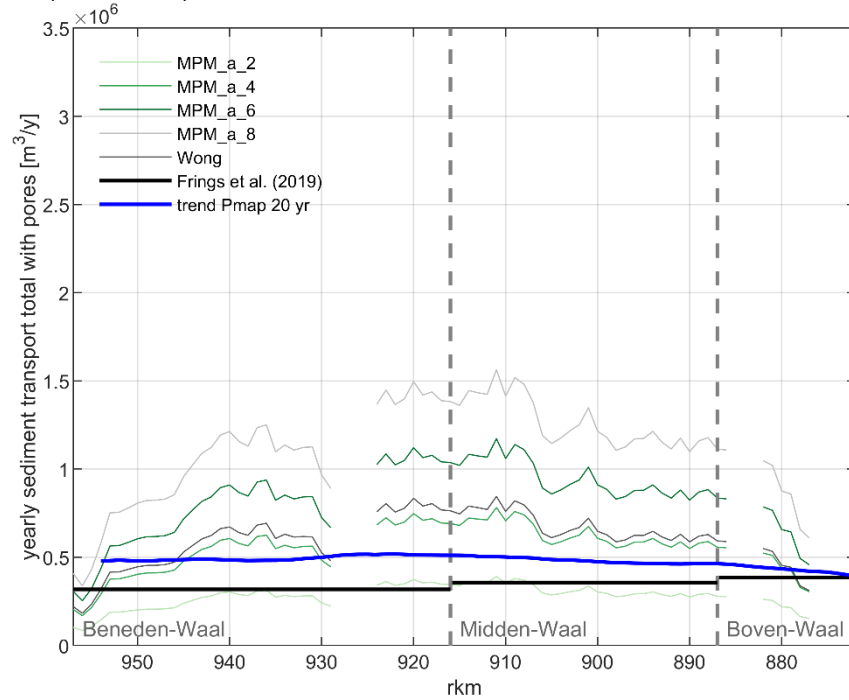


Figure 6.1 Yearly total sediment transport with pores, changing parameters a (green solid lines) compared to MPM_a_8 default setting (light grey), Wong et al. (2009) (grey), and sediment transport estimates from Frings et al. (2019) and Pmap (20 years). Computed transports at the locations of fixed layers are not shown because averaging over the main channel width (half alluvial, half fixed) yields unrealistic values in these cases.

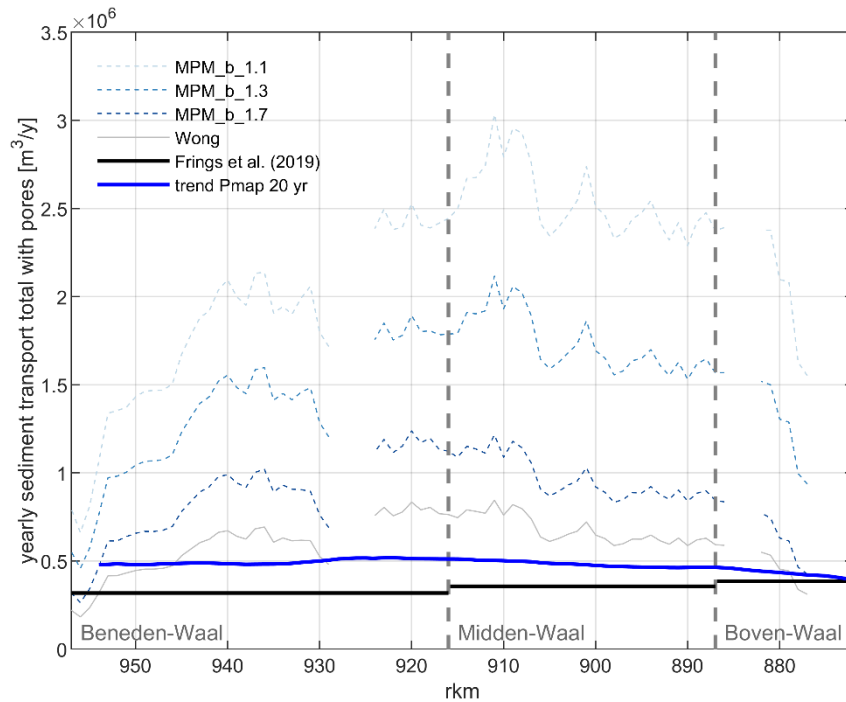


Figure 6.2 Yearly total sediment transport with pores changing parameter b (blue dashed lines), Wong et al. (2009) (grey) and sediment transport estimates from Frings et al. (2019) and Pmap (20 years). Computed transports at the locations of fixed layers are not shown because averaging over the main channel width (half alluvial, half fixed) yields unrealistic values in these cases.

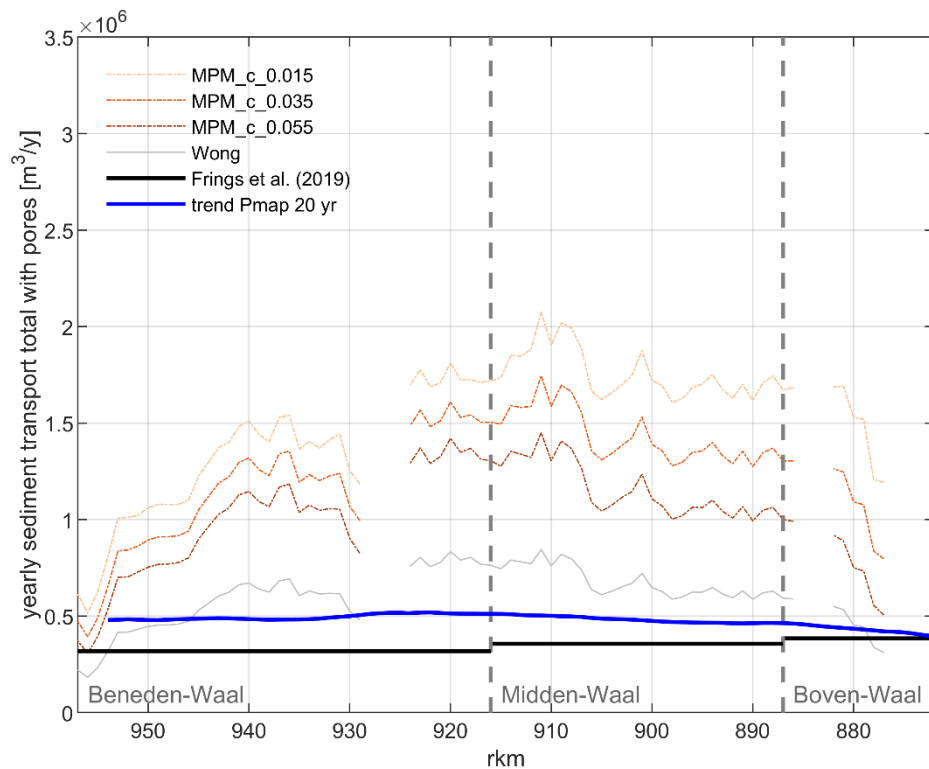


Figure 6.3 Yearly total sediment transport with pores changing parameter c (orange dashed-dotted lines) compared to Wong et al. (2009) (grey) and sediment transport estimates from Frings et al. (2019) and Pmap (20 years). Computed transports at the locations of fixed layers are not shown because averaging over the main channel width (half alluvial, half fixed) yields unrealistic values in these cases.

Similar conclusions are drawn when analyzing the offline sediment transport results for gravel and sand separately (Figure 6.4 to Figure 6.9). Plotting gravel and sand separately shows that the fractions respond differently to the change in parameters. Gravel transport is more sensitive to changes in b than sand. On the other hand, sand transport is more sensitive to changes in the calibration parameter a .

For calibration of the sediment transport settings, we mainly look at the total transport predicted by the model in comparison to the values resulting from Pmap analysis, because the transport of sand and gravel separately is much more uncertain. It is however still useful to look at the modelled sand and gravel transport, because the ratio between these transports is relevant, especially looking ahead to the coupling with the Boven-Rijn, that is more dominated by gravel.

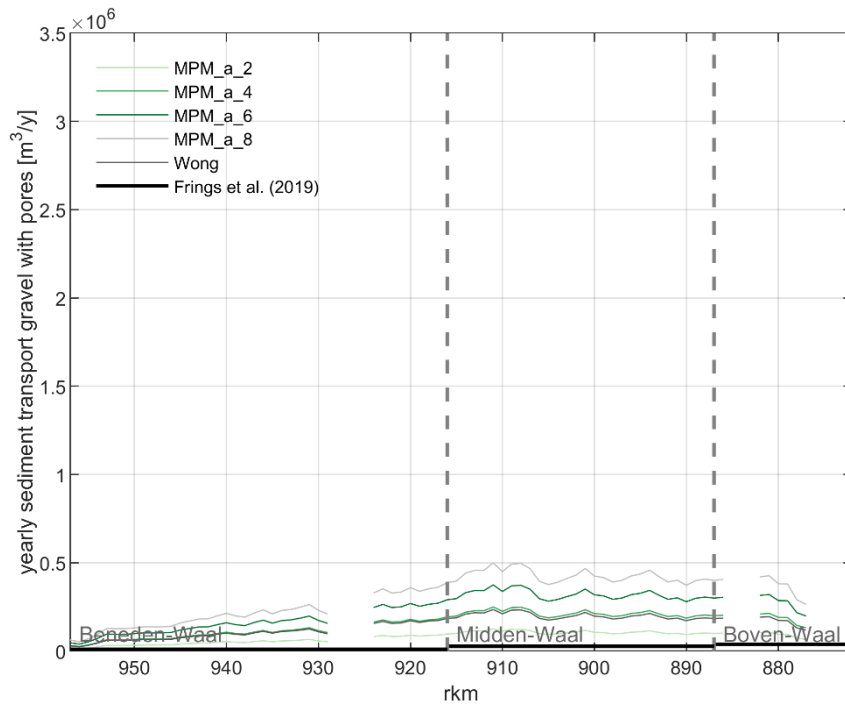


Figure 6.4 Yearly sediment transport for gravel with pores changing parameter a (green solid lines) compared to MPM_a_8 default setting (light grey), Wong et al. (2009) (grey) and sediment transport estimates from Frings et al. (2019). Computed transports at the locations of fixed layers are not shown because averaging over the main channel width (half alluvial, half fixed) yields unrealistic values in these cases.

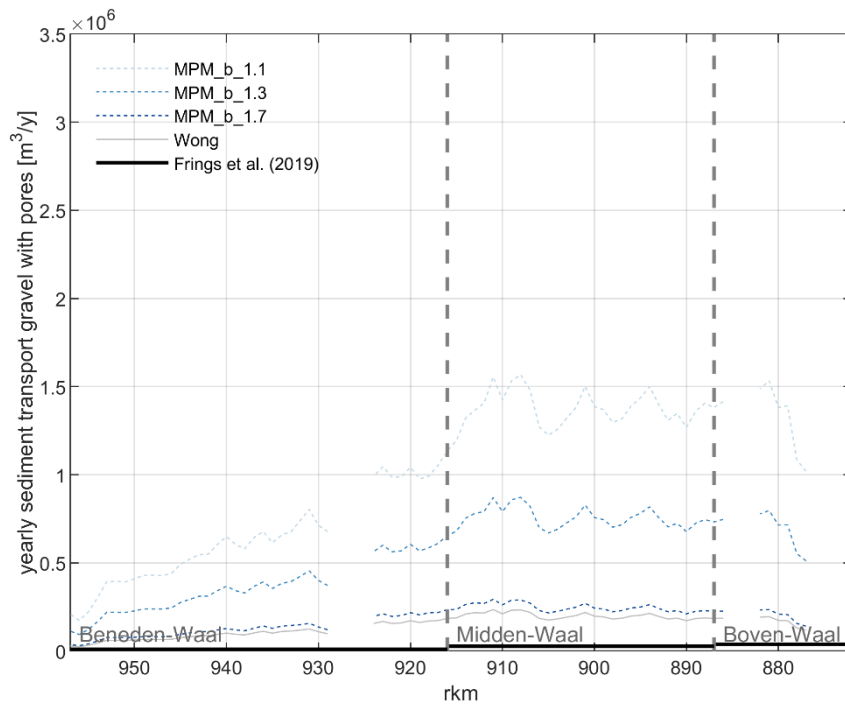


Figure 6.5 Yearly sediment transport for gravel with pores changing parameters b (blue dashed lines) compared to Wong et al. (2009) (grey) and sediment transport estimates from Frings et al. (2019). Computed transports at the locations of fixed layers are not shown because averaging over the main channel width (half alluvial, half fixed) yields unrealistic values in these cases.

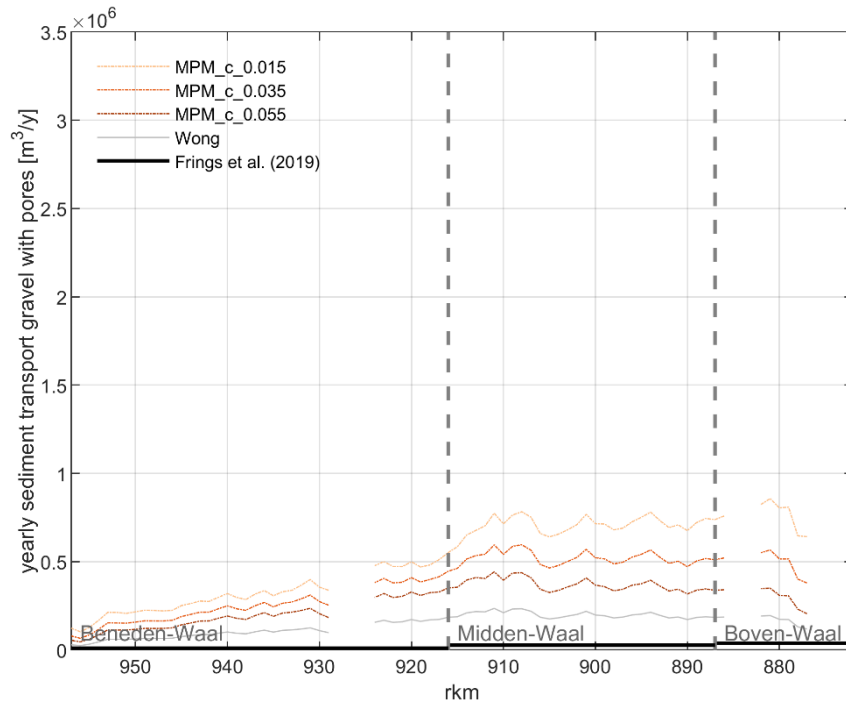


Figure 6.6 Yearly sediment transport for gravel with pores changing parameters c (orange dashed-dotted lines) compared to Wong et al. (2009) (grey) and sediment transport estimates from Frings et al. (2019). Computed transports at the locations of fixed layers are not shown because averaging over the main channel width (half alluvial, half fixed) yields unrealistic values in these cases.

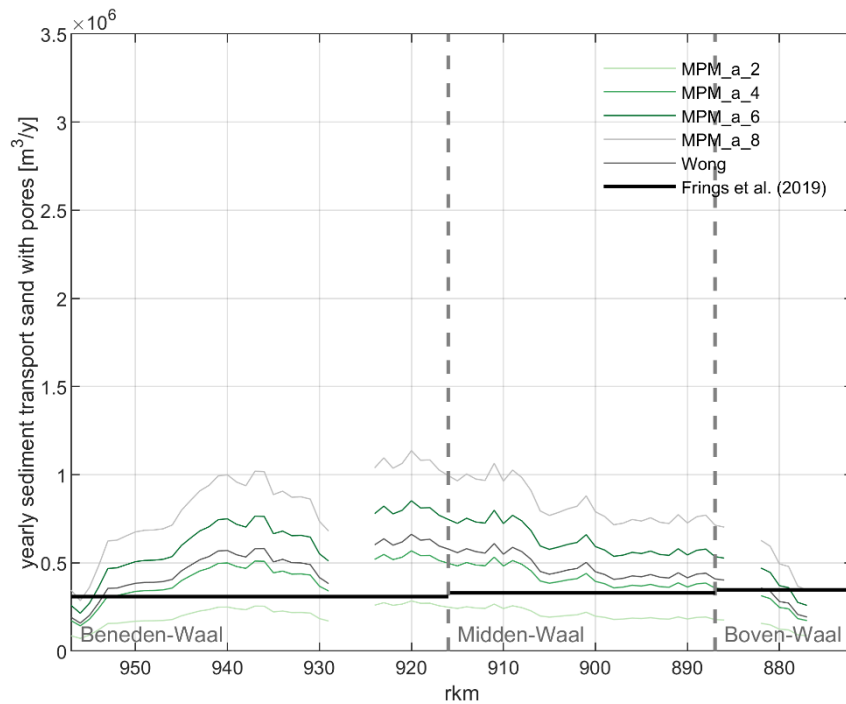


Figure 6.7 Yearly sediment transport for sand with pores changing parameter a (green solid lines) compared to Wong et al. (2009) (grey) and sediment transport estimates from Frings et al. (2019). Computed transports at the locations of fixed layers are not shown because averaging over the main channel width (half alluvial, half fixed) yields unrealistic values in these cases.

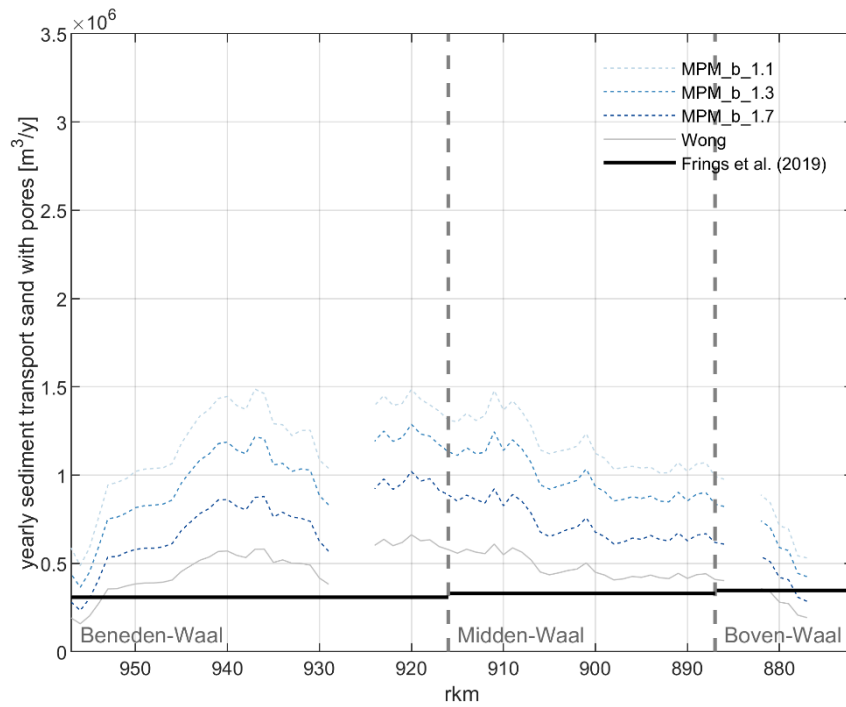


Figure 6.8 Yearly sediment transport for sand with pores changing parameters b (blue dashed lines) Wong et al. (2009) (grey) and sediment transport estimates from Frings et al. (2019). Computed transports at the locations of fixed layers are not shown because averaging over the main channel width (half alluvial, half fixed) yields unrealistic values in these cases.

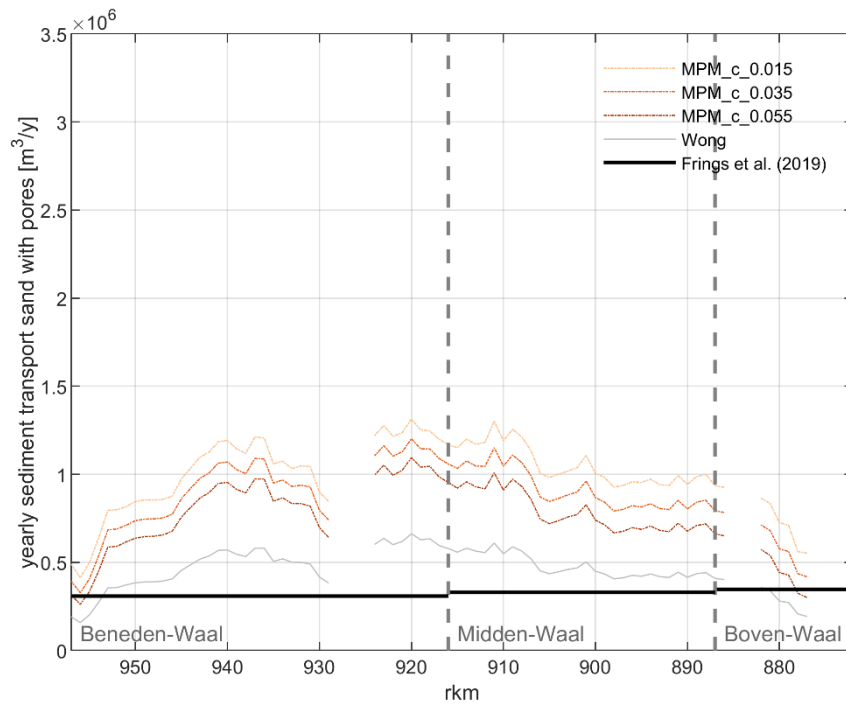


Figure 6.9 Yearly sediment transport for sand with pores changing parameters c (orange dashed-dotted lines) compared to Wong et al. (2009) (grey), DVR settings (black), and sediment transport estimates from Frings et al. (2019). Computed transports at the locations of fixed layers are not shown because averaging over the main channel width (half alluvial, half fixed) yields unrealistic values in these cases.

Hiding and exposure and the ripple factor were also tested. Hiding and exposure formulas 0, 1, 2 and 3 (see Table 6.2) were tested. In 2, the hiding coefficient was fixed to -0.8, no variations were tested.

Table 6.2 Hiding and exposure formulation options (Deltares, 2022). With D_i the characteristic grain size of the sediment fraction considered [m] and D_m the mean grain size of the total sediment mixture [m].

hiding and exposure option	formula
0 = No hiding and exposure	$\xi = 1$
1 = Egiazaroff (1965)	$\xi = \left(\frac{\log_{10} 19}{\log_{10} 19 + \log_{10} D_i/D_m} \right)^2$
2 = Power law (Parker, Klingeman & McLean or Soehngen, Kellerman & Loy)	$\xi = \left(\frac{D_i}{D_m} \right)^\alpha$, with alpha as calibration factor, e.g. -0.8
3 = Ashida-Michiue (1972)	$\xi = 0.8429 \frac{D_i}{D_m}$ if $\frac{D_i}{D_m} < 0.38889$ $\xi =$ as Egiazaroff otherwise

Sediment transport is affected relatively little by changes in the hiding and exposure settings (Figure 6.10), also not upstream in the section with clearly graded sediment in the bed. The ripple factor, on the other hand, has a larger effect on the sediment transport. Decreasing the ripple factor from 1 to 0.4 (using method 1 – constant μ) leads to a decrease of approximately 200.000 m³/year in the Waal (Figure 6.11).

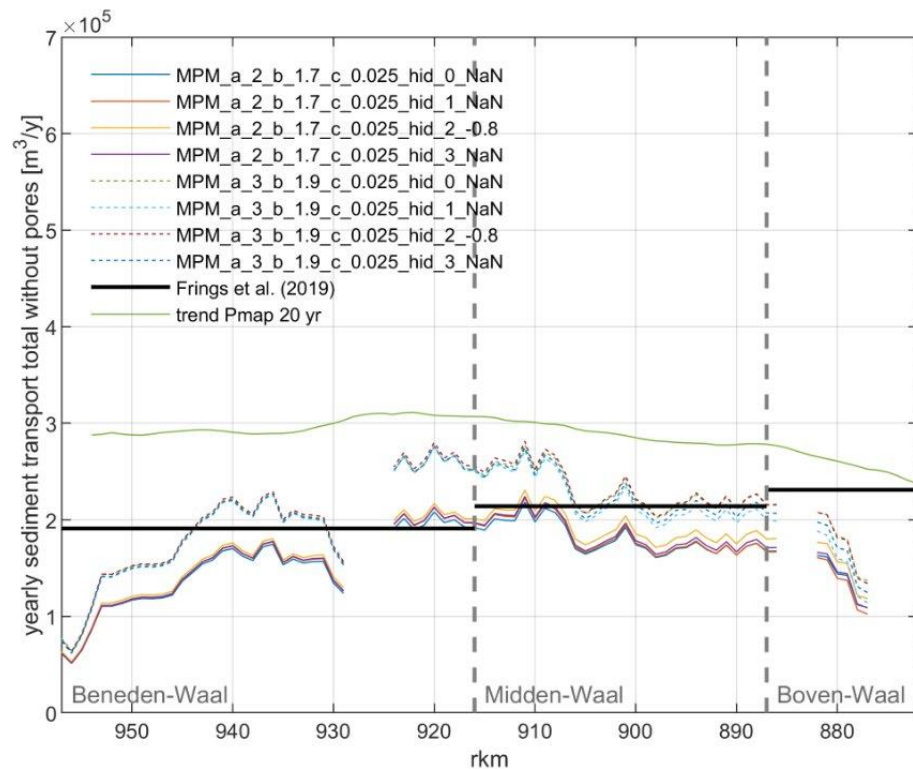


Figure 6.10 Sensitivity test of sediment transport for different hiding and exposure settings. Computed transports at the locations of fixed layers are not shown because averaging over the main channel width (half alluvial, half fixed) yields unrealistic values in these cases.

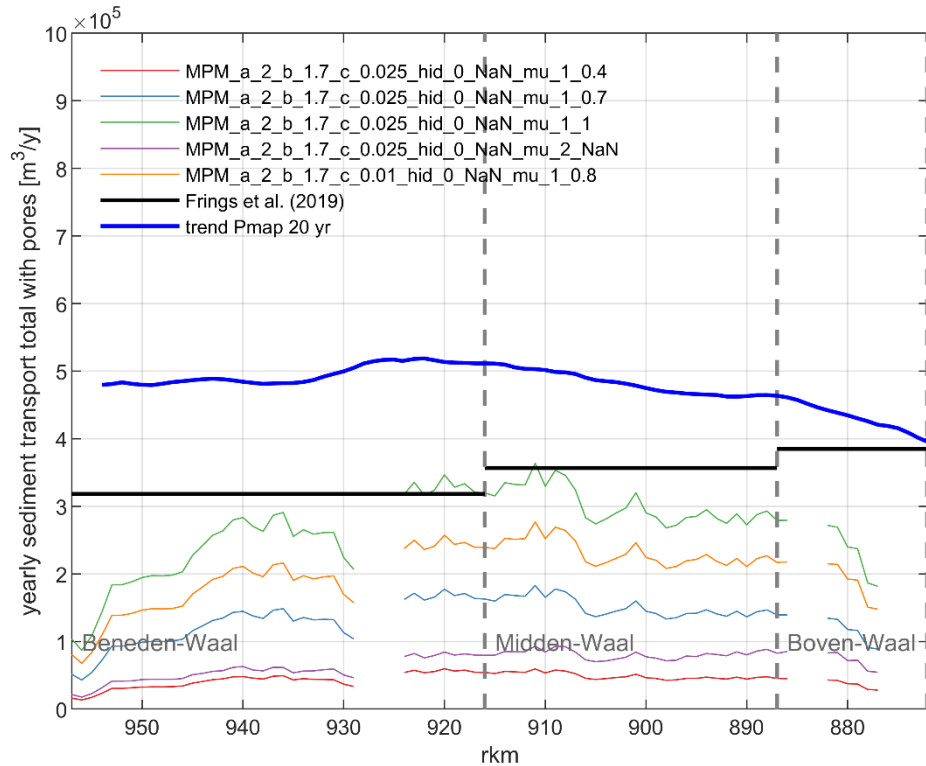


Figure 6.11 Sensitivity test of sediment transport for different ripple factors (μ). Computed transports at the locations of fixed layers are not shown because averaging over the main channel width (half alluvial, half fixed) yields unrealistic values in these cases.

Based on the results and discussions with Rijkswaterstaat, the decision was made to use parameters based on the recent literature of Wong & Parker (2006). The main reason was that we did not want to deviate from a formulation that was published in scientific literature, because that would change the character of the transport formula into something that has not been tested scientifically. The only parameter that got a different value is the calibration factor (a), which is meant to be varied for calibration to better fit the measured data. It still needs to be decided whether the same set of parameters should be used for all branches, or if we want to build separate branch models with each using the ideal settings per branch. This will be done once the models of Boven-Rijn, Pannerdensch Kanaal and Neder-Rijn/Lek have been set up as well.

For the Waal and IJssel, the set of parameters presented in Table 6.3 was used for initial calibration runs.

Table 6.3 Final parameters settings used in the model.

Settings	Sediment transport formula	Parameters
Final parameter set	Meyer-Peter-Müller (all fractions)	$a = 2$; $b = 1.6$; $\theta_c = 0.047$
	Hiding and Exposure	Power Law with $\alpha = -0.8$
	Ripple factor	Constant user input = 1.0

Final results of the offline run with these parameters can be seen in Figure 6.12.

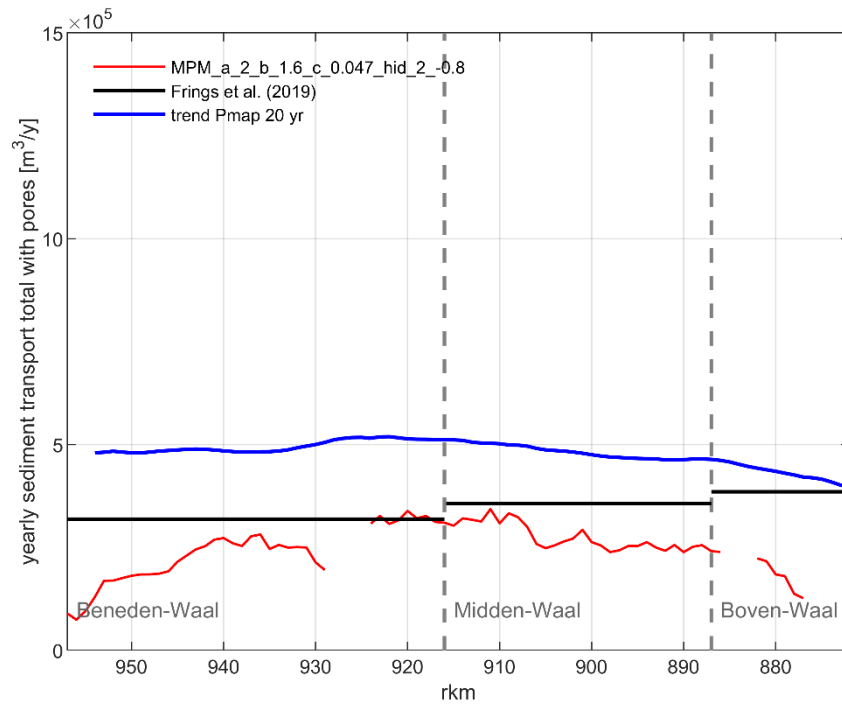


Figure 6.12 Offline yearly total sediment transport with MPM sediment transport formula with $a=2$, $b=1.6$, $\theta_c=0.047$, hiding and exposure (2) with $\alpha = -0.8$, ripple factor $\mu=1.0$. Computed transports at the locations of fixed layers are not shown because averaging over the main channel width (half alluvial, half fixed) yields unrealistic values in these cases.

6.2.2 Gradient analysis

As part of the offline calibration, the sediment transport results were compared to velocity and grain size gradients (Figure 6.13). As with the sediment transport, velocities were averaged within the main channel and per river kilometer. Figure 6.14 shows the results of the sediment transport per fraction (1-11) and the velocities for three flow conditions: low (1.020 m³/s at Lobith), medium (3.053 m³/s at Lobith) and high flow (8.592 m³/s). Based on these outputs the following conclusions can be drawn:

- For low flows moving in the downstream direction up to km 910, we see that although there are no big changes in velocity, there is a positive gradient in sediment transport. This is due to the reduction of the mean particle size in this transition between gravel and sand. After km 910, the downstream fining is less strong. Then the negative gradient in velocity plays a bigger role, leading to a reduction in the sediment transport.
- Similar results are observed for medium flows. In medium flows, also larger particles are entrained (5-11).
- For high flows, the influence of grain size on sediment transport is still visible in the downstream part, especially for the finer fractions. From approximately rkm 910 and further upstream, the velocity gradient takes over.
- Sudden drops in sediment transport rate are related to the presence of fixed layers.

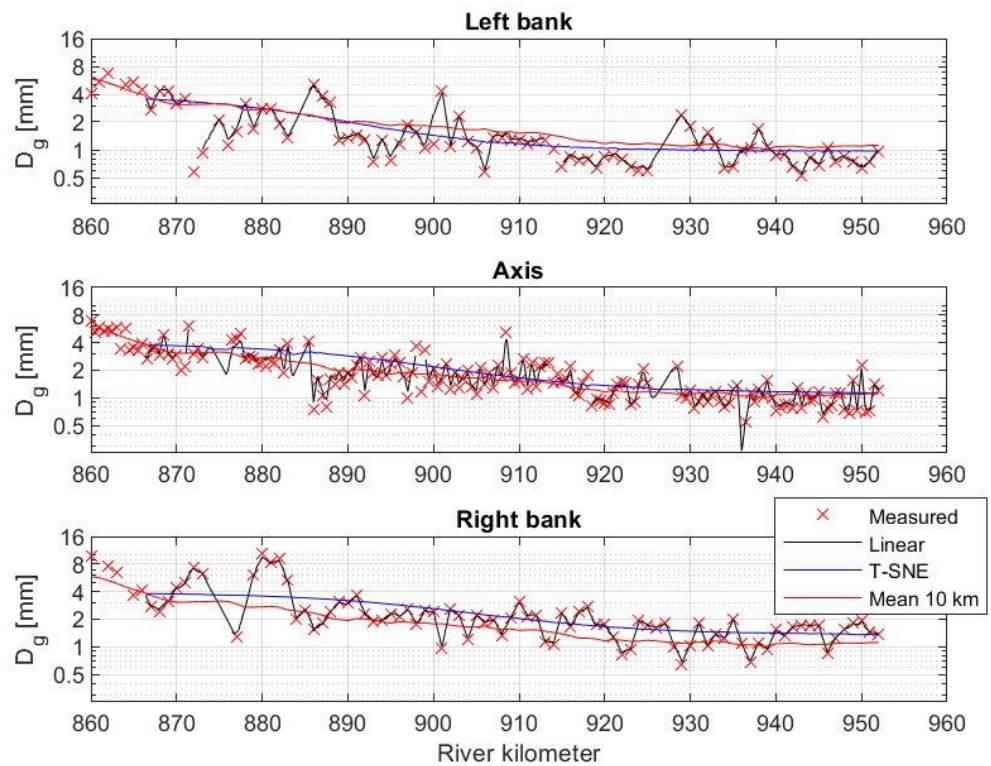


Figure 6.13 Geometric mean of the sieve curves on the Waal derived from the 2020 measurements (red crosses) and derived using the rolling mean (solid red line) (Becker et al., 2023). The black line is a simple linear interpolation between the 2020 measurements, and the blue line is the result of applying a statistical method (Becker et al., 2023). Note that rkm increases from left to right.

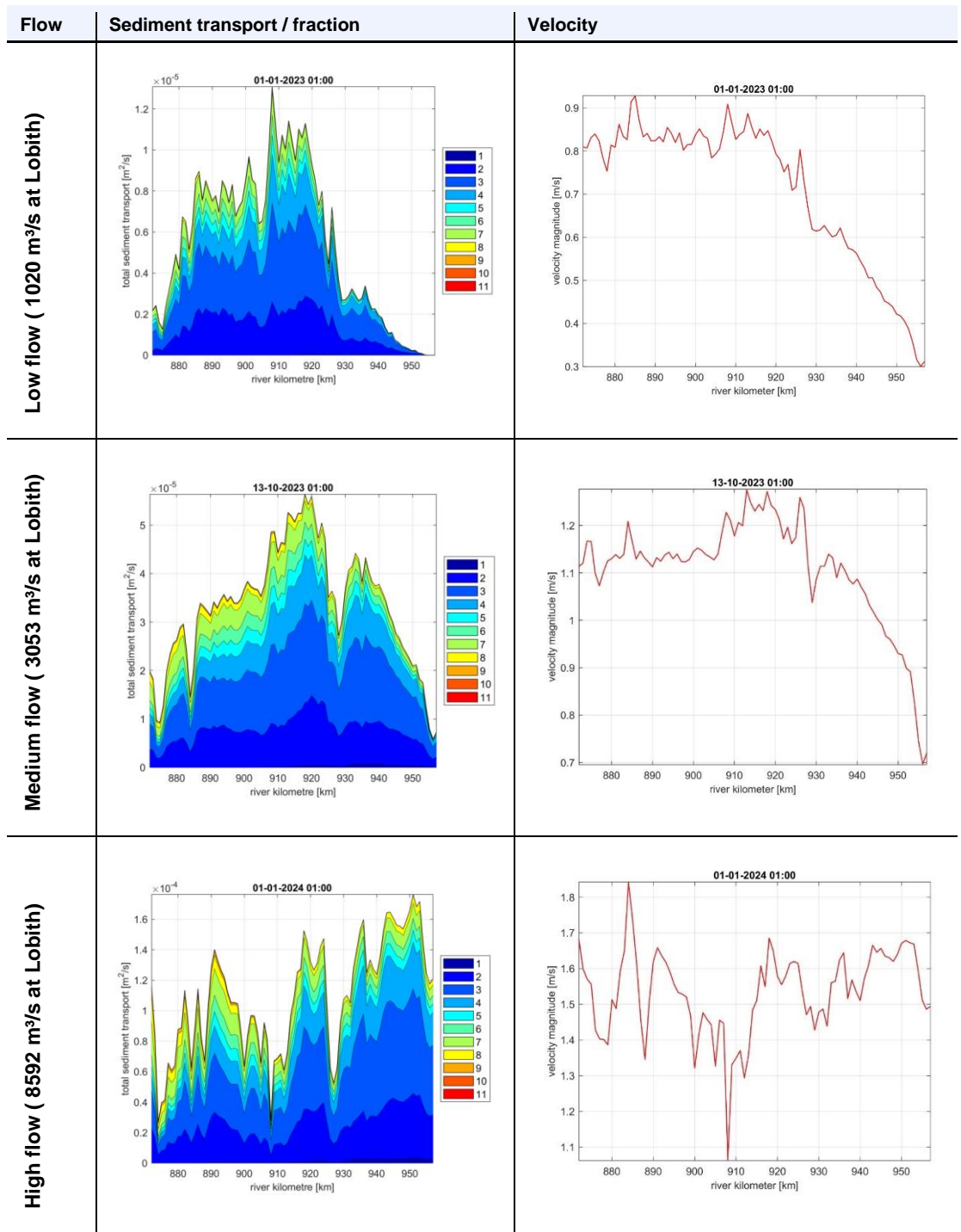


Figure 6.14 – Total sediment transport per fraction and velocity gradient for low, medium and high flows in the Waal for Meyer-Peter and Müller transport formula ($a = 2$, $b = 1.6$, $c = 0.047$). Note that rkm increases from left to right.

7 First steps in 1D calibration

7.1 Calibration procedure

Calibration will be carried out in 2 steps, a 1D and a 2D calibration, as described in the “plan van aanpak” (Spruyt, 2022). The 1D calibration focusses on the following parameters:

- 1 Yearly sediment transport rates and transport gradients (longitudinal profiles of sediment transport)
- 2 width averaged bed levels and bed level trends (longitudinal profiles L3R3 per km)
- 3 celerity of bed disturbances per river section. This step has not yet been carried out. Indicative values for the celerities have been derived by Sieben (2020), see Becker et al. (2023), these will have to be verified with the data by De Joode (2023) (see Becker et al., 2023).

The 2D calibration is meant to adjust:

- 4 2D patterns, e.g. transverse slope in bends (longitudinal profiles along the river axis and lines to the left (L3) and right (R3) of the river axis)

Section 7.2 presents the first results of morphological simulations for 1D calibration, for the period 2000 - 2009. In 2025, the simulation duration will be extended to cover the entire period that was selected for calibration (1999 – 2012). Note that these results are coming from simulations that start from initial bed levels and composition without prior spin-up and still use the hydrograph of the old DVR-model, which in 2025 needs to be replaced by the new hydrograph presented in section 4.3. With these modifications, all analyses of the 1D calibration mentioned below need to be deepened in 2025.

These results thus have to be regarded as preliminary, which is why the resulting model version is called v0.5. In 2025, we intend to finish 1D calibration to reach model version v0.8 and then continue with 2D calibration leading to model version v1.0.

7.2 1D calibration results

7.2.1 Yearly sediment transport rates and transport gradients

Figure 7.1 shows yearly sediment transport along the Waal for both an offline and an online computation (2000 – 2009) using the sediment transport settings selected from the offline analysis (Table 6.3). Clearly, the transport is underestimated compared to the transport derived from bed level changes by Sloff (2019). However, from bed level changes only gradients in transport can be derived. The data does not give information on absolute values for the transport itself. For the incoming transport at the upstream end of the Waal, Sloff (2019) therefore used an estimate based on model simulations. For the new morphological model, the goal is to use the same transport formula settings for all branches. The current selection of transport settings is based on an analysis for both the Waal and the IJssel. Given the uncertainty of the incoming load at the upstream end of the Waal, it was accepted that the selected settings give a much lower incoming transport (while for the IJssel on the other hand, the transport is slightly overestimated compared to the numbers given by Sloff (2019)). Results of the models of Boven-Rijn and Pannerdensch Kanaal, which will be set-up in 2025, have to show if this choice needs to be modified.

In terms of transport gradients, our observations are similar to previous results with different transport settings (Becker et al., 2023). The positive gradients observed up to rkm 925 are overestimated in the model. From rkm 925 up to the downstream boundary the model shows a strong decline in transport rates, while the bed level analysis shows a decline only for rkm 925 – 935 after which the transport rate stays more or less constant. This is partly explained by the effect of sand mining: the transport gradient is actually negative (leading to sediment deposition), but when deposited sediment is regularly extracted bed levels remain more or less stable. This is why the negative gradient is not visible in the data analysis.

While the negative transport gradient is underestimated in the analysis based on bed level changes, we expect the negative gradient in the model to be an overestimation with respect to reality. In Section 4.2 we explain that velocities near the downstream boundary are underestimated due to the choice of downstream boundary condition. Furthermore, in last year's report we showed that the application of a constant Chézy coefficient leads to an overestimation of the velocity gradient for medium and high discharges ($Q_{Lobith} > 3000 \text{ m}^3/\text{s}$). By applying a smoothly varying roughness along the channel this can be corrected without introducing sudden transitions in roughness. The ADCP measurements that were made recently by RWS-ON can be used to further validate the modelled flow velocities. The velocities in the original hydrodynamic model have already been validated against measurements of the flood of 2021 (Gradussen, 2023), and a validation against ADCP measurement on the section with longitudinal training walls will be carried out in 2025 in the SITO model schematisations project. Both provide material for additional validation of velocities in the morphodynamic model.

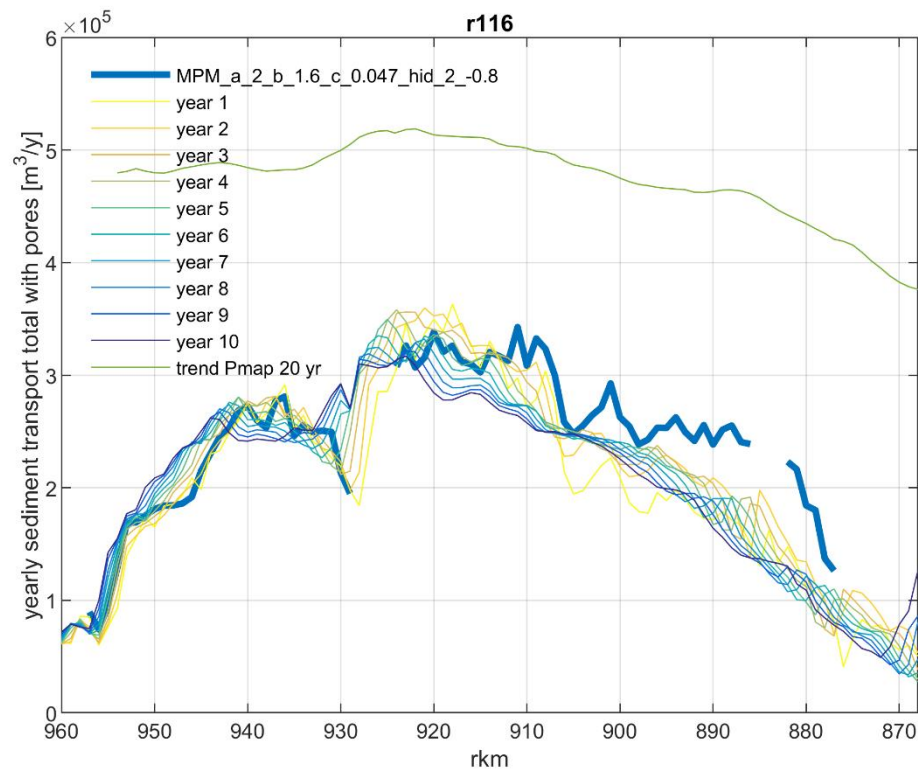


Figure 7.1 Total yearly sediment transport including pores for an offline (thick blue line) and online (thin coloured lines) computation (2000 – 2009). The green line indicates the yearly transport derived from Pmap data.

7.2.2 Bed level development

Figure 7.2 compares the width- and km-averaged bed level development in the model to measurements.

Following the gradients in sediment transport as presented in Figure 7.1, the model shows an overall trend of degradation roughly up to rkm 920, after which aggradation is mostly observed, except between rkm 932 and 940. These large-scale patterns correspond to the measurements.

Model results show an initial spike in the bed level at rkm 908, which is the location of the overnachtingshaven IJzendoorn, see Figure 7.3. The spike rapidly decreases during the first 2 years of simulation as the model adapts to the boundary conditions. Further investigation by RWS has revealed that the model schematization contains inaccuracies at this location, which lead to an underestimation of flow velocities in the main channel for high discharges. This should be taken into account in the interpretation of the model results.

Other spikes in the bed level are mainly visible downstream of fixed layers (Erlecom at rkm 876, Nijmegen at rkm 885 and St. Andries at rkm 928), and remain present throughout the simulation. The sedimentation front in the section downstream of St. Andries, which is visible both in the model and the measurements, may be the result of the construction of the fixed layer, that was finished in 1998. The propagation of this front is also visible in Figure 7.4, that shows changes in bed level for the periods 2000 – 2003, 2003 – 2006 and 2006 – 2009.

Table 7.1 shows the average yearly bed level change for the Boven-Waal, Midden-Waal, Beneden-Waal and Getijden-Waal. Because the model overestimates the transport gradients (see Figure 7.1), we see that overall, bed levels change more rapidly in the model compared to the prognosis by Sloff (2019). Compared to the measurements between August 1999 and November 2009, the deviations are even larger. On the Boven-Waal and Midden-Waal, the degrading trend is too strong. On the Beneden-Waal, the net change in average modelled bed level is close to zero, while the measurements show an aggrading trend of more than 1 cm/y. On the Getijden-Waal, the model predicts aggradation while the measurements show net degradation in the period 1999-2009. The aggradation in this section of the model occurs despite the implementation of sand mining in the model. This is further explained in Section 7.2.4.

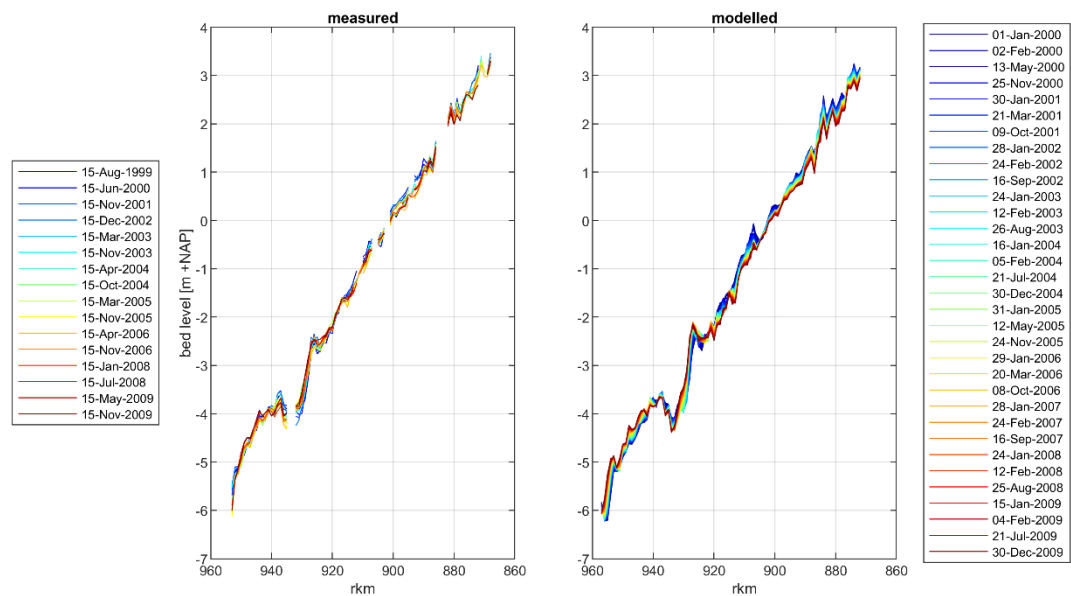


Figure 7.2 Width-averaged (R3L3) and km-averaged bed levels along the Waal. Left: observed; right: modelled using the transport formula and settings resulting from the offline calibration.

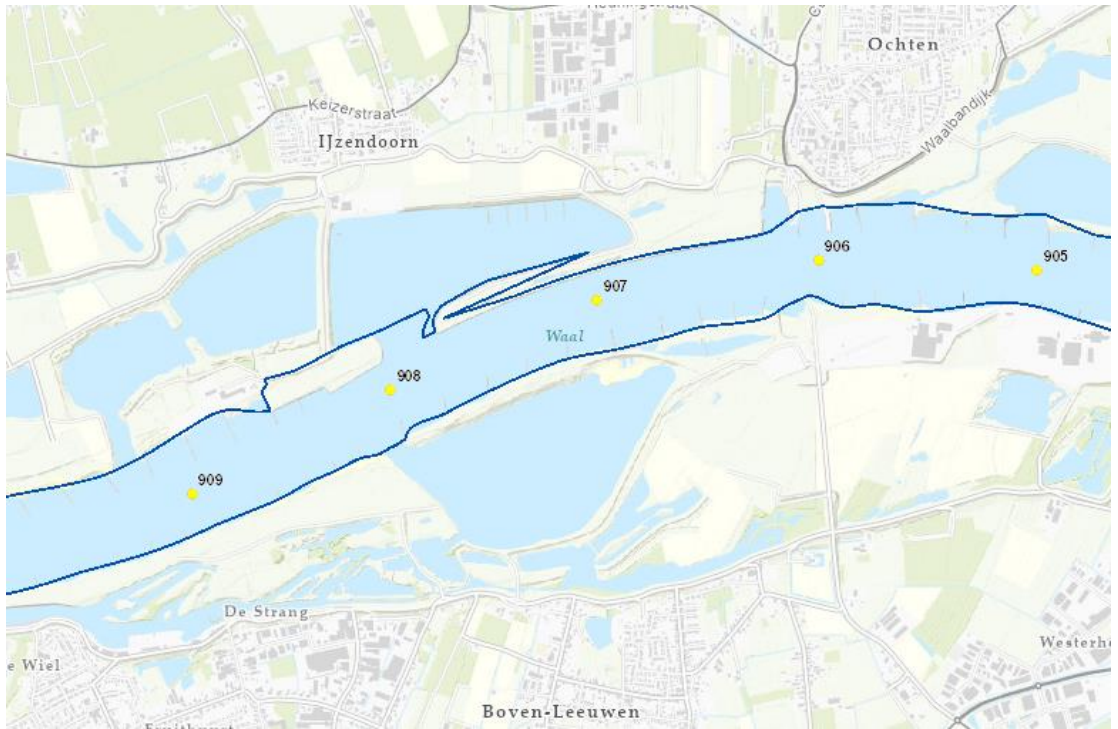


Figure 7.3 Overnachtingshaven IJzendoorn at rkm 908 (right bank). Source: Legger Rijkswaterstaatswerken (2022).

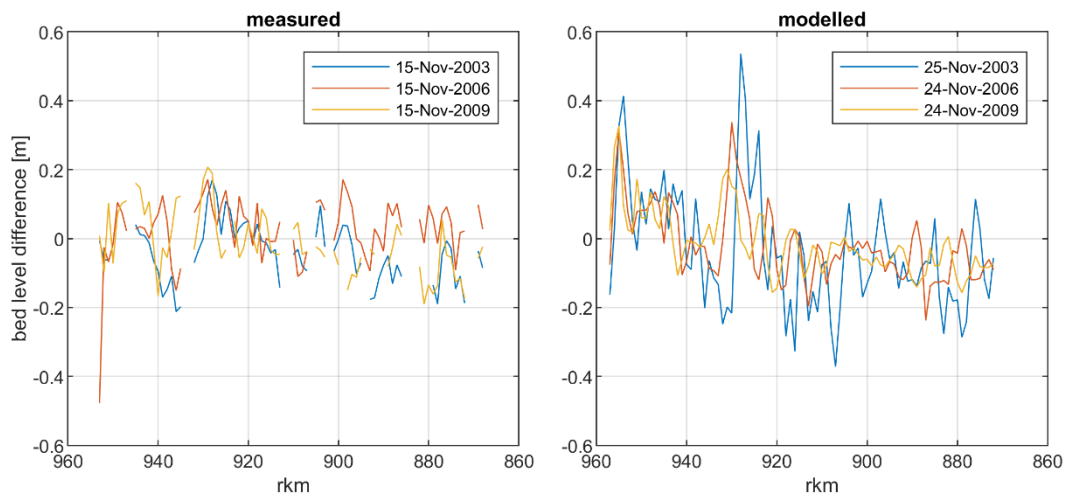


Figure 7.4 Total width-averaged (R3L3) and km-averaged bed level change in model and measurements, for the periods 2000 – 2003, 2003 – 2006 and 2006 – 2009.

Table 7.1 Section-averaged bed level changes.

Section	rkm	model 10 yr [cm/y]	measured 1999 – 2009 [cm/y]	Prognosis [cm/y] (Sloff, 2019)
Boven-Waal	867 – 887	-2.55	-1.38	-1.59
Midden-Waal	887 – 911.5	-2.06	-0.69	-0.92
Beneden-Waal	911.5 – 932.4	-0.07	1.08	-0.17
Getijden-Waal	932.4 – 952.7	0.78	-0.74	0.09

7.2.3 Grain size distribution changes

Figure 7.5 shows the development of grain sizes at the end of the calibration simulation. Variations in final grain sizes are mostly due to bend effects (visible on the left and right side of the main channel) and the presence of fixed layers, which lead to strong erosion and coarsening directly downstream. The variations largely remain within the range of the measurements. The large changes in grain size near the upstream boundary, mainly on the right side of the main channel, are a modelling artifact. Model results at this location are largely influenced by the choice of upstream boundary condition. More detailed investigation of these results will be carried out next year during 2D calibration.

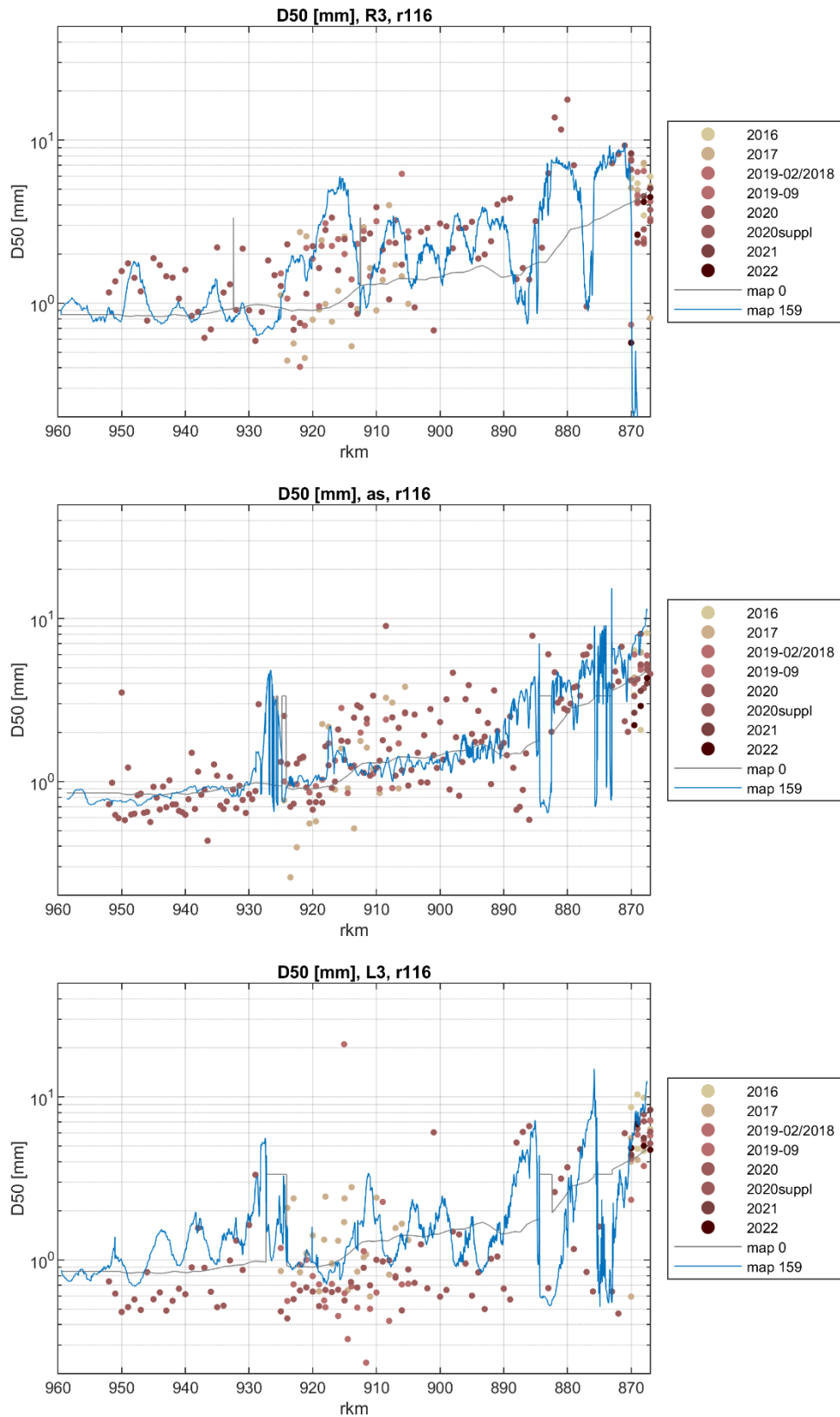


Figure 7.5 Mean sediment diameter D_{50} after 10 years (blue line) compared to the initial value (grey line). Dots indicate measurements that were used to derive the initial composition of the bed.

7.2.4 Fairway maintenance and sediment extraction

In developing and improving the dredging and dumping routine for the new morphological model, a large number of test simulations were carried out. Comparing the results of these test simulations, information can be gathered on the sensitivity to different dredging and dumping parameters. In this section, attention will be paid to the most important conclusions drawn from these comparisons. Furthermore, model results with the latest dredging and dumping routine will be compared to reported dredging and sand mining volumes (see Section 3.1).

For the test simulations, use was made of the same sediment transport formulations as used in the 1D IRM-model (Chavarrías et al., 2020): Engelund-Hansen with $a=0.18$ and $n=5$ for fractions 1-4 and Meyer-Peter-Müller with $a = 2.56$, $b = 1.5$, $\theta_c = 0.025$ and $\mu = 1$ for fractions 5-11. Based on further discussions and the results of the offline calibration (Chapter 6) it was decided to not use these settings anymore. However, conclusions regarding the relative effects of different dredging/dumping parameters are expected to still be valid with different sediment transport settings.

For the validation of computed dredging volumes, a simulation was carried out with the transport settings chosen based on the offline calibration, see Table 6.3.

7.2.4.1 Effect of dredge depth and clearance

As expected, most changes described in Section 5.6 do not have a major influence on the long-term morphological development. An exception is the change in required water depth below OLR for the Boven-Merwede. Using the intervention depth from RBK instead of the 'Leggerdiepte CEMT-92', the required depth below OLW increases by 0.45 m. Additionally, the clearance has increased from 0.45 m in the previous model to 0.75 m in the current model. This leads to an increase in dredging volumes on the Boven-Merwede. For sand mining on the Boven-Merwede, the previous routine used a depth of 5.40 m (the maintenance depth) and a clearance of 0.45 m. In the new routine the requirements for sand mining are the same as for dredging, which means a depth of 4.95 m + 0.75 m clearance. Hence, for sand mining the dredge depth is reduced somewhat. Combined with the increase in dredging volumes, which leaves less sediment for sand mining, this leads to a decrease in sand mining volumes and a larger increase in bed levels on the Boven-Merwede during the calibration period.

Also on the Beneden-Waal, depth requirements for sand mining were changed significantly. Where in the old routine, a depth of 5.40 m was used with a clearance of 0.30 m, the new model uses depths ranging from 3.14 m to 3.97 m with the same clearance, to align with the requirements for dredging. This leads to a significant reduction in sand mining volumes, and an increase in bed levels.

Figure 7.6 and Figure 7.7 show modelled bed level development before and after the changes in depth requirements on the Beneden-Waal and Boven-Merwede. Note that for the results shown in Figure 7.6, changes were already made to the old dredging routine. Most importantly, clearance on the Boven-Merwede was changed from 0.45 m to 0.30 m. In Figure 7.7, a clearance of 0.75 m was used on the Boven-Merwede.

Roughly from rkm 930 onward, we see a large difference in bed level development, which is due to the changes described above. The bed level development after the changes shows less correspondence to the measurements. We also see large differences in the sand mining volumes, see Figure 7.8 and Figure 7.9 (note the difference in scale). The volumes shown in Figure 7.8 are of the same order of magnitude as reported numbers (see Section 3.1.2 and Table 3.1). After the changes in the dredging and dumping routine, modelled sand mining volumes are much smaller than reported.

At this moment, it is not known whether the observed differences between model results and measurements are due to differences between the dredging/sand mining routine in practice and the one implemented in the model, or caused by other shortcomings of the model. This needs further investigation.

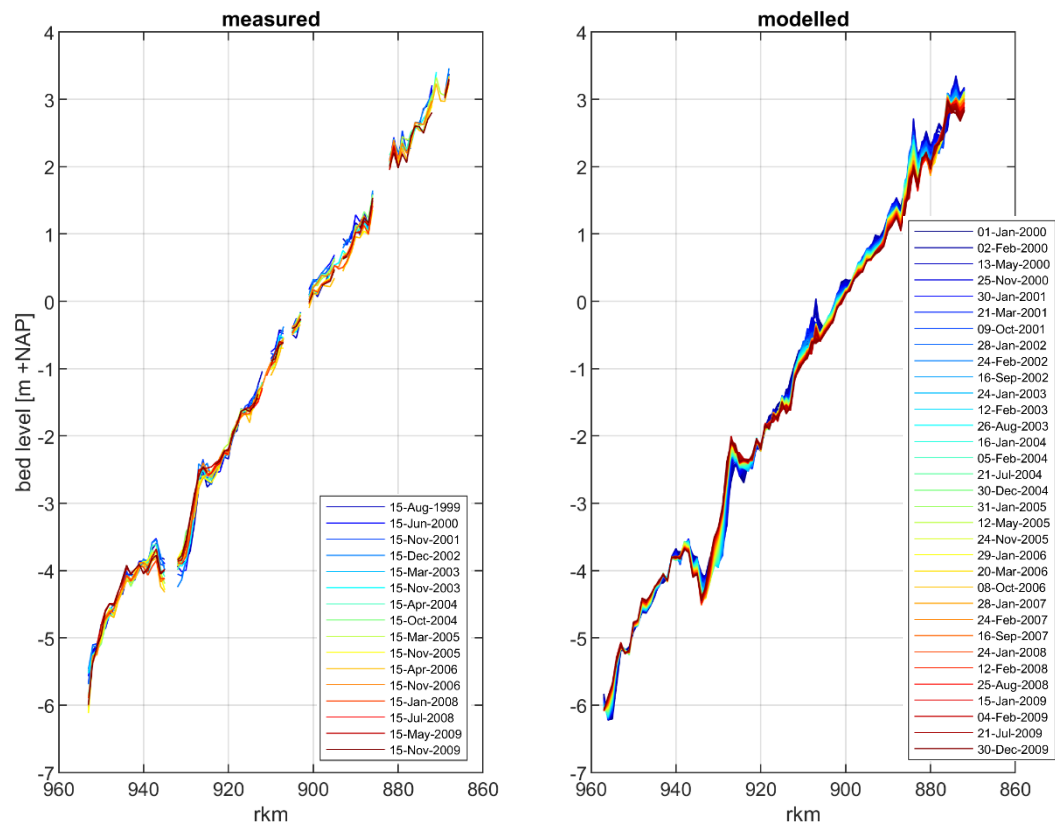


Figure 7.6 Measured and modelled bed levels in run 110, with old depth requirements on Boven-Merwede and Beneden-Waal. Note that in this simulation, the clearance for Boven-Merwede was set to 0.30 m instead of 0.45 m that was used previously.

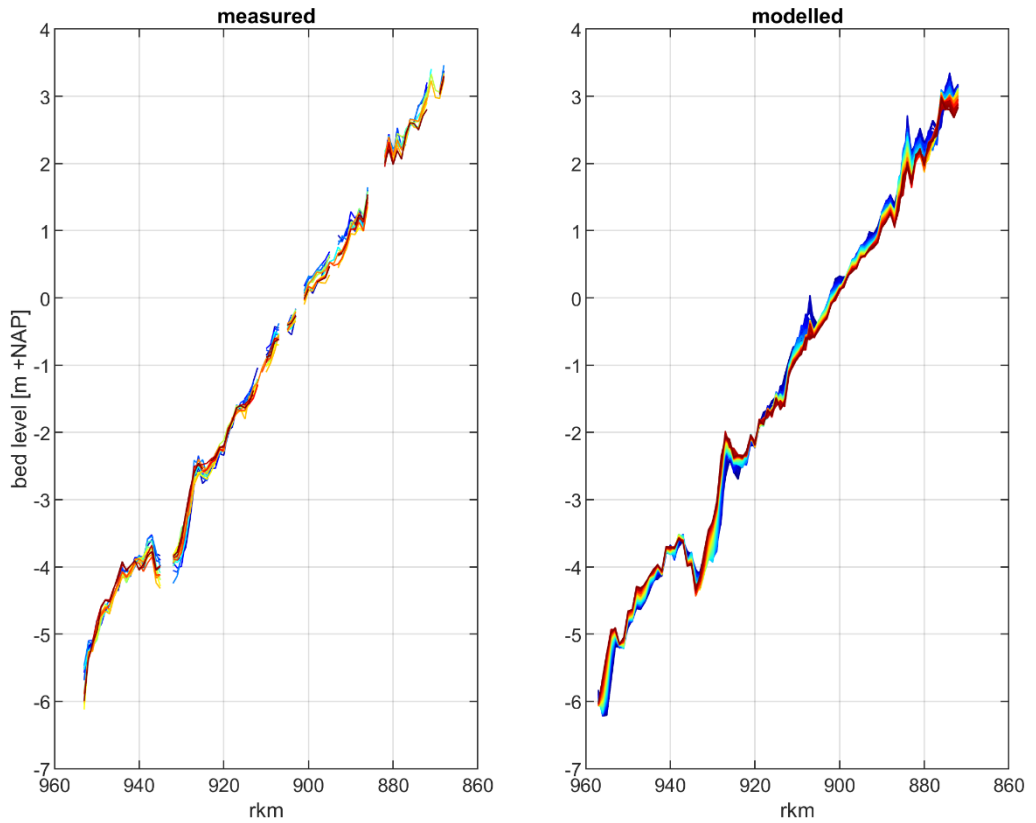


Figure 7.7 Measured and modelled bed levels in run 111, with new depth requirements on Boven-Merwede and Beneden-Waal.

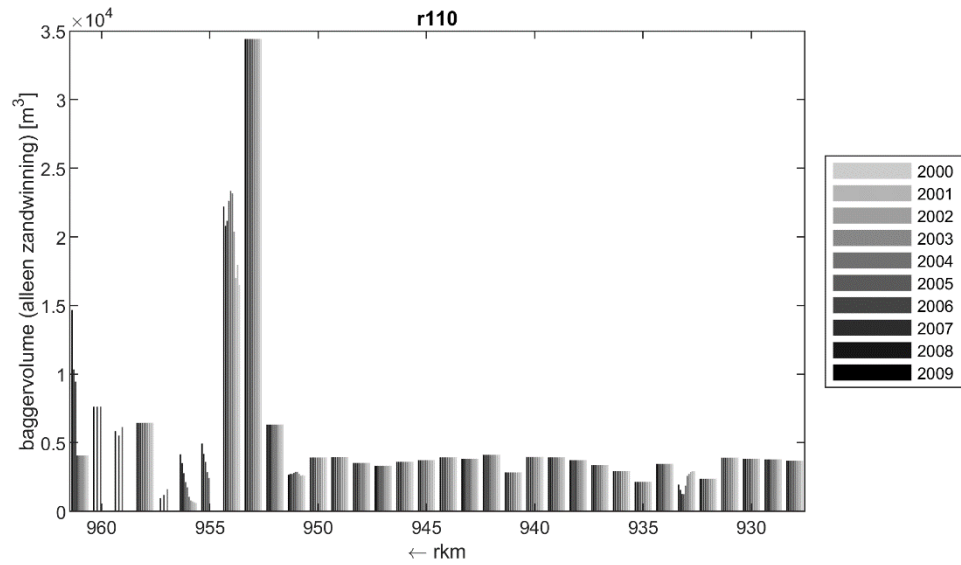


Figure 7.8 Sand mining volumes in run 110, with old depth requirements on Boven-Merwede and Beneden-Waal

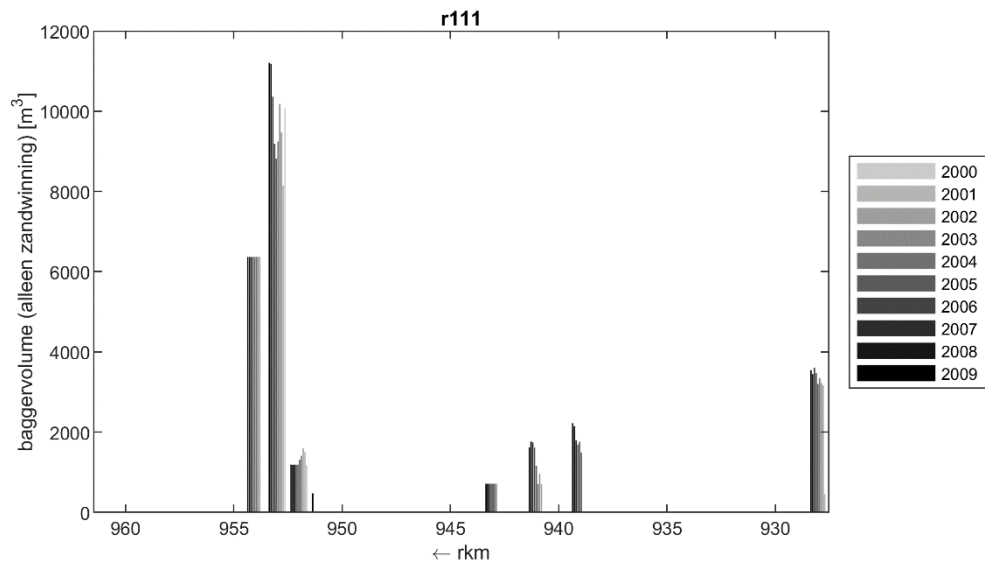


Figure 7.9 Sand mining volumes in run 111, with new depth requirements on Boven-Merwede and Beneden-Waal. Note the difference in scale with respect to Figure 7.8.

7.2.4.2 Effect of parameter TriggerAll

Another parameter that has a significant effect on the results is whether or not the whole area inside a polygon is dredged up to clearance when dredging is triggered anywhere within that polygon. This behaviour can be switched on with the keyword TriggerAll.

Figure 7.10 shows that TriggerAll=1 (true) leads to larger dredging volumes, but smaller sand mining volumes. Especially between rkm 950 and 955 differences are observed. Because sand mining occurs before dredging in each timestep, TriggerAll=1 would in principle result in an increase of sand mining volumes. This is not the case, most probably because sand mining is often limited by the maximum volume rate imposed (see Section 5.6.8). Because no maximum volume rate is imposed for dredging, dredging volumes can increase rapidly in a short amount of time, while sand mining volumes cannot.

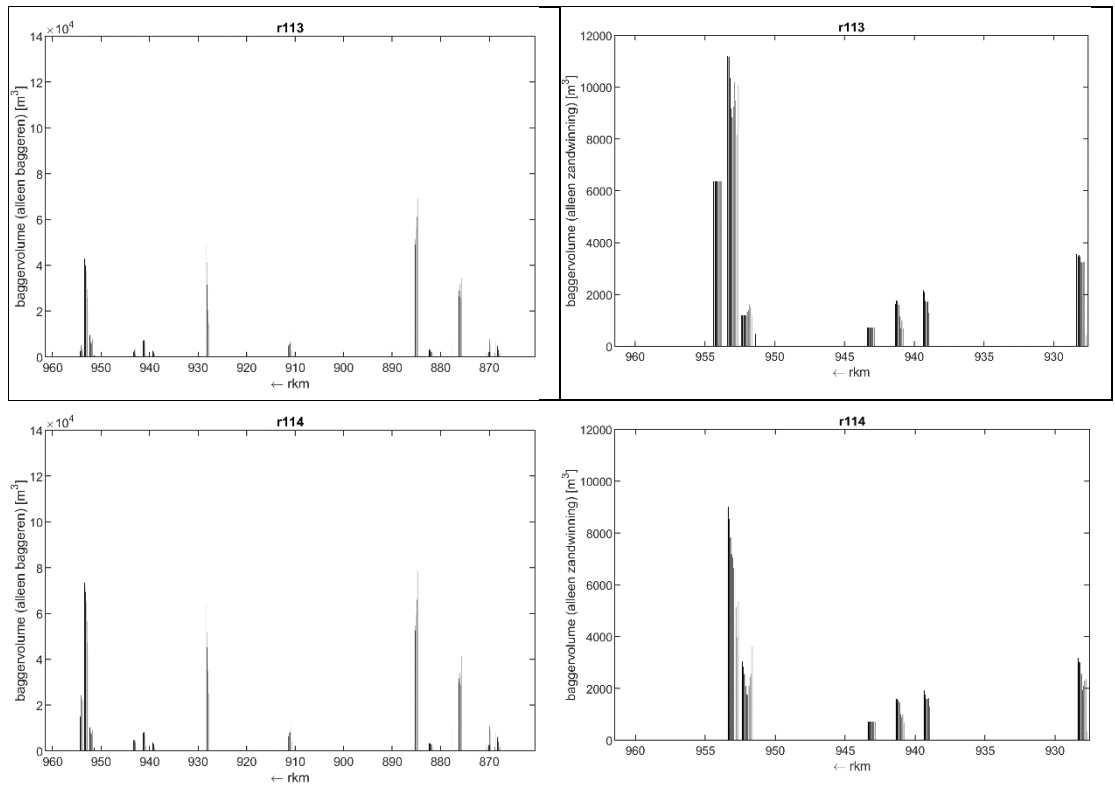


Figure 7.10 Dredging (left) and sand mining (right) volumes in run 113 (top, with $TriggerAll=0$) and run 114 (bottom, with $TriggerAll=1$). Note the difference in scale of the horizontal axis between left and right figures.

7.2.4.3 Comparison between modelled and reported dredging volumes

Figure 7.11 shows measured and modelled dredging volumes for a simulation with sediment transport settings according to Table 6.3. We note the following:

- Modelled and reported dredging volumes are of the same order of magnitude.
- Both model and measurements show large dredging volumes directly downstream of the fixed layers, at rkm 876, 885 and 928.
- In the model, dredging is concentrated at a few locations, while in reality dredging occurs throughout the domain.
- No dredging activities have been reported downstream of rkm 930 in the period considered, while the model shows large dredging volumes around rkm 953. Possibly, the data for this section are missing for the period considered.

Figure 7.12 contains modelled dumping volumes for the same simulation. Comparing to the modelled dredging volumes, we see that for most locations dredged material can always be deposited within the same river kilometer. Exceptions are rkm 928, where dredged material is dumped either within the same rkm or at rkm 929, and rkm 953, where dredged material is sometimes dumped at rkm 954.

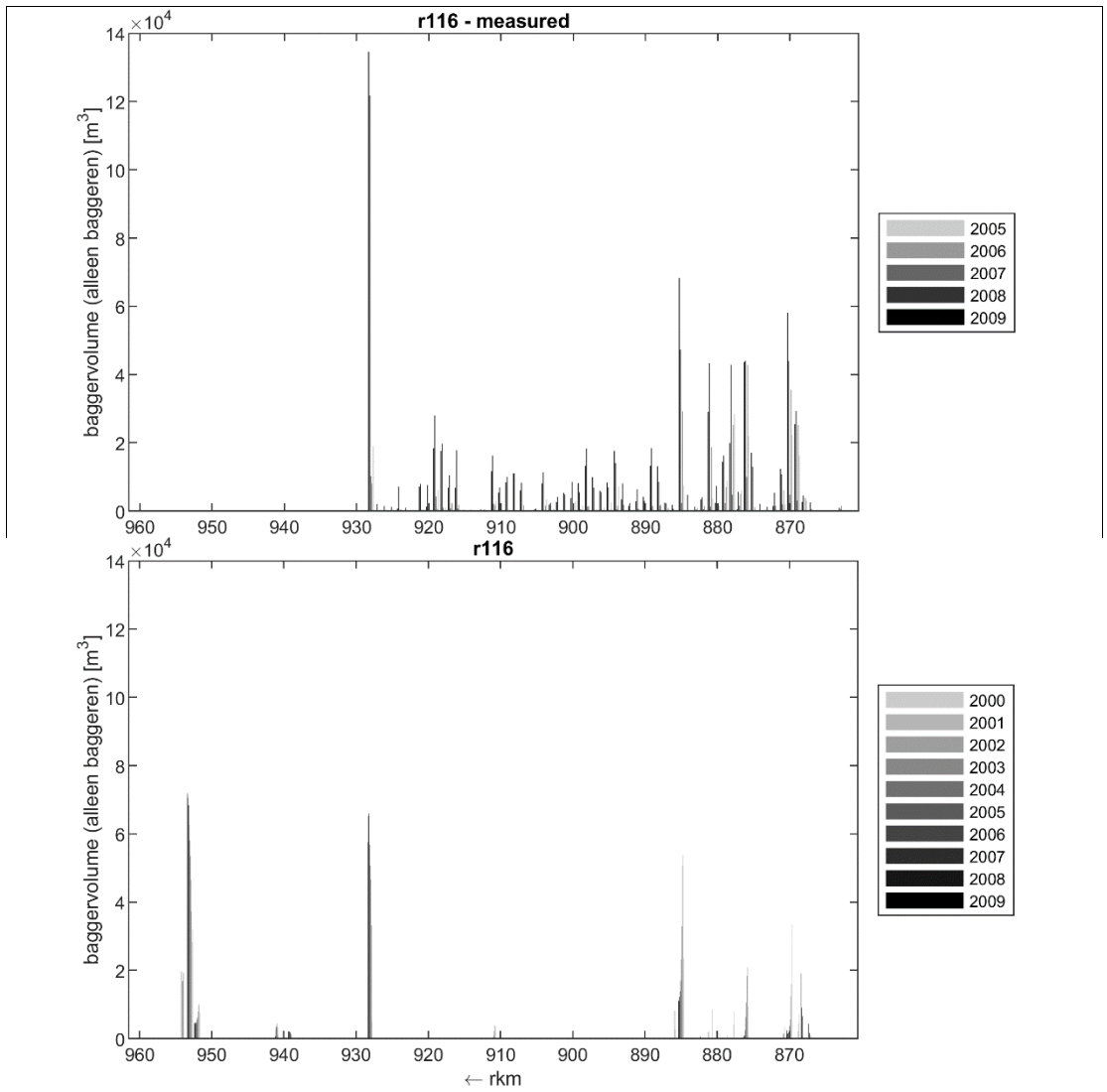


Figure 7.11 Measured (top) and modelled (bottom) dredging volumes.

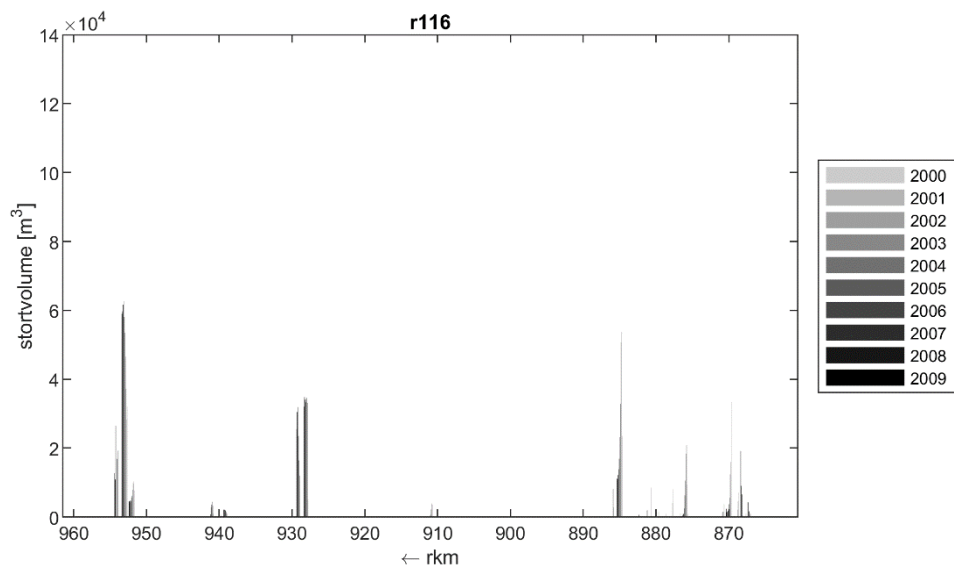


Figure 7.12 Modelled dumping volumes.

8 Conclusions and recommendations

In 2024, the morphological Waal model developed in 2023 (model version v0) was improved in several ways, which led to model version v0.5. With these changes, the numerical stability has been improved significantly, and simulation times have decreased to acceptable values through optimization of the morphological factor and the number of sediment fractions. Furthermore, significant attention has been paid to the implementation of fairway maintenance (dredging and dumping) and sediment extraction in the model. For this, information on the current practice and data on dredging volumes has been collected. Through several discussions with Rijkswaterstaat, it was decided how the practice of fairway maintenance and sediment extraction could best be schematized in the model. The modelled dredging, dumping and extraction volumes resulting from this implementation were subsequently analysed and compared to reported volumes. Furthermore, the computation of dune heights in the model was validated. By taking into account dune heights, the dredging and dumping routine can possibly be improved further.

This report also presents the results of several analyses of the model results, regarding the accuracy of the downstream boundary condition, the roughness of the fixed layers and the sensitivity of model results to the parameters of the sediment transport formula. Based on the latter, a set of sediment transport parameters has been selected as starting point for the 1D calibration.

The first analyses needed for the 1D calibration were carried out, but 1D calibration has not yet been finished. The resulting model is therefore called “version 0.5”. In that model, modelled sediment transport is significantly lower than the estimate based on bed level changes by Sloff (2019), and than the results of 2023 (which used a different transport formula, which was abandoned in discussion with RWS). In the final model, sediment transport on the Waal should match the incoming sediment transport from Boven-Rijn. That model will be set-up in 2025. First model results need to show if the parameter settings in the transport formula for the Waal need to be changed to achieve a better match.

The modelled transport gradients are somewhat too high, resulting in faster bed level changes than observed in reality. On the upstream part of the Waal, this can be changed by either applying an even smaller calibration factor (which would result in even lower sediment transport) or changing the gradient in initial sediment composition. Improving the gradients in flow velocities by introducing a varying main channel roughness (but fit for morphological simulations) might help to reduce the gradients as well, but it's not sure if that on its own would be sufficient. It is recommended to analyse these options with the offline calibration tool in 2025. On the downstream part, bed level development is largely influenced by sand mining. It needs to be discussed further which sand mining volumes need to be achieved by the model.

Table 8.1 recommends which steps to take next year. First, the 1D calibration should be improved further by analysing the influence of a different initial sediment composition and different gradients in flow velocity and roughness, and by agreeing on the sand mining volumes to be achieved by the model. Possibly, the downstream boundary conditions also need to be modified.

Furthermore, the model should be properly spun-up for the final 1D calibration runs. A method for this was proposed in 2023, but it is being refined further at the moment in other projects, because it turned out that the sections around the fixed layers need more spin-up than the rest of the model. The refined method can be used next year for the new model as well.

Once the model is sufficiently calibrated for the long-term and on the larger scale (model version v0.8), we can proceed to a detailed 2D calibration to achieve model version 1.0 (fully calibrated). As a starting point, the newly available ADCP-measurements across Waal bends, with and without fixed layers, should be used to calibrate the roughness of fixed layers and inner bends. This could also improve the spin-up of the model. Furthermore, the analysis of bed mobility by Olink & Sieben (2024) should be used to identify sections of the main channel that are less mobile or even immobile, since this can have a strong influence on the formation of 2D patterns in bed level development.

In first calibration runs for the IJssel (with model version v0.5), it turned out that the model is very close to ill-posed near the upstream boundary, which means that it easily becomes unstable. Due to this, a large sedimentation wave enters the model. A similar behaviour has been observed in some of the Waal model runs of 2023 (v0), without making the connection to ill-posedness yet. It is recommended to check whether also the Waal model is close to ill-posedness. And the possibility to add extra diffusion to the model in case of ill-posedness should be added in the software.

In order to bring the models for morphological and hydrodynamic simulations closer to each other, it is furthermore recommended to:

- check what value of *epshu* is appropriate for unsteady hydrodynamic simulations, and
- introduce a smooth gradient in main channel roughness as proposed in 2023.

Next to the work on the Waal, the calibration of the IJssel model will be refined further (v0.8 and v1.0), and first models (v0) for Boven-Rijn, Pannerdensch Kanaal, Neder-Rijn and Lek will be set up.

Table 8.1 Recommended steps to continue model development in 2025.

activity areas	associated activities	model version	steps for 2025
data collection	<ul style="list-style-type: none"> Collection of all data needed to set-up a model, e.g. boundary conditions, calibration data hydrodynamics and sediment transport and morphology, bed composition, etc. 	v0 v1	non- or less erodible layers Waal v1 (Olink & Sieben, 2024); ADCP measurements Waal bends: further validation of modelled flow velocities
hydrodynamic model schematization ⁶	<ul style="list-style-type: none"> modification of the hydrodynamic model, that forms the basis of the morphological model, where needed⁵ 	v0 v1	develop and test a Qh-relation that better approximates the tidal signal at the downstream boundary in terms of resulting sediment transport
morphodynamic model schematization: towards a well-working basic model (v0)	<ul style="list-style-type: none"> set-up of a first running model including: <ol style="list-style-type: none"> dynamic river bed representative initial bed elevation (e.g. smoothing of bed forms) suitable roughness formulation for morphology sediment (grain sizes and sediment layers, with focus on active/upper layer) secondary flow first choice of transport formula and parameters (uncalibrated) non-erodible and less erodible layers suitable grid resolution testing phase v0 model, identification of problems and modification of the schematization accordingly 	v0	non- or less erodible layers Waal v1
extending the basic model to a v1 model	<ul style="list-style-type: none"> more sophisticated description of <ol style="list-style-type: none"> main channel roughness composition and thickness of underlayers, including non-erodible layers set-up of a dredging and dumping module testing phase v1 model, and iterative modification of model schematization if necessary 	v1	Waal v1: more sophisticated main channel roughness (test effect with offline calibration tool first!)
development of methodologies and tools for running the model	<ul style="list-style-type: none"> approach and tools for model simulation (i.e. Simulation Management Tool) strategy for model spin-up strategy and tools for model evaluation and presentation of results strategy and tools for simplification of model set-up and improving reproducibility 	v0 v1	Waal v1: Snakemake workflows; analysis time dependent morfac

⁶ This should be done in SITO Modelschematisaties, as part of the development of the hydrodynamic model.

activity areas	associated activities	model version	steps for 2025
model calibration and validation	<ul style="list-style-type: none"> • calibration and validation strategy • adapting the hydrodynamic model to make it suitable for morphodynamic simulations • hydrodynamic validation • “offline” calibration giving a first estimate of morphological response based on the flow field in the hydrodynamic simulations • 1D morphodynamic calibration and validation (focusing on width-averaged, large-scale and long-term trends) • 2D morphodynamic calibration and validation (focusing on 2D patterns in the river bed, such as bank patterns and bend profiles) • validation of dredging and dumping module 	v1	Waal v1: test influence of gradients in grain size and gradients in flow velocity with offline calibration tool; finish 1D calibration and validation; roughness of fixed layers; 2D calibration and validation
exploring model uncertainties	<ul style="list-style-type: none"> • influence of unknown physical variables (e.g. roughness in transport, bed composition, active layer thickness) • influence of model settings (e.g. initial geometry/composition and boundary conditions) or modelling concepts (e.g. Hirano model) • influence of simulation strategy and approaches (e.g. methods for optimizing simulation time, schematization of the hydrograph, choice of simulation period) 	v1-v3	-
development of modeling strategies and development for future use of the model	<ul style="list-style-type: none"> • identifying types of application and requirements • development of strategies for application of the model (e.g. choice of scenarios, choices for model settings and geometry, type of interventions) • identifying needs for further development of the model schematization (including needs for knowledge development and data requirements) • implementation and testing 	v1-v3	-
verification of model application	<p>testing the model application in test cases of</p> <ol style="list-style-type: none"> a. effect of interventions b. planning study (“planstudie”) c. (long-term) forecast of system behaviour <p>improvement of the model schematization, modeling strategies, methodologies and tools based on the outcomes of the test cases</p>	v1-v3	-
Implementation of new functionality in D-HYDRO	<ul style="list-style-type: none"> • Identifying requirements of new functionality • functional design of needs • design of implementation • implementation and testing • updating user manuals 	v2-v3	option to add diffusion in case of ill-posedness

9 Literature

- Becker, A., Kusters, A., Nunes de Alencar Osorio, A.L., Chavarrías, V. and Ottevanger, W. (2023). Morphological model for the river Rhine. First (v0) model of the Waal branch. Deltares report 11209261-003-ZWS-0002.
- Becker, A. (2024). Bagger- en stortrutines in DVR-model. Deltares memo 11210364-003-ZWS-0002, February 26, 2024.
- Castañón, A.L., A. Becker, A. Kusters, W. Ottevanger, V. Chavarrías (2024): Morphological model for the river Rhine. First (v0.8) model of the IJssel branch.
- Chavarrías, V., Busnelli, M. and Sloff, K. (2020). Morphological models for IRM. Rhine branches 1D. Deltares report 11206792-014-ZWS-0001.
- Chavarrías, V., W. Ottevanger, K. Sloff, and E. Mosselman (2022), Modelling morphodynamic development in the presence of immobile sediment, *Geomorphology*, 410, 108,290, doi: <https://doi.org/10.1016/j.geomorph.2022.108290>.
- Chavarrías, V. (2024). Dunes in the Waal. Deltares memo 11210364-003-ZWS-0012_v1.12, d.d. 2024-11-07.
- Deltares. (2022). User Manual Delft 3D FM Suite.
- Frings, R.M., G. Hillebrand, N. Gehres, K. Banhold, S. Schriever and T. Hoffmann (2019): From source to mouth: Basin-scale morphodynamics of the Rhine River. *Earth-Science Reviews*, Volume 196, ISSN 0012-8252, <https://doi.org/10.1016/j.earscirev.2019.04.002>.
- Gradussen, B. (2023): Validatie Waalmodel hoogwater 2021. Deltares-rapport 11209233-003-ZWS-0023, 18 december 2023.
- Gradussen, B. (2024). Jaarlijkse Actualisatie Modellen RMM 2024. dflowfm2d-rmm_vzm-j24_6-v1a. Deltares report 11210333-004-ZWS-0006.
- Krabbendam, J. (2024). Bagger- en stortgegevens Rijntakken. Memo, Rijkswaterstaat Oost-Nederland, version 1 d.d. July 2, 2024.
- Lesser, G. R., J. A. Roelvink, J. A. T. M. van Kester, and G. S. Stelling (2004), Development and validation of a three-dimensional morphological model, *Coastal Eng*, 51 (8--9), 883--915, doi:10.1016/j.coastaleng.2004.07.014.
- Meyer-Peter, E., and R. Müller (1948): Formulas for bed-load transport. In: Proc. 2nd IAHR World Congress, 6-9 June, Stockholm, Sweden, pages 39-64.
- Olink, E., and J. Sieben, J. (2024): Korte verkenning scan rivierbodem met hardere ondergrond. Memo RWS-WVL of 11-06-2024.
- Onjira, P. (2023), Living lab Rhine (LiLaR): Comparison of sediment measurement methods between the Netherlands and Germany, Tech. Rep., BfG.
- Ribberink, J. S. (1987). Mathematical modelling of one-dimensional morphological changes in rivers with non-uniform sediment. Ph.D. thesis, Delft University of Technology, Delft, the Netherlands.
- Rijkswaterstaat-ON (2010): Sedimentbeheer Rijntakken 2010-2015. RWS/DON-20 10/9366, 11 oktober 2010.

Rijkswaterstaat-ON (2022): Trajectindeling ten behoeve van monitoring van bodemtrends voor de Rijntakken. Memo Rijkswaterstaat Oost-Nederland 3 maart 2022.

Rijkswaterstaat-WVL (2017): Advies sedimentbeheer Rijn-Maasmonding. RWS-2017/15177, 22 maart 2017.

Sieben, J., R. van der Veen, D.F. Kroekenstoel and M. Schropp (2005): Morfologische effecten Ruimte voor de Rivier in het Bovenrivierengebied. Tech. Rep. 20005.044X, RIZA, Directoraat-Generaal Rijkswaterstaat, Arnhem, The Netherlands.

Sieben, J. (2014). Schatting alluviale ruwheid in binnenbochten met constructies, Arjan Sieben 18-03-2005, met aanvulling vaste laag Boven-Rijn 2013 d.d. 26-03-2014. Memo.

Sloff, K., A. Paarlberg, A. Spruyt, M. Yossef (2009): Voorspelinstrument Duurzame Vaardiepte Rijndelta. Continued development and application of morphological model DVR Part 2: model adjustment. Deltares report 1002069-002-ZWS-0005, June 2009.

Sloff, K. (2019): Prognose bodemligging Rijntakken 2020-2050. Trends voor scheepvaart en waterbeschikbaarheid. Deltares-rapport 1203738-005-BGS-0008, 20 december 2019.

Tönis, R. (2010). Sedimentbeheer Rijntakken 2010-2015. RWS Oost-Nederland, 11 oktober 2010.

Treurniet, M. and Tönis, R. (2019). Sedimentmanagement Rijntakken. RWS Oost-Nederland.

Van der Wijk, R. (2022). Afleiden QH-relatie Rijn-Maasmonding voor Rijntakken en Maas. Deltares memo 11206813-006-ZWS-0008.

Van Dongeren, A., M. van der Lugt, B. Röbbke, C. Swinkels, A. Luijendijk, E. Moerman, and M. Gawehn (2018), Delft3D FM morphology: results of testing, rapport Deltares, concept I1000394-002, Deltares, Delft, 25 pp.

Van Doorn, S. (2023). Rivierkundig Beoordelingskader voor ingrepen in de Grote Rivieren. Version 6.0. Rijkswaterstaat Water, Verkeer en Leefomgeving, January 23, 2023.

Van Vuren, S. and Ottevanger, W. (2006). Inbouw duinhoogte- en ruwheidsvoorspellers in Delft3D-MOR. Report Q4190, Delft Hydraulics, November 2006.

Wong, M., & Parker, G. (2006). Re-analysis and correction bedload relation of Meyer-Peter and Muller using their own database. Journal of Hydarulic Engineering, Volume 132, Issue 11.

Yossef, M. F. M., H. R. A. Jagers, S. van Vuren and A. Sieben (2008): Innovative techniques in modelling large-scale river morphology." In M. Altinakar, M. A. Kokpinar, 'Ismail Aydin, S. evket Cokgor and S. Kirgoz, eds., Proceedings of the 4th International Conference on Fluvial Hydraulics (River Flow), 3-5 September, Cesme, Izmir, Turkey. Kubaba Congress Department and Travel Services, Ankara, Turkey.

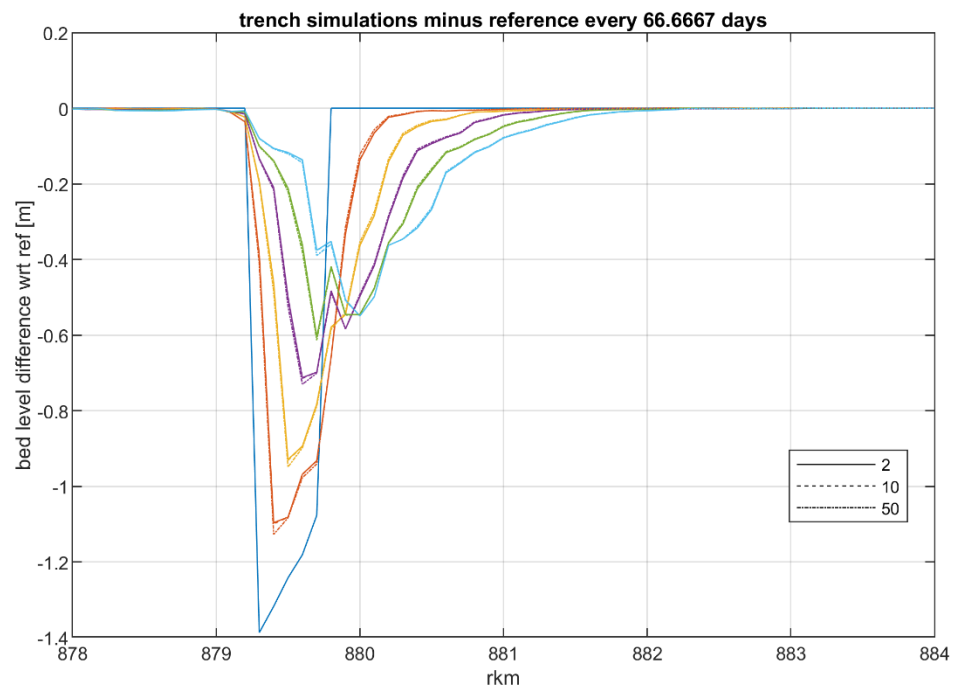
A Results analysis of morphological factor

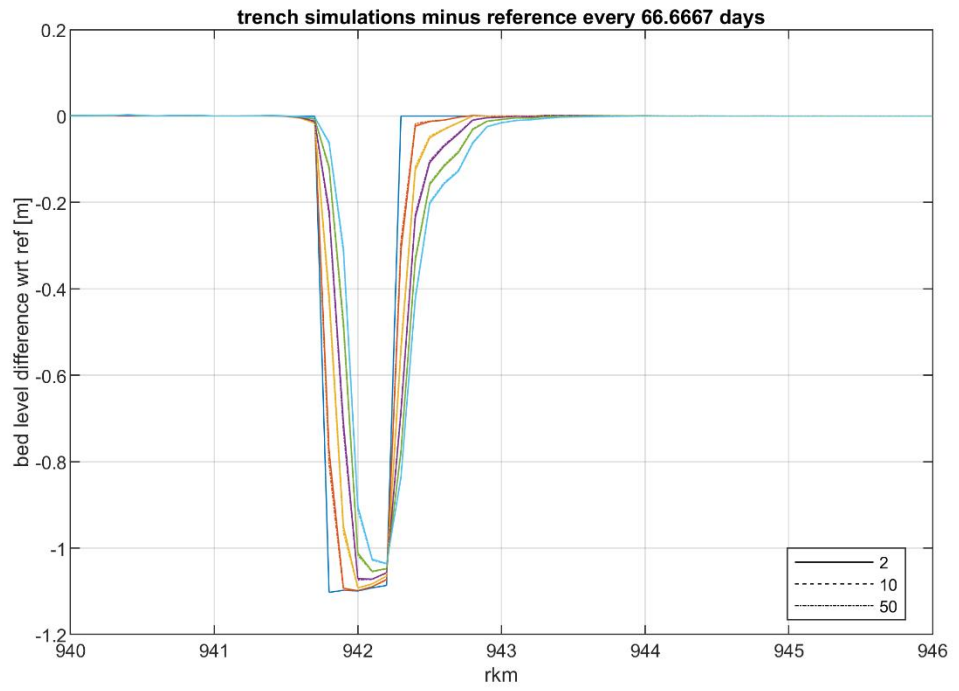
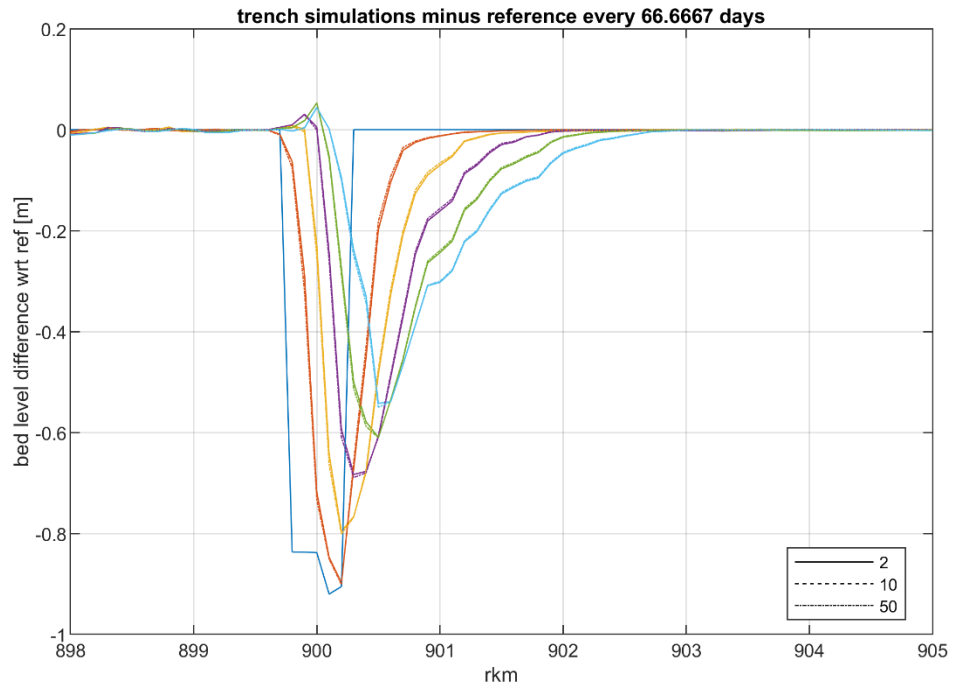
A.1 Trench movement

The figures below show the trench movement. For each discharge level and each selection of morphological factors, three figures are presented, which represent one of the three trenches each, on Boven-Waal (km 879.5), Midden-Waal (km 900), and Beneden-Waal (km 942).

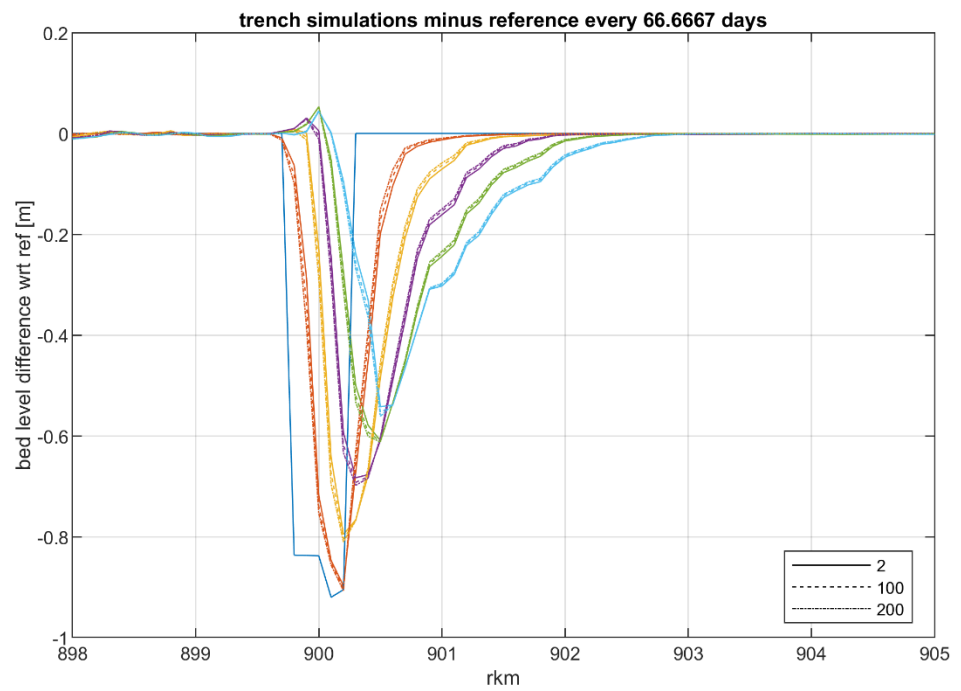
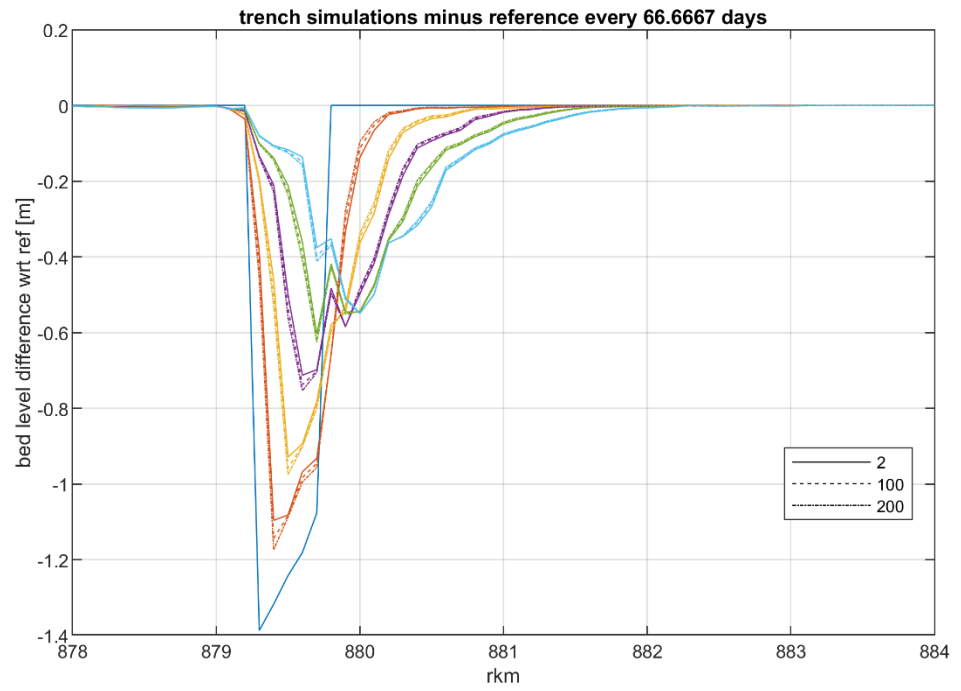
A.1.1 $Q_{\text{Lobith}} = 1.635 \text{ m}^3/\text{s}$

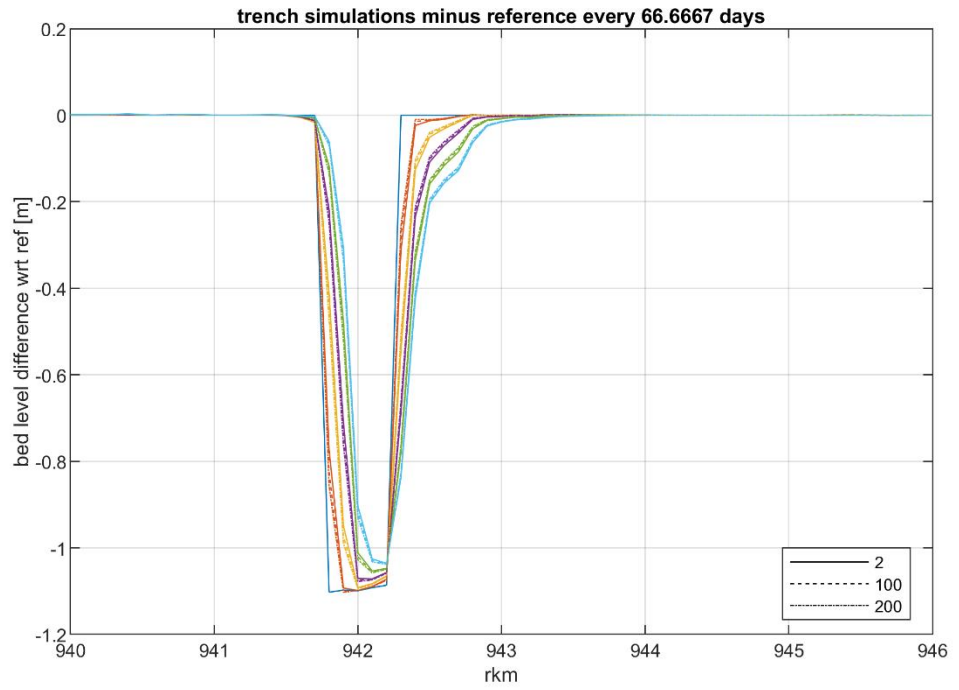
A.1.1.1. Morfac = 2, 10 and 50



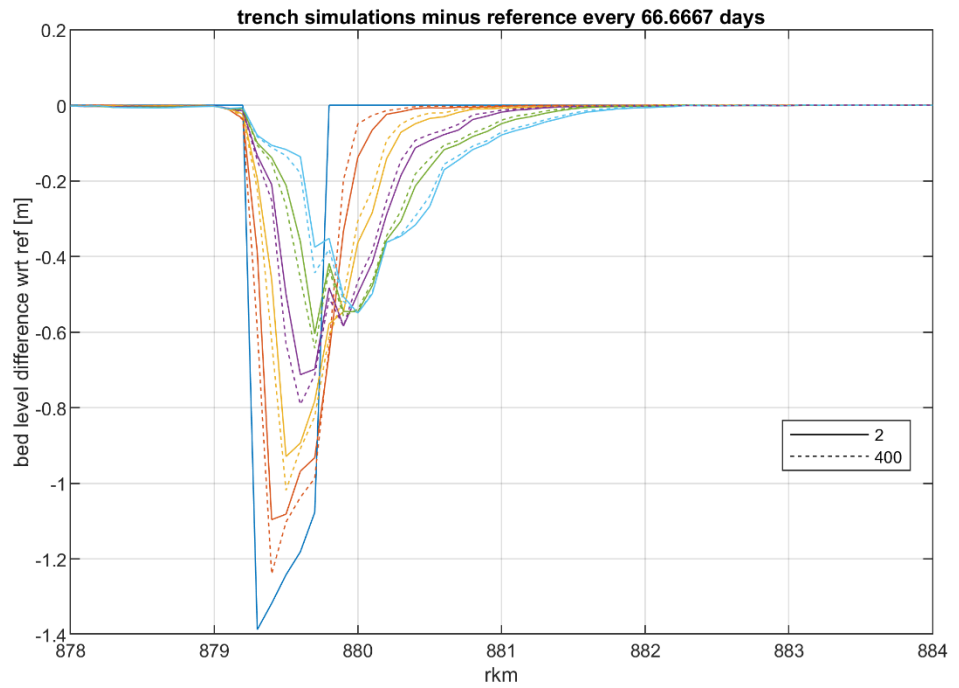


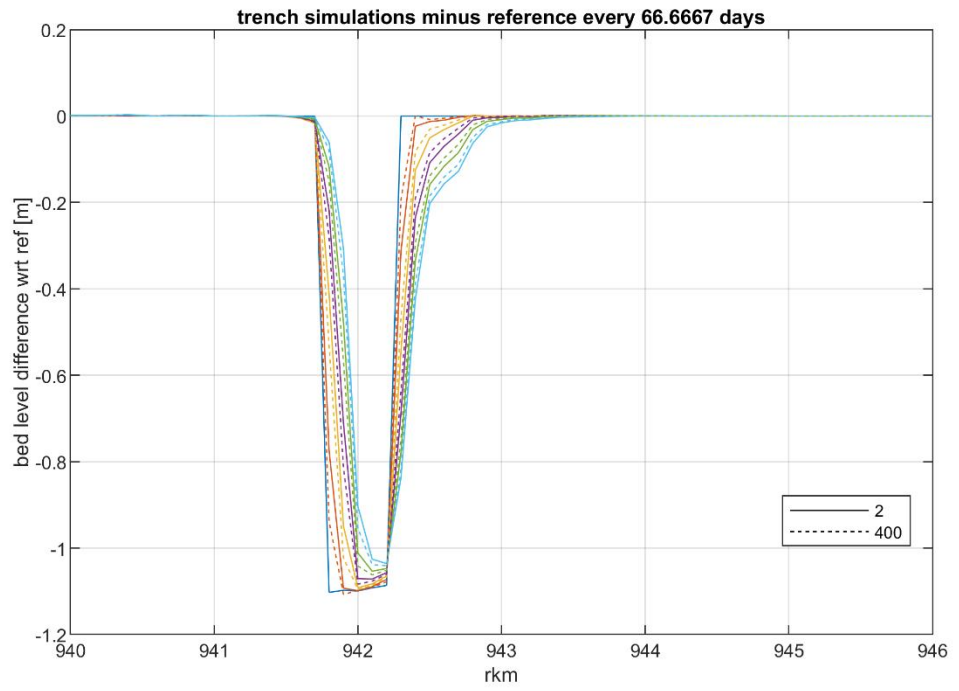
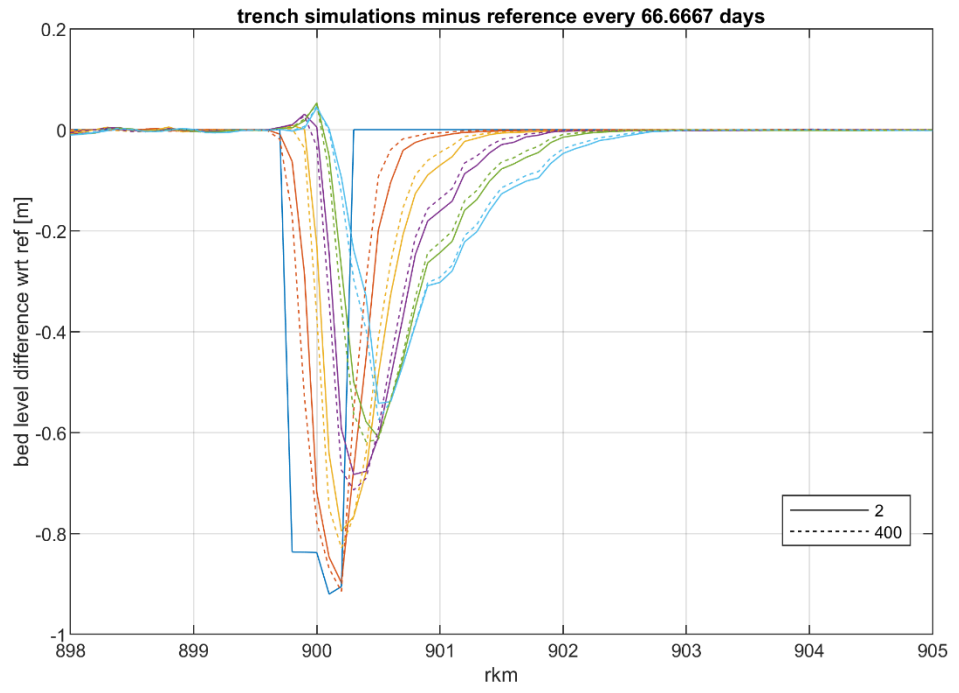
A.1.1.2. Morfac = 2, 100 and 200





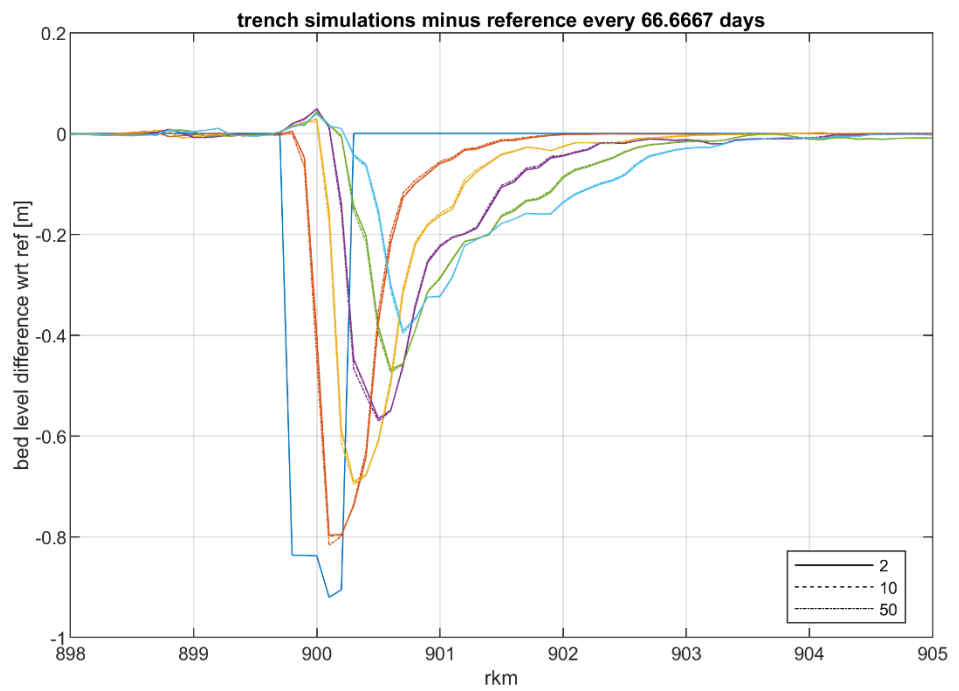
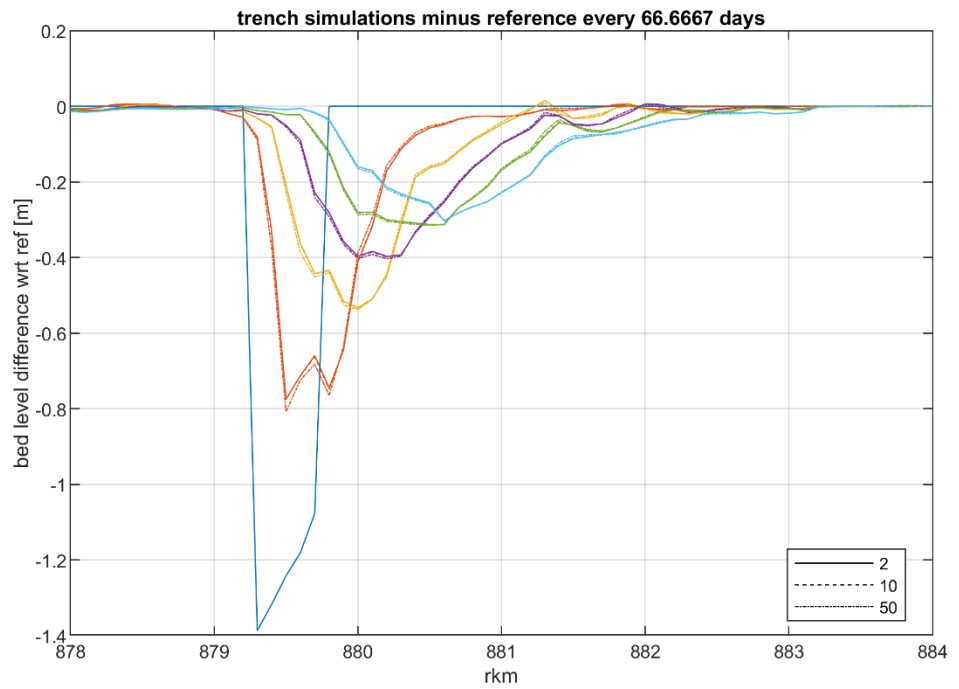
A.1.1.3. Morfac = 2 and 400

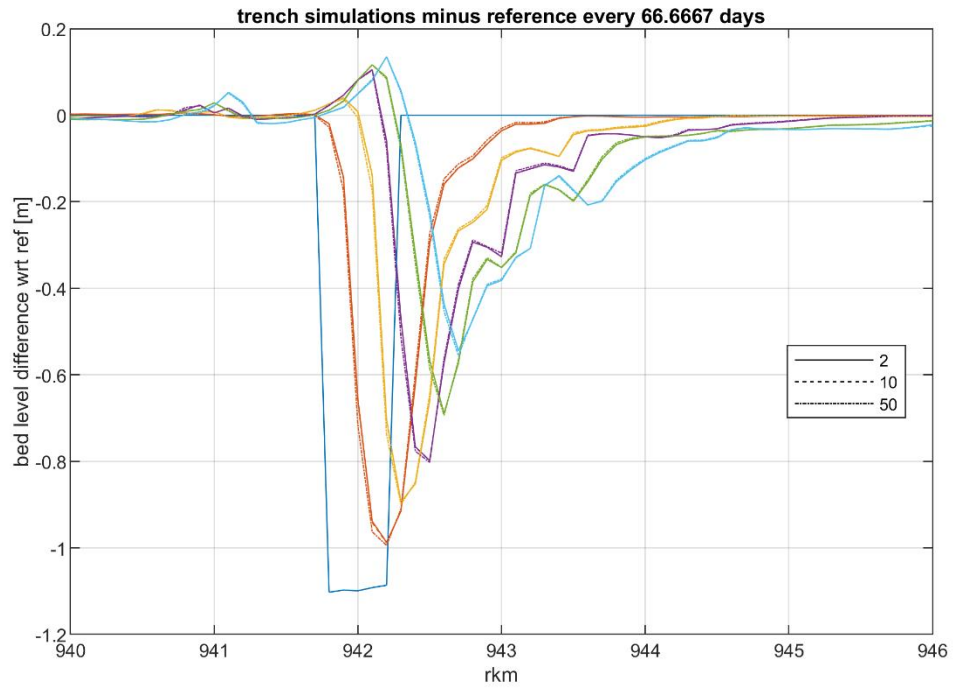




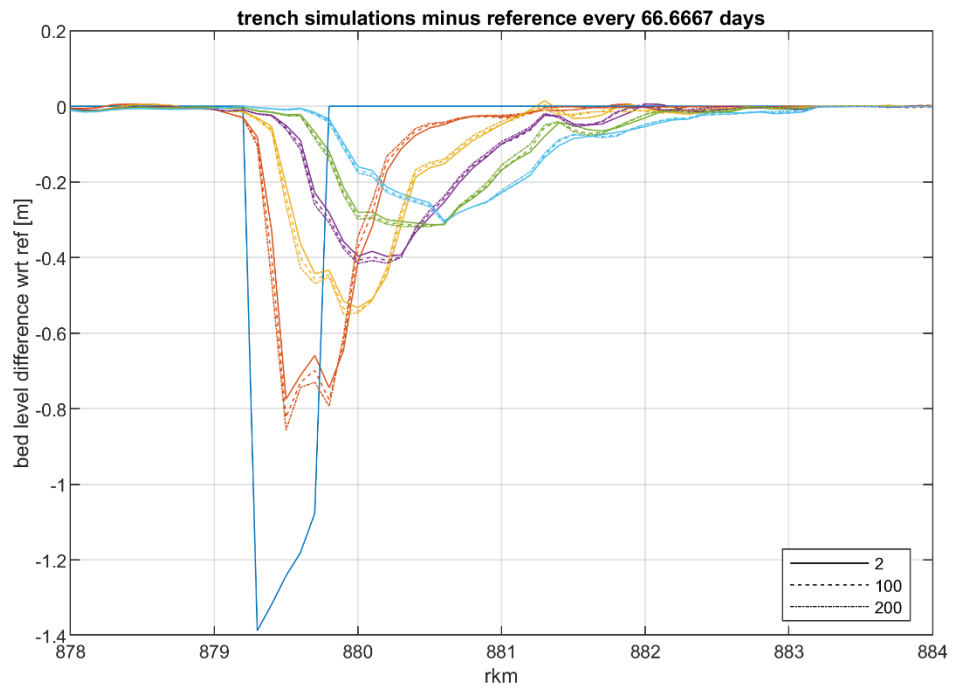
A.1.2 QLobith = 3.824 m³/s

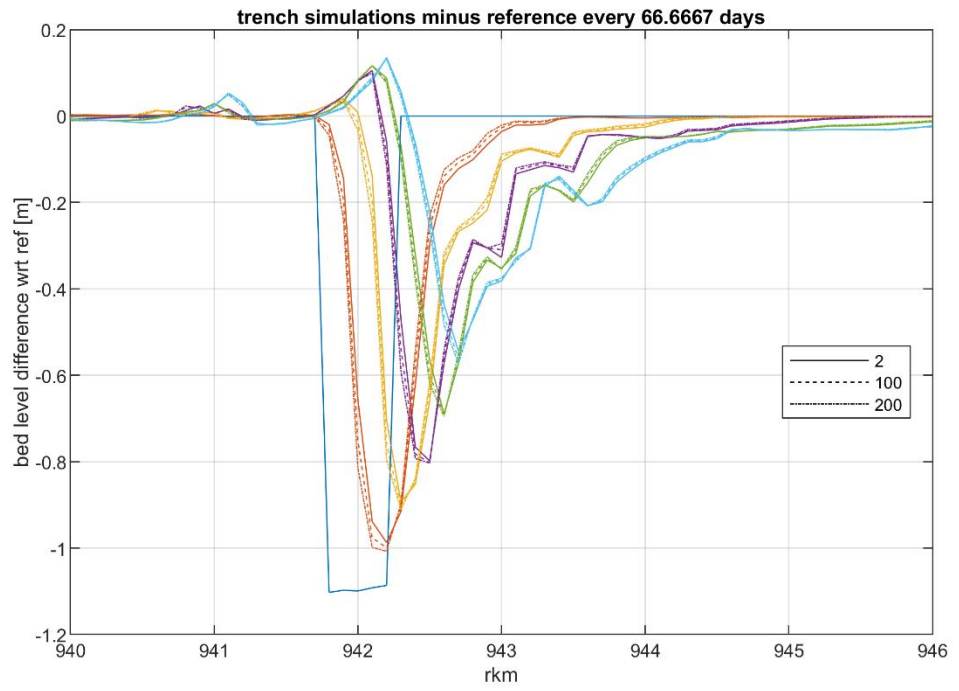
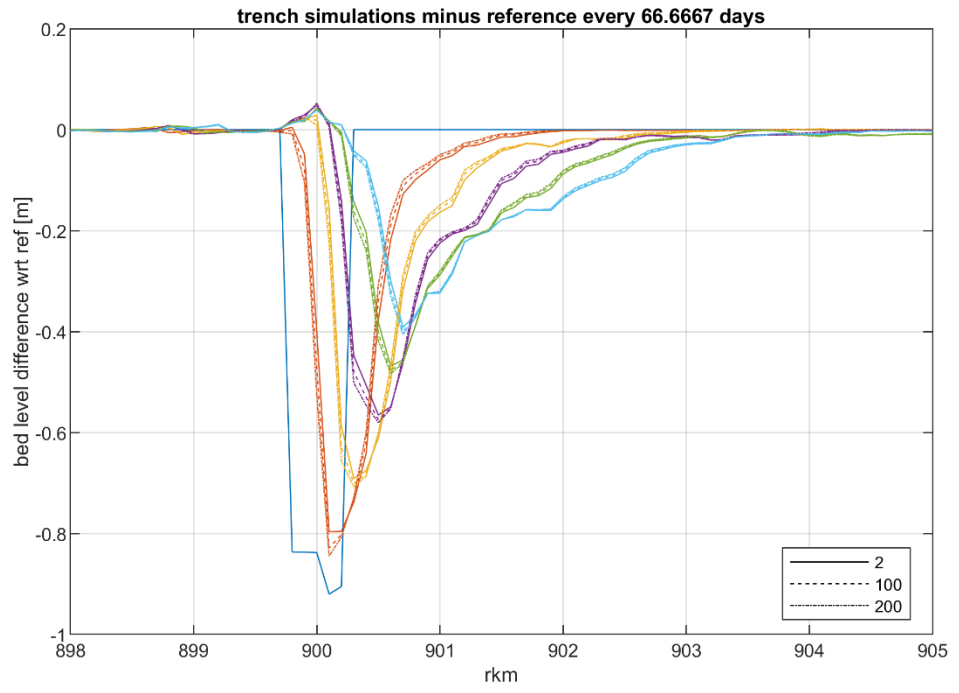
A.1.2.1. Morfac = 2, 10 and 50



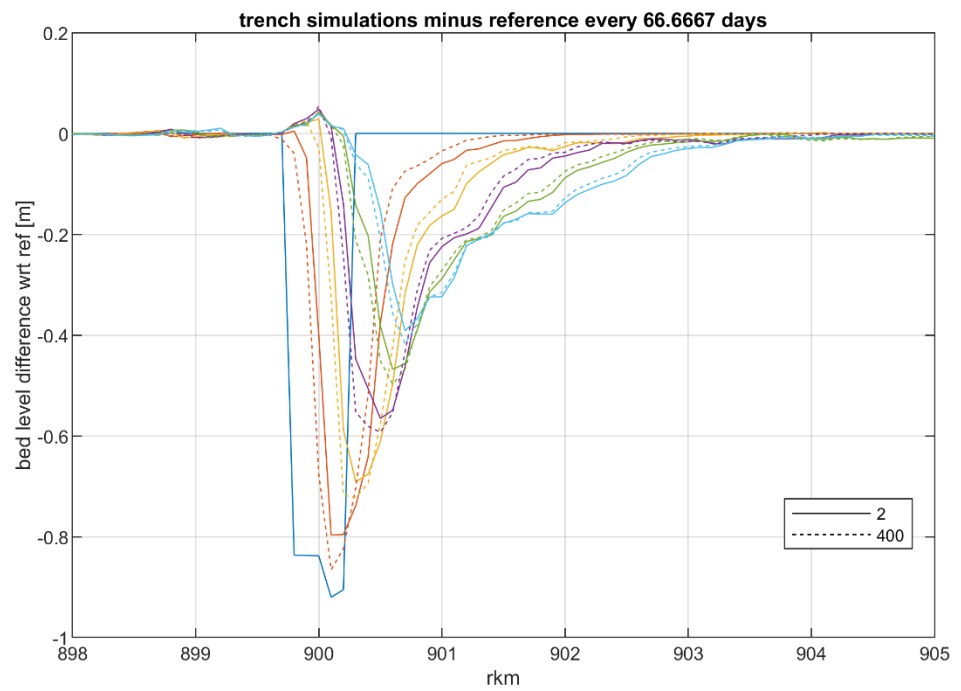
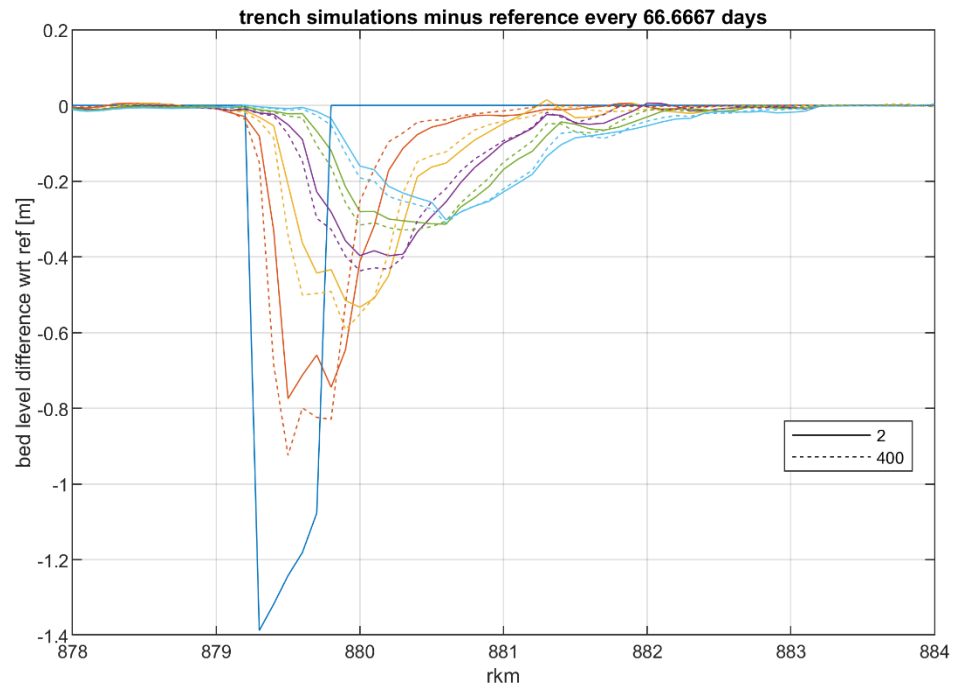


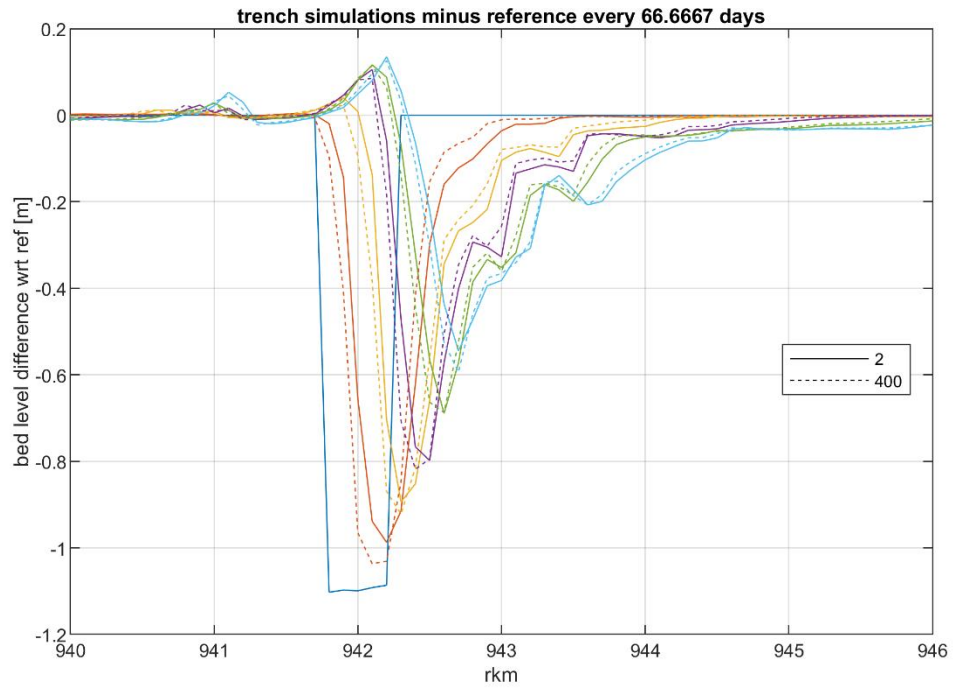
A.1.2.2. Morfac = 2, 100 and 200





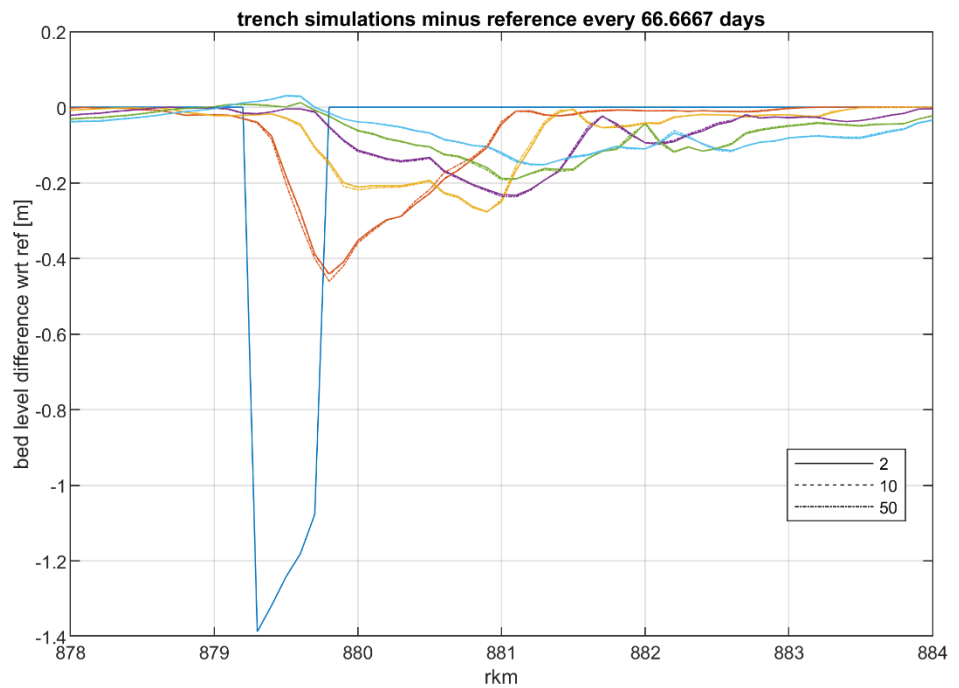
A.1.2.3. Morfac = 2 and 400

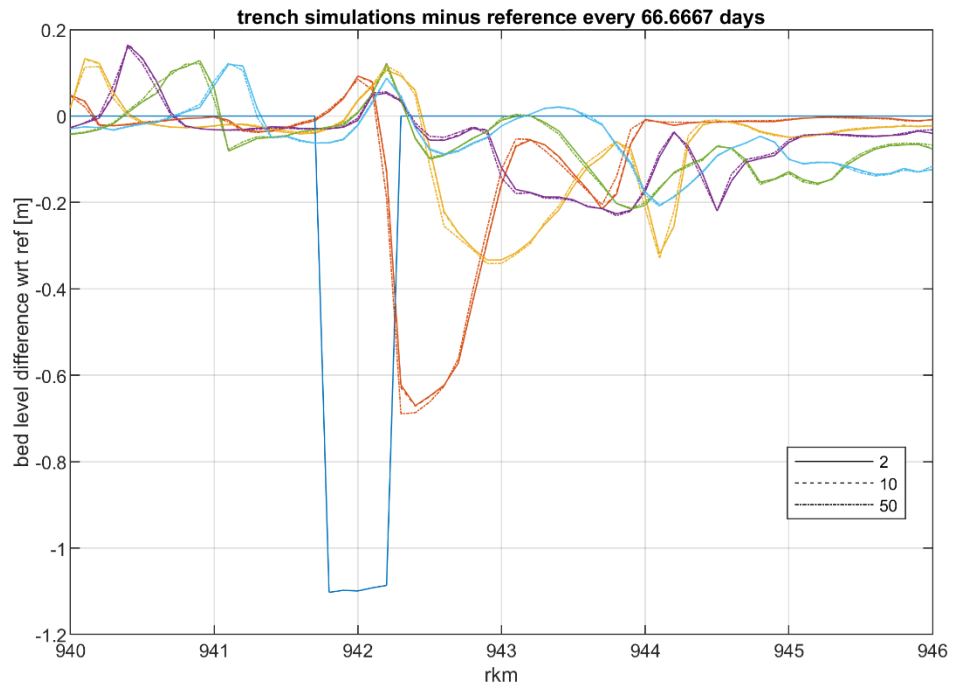
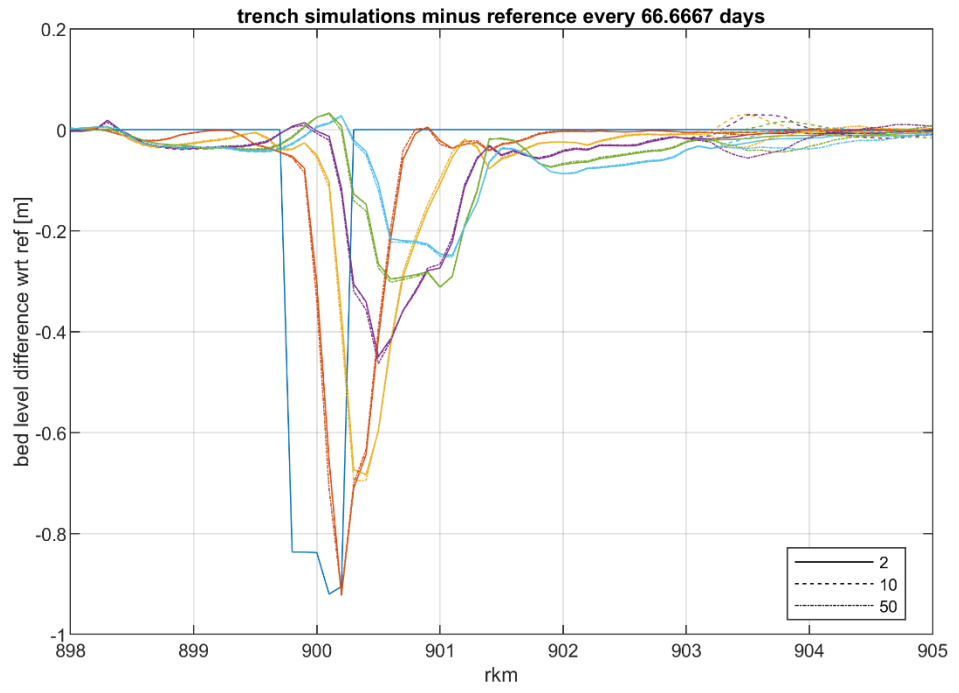




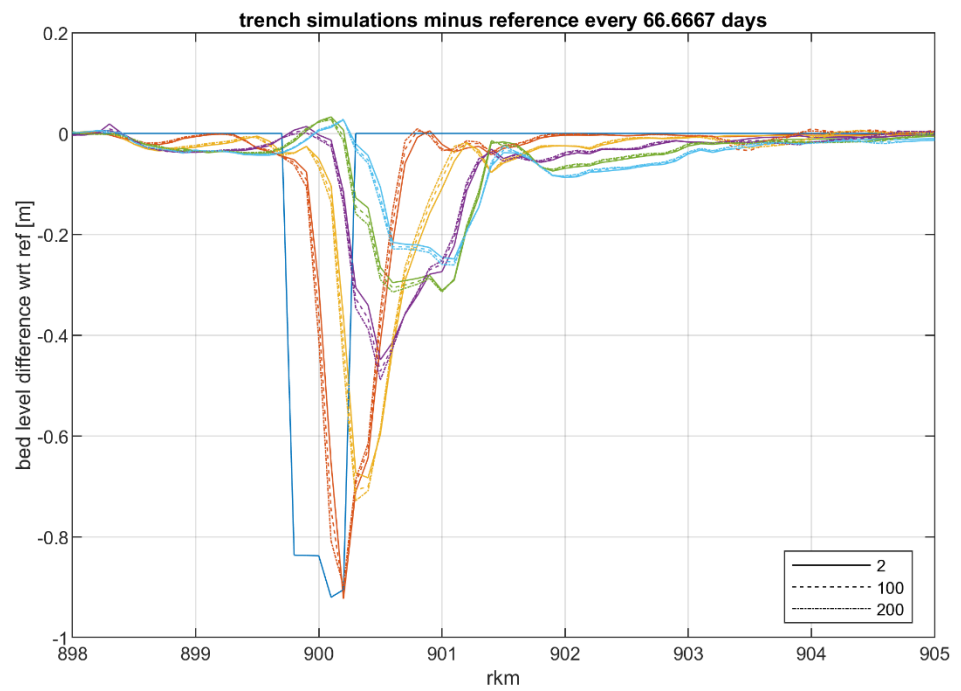
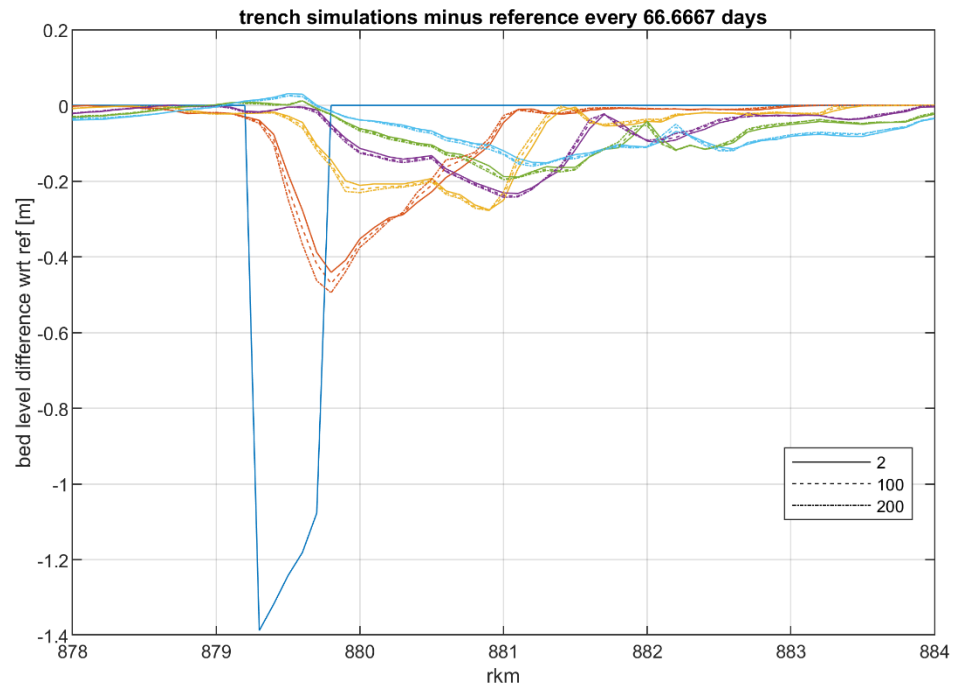
A.1.3 $Q_{Lobith} = 8.592 \text{ m}^3/\text{s}$

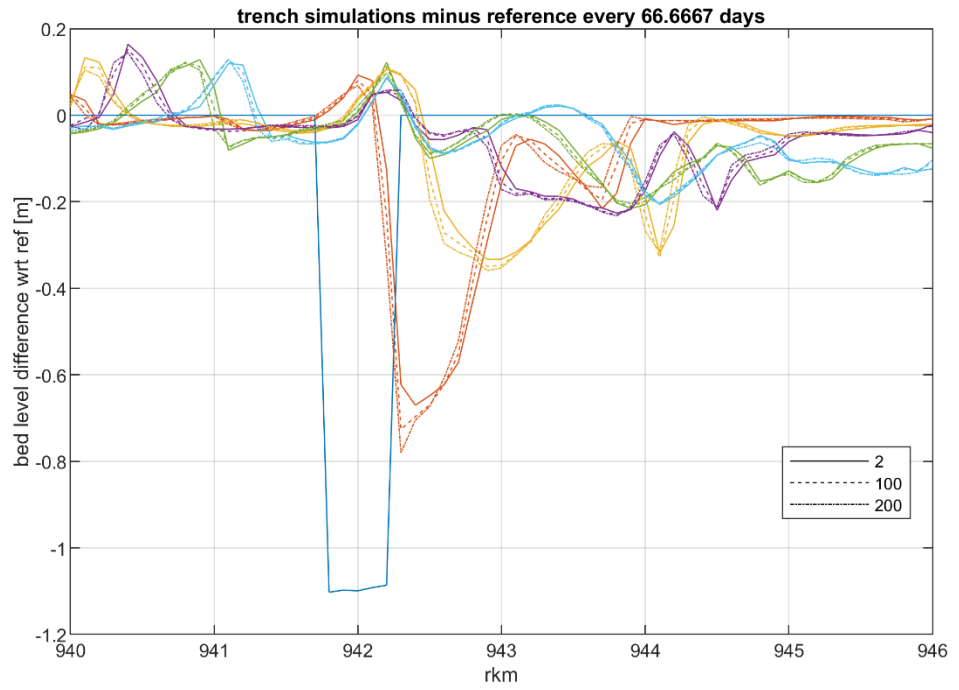
A.1.3.1. Morfac = 2, 10 and 50



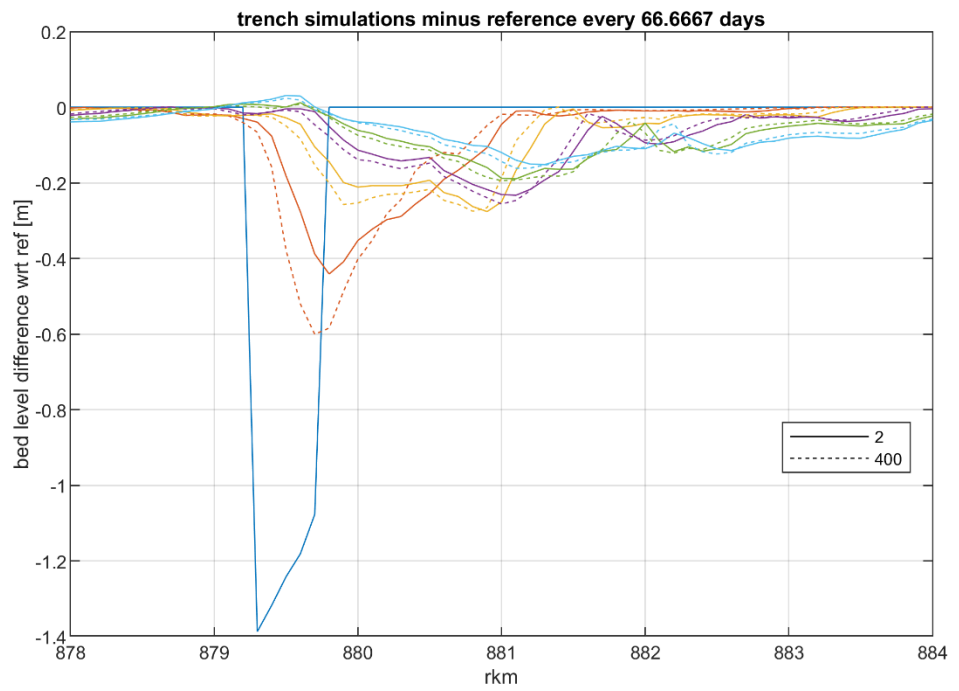


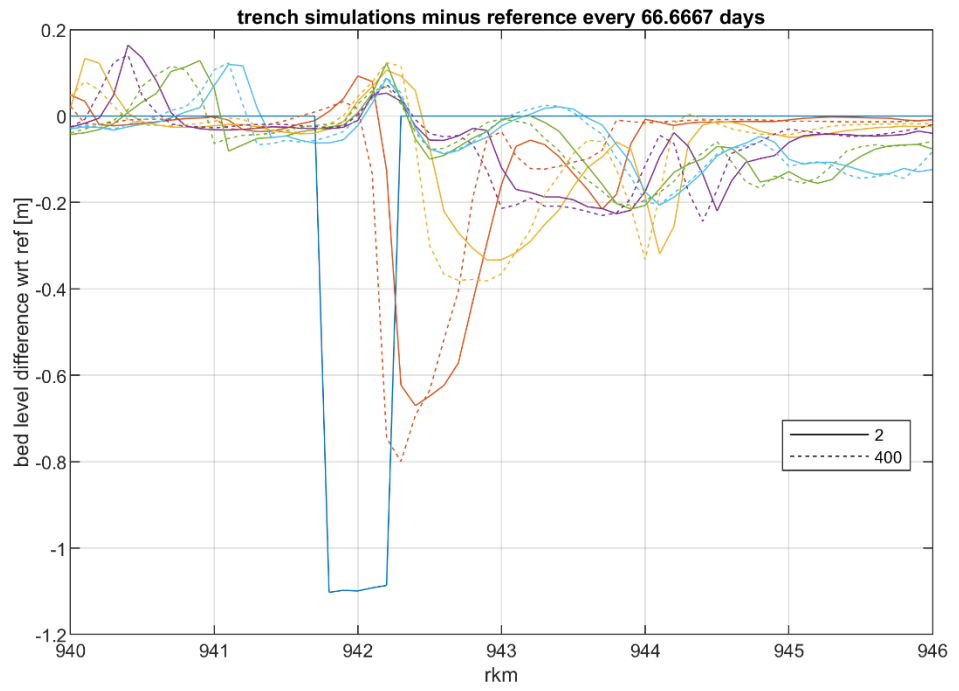
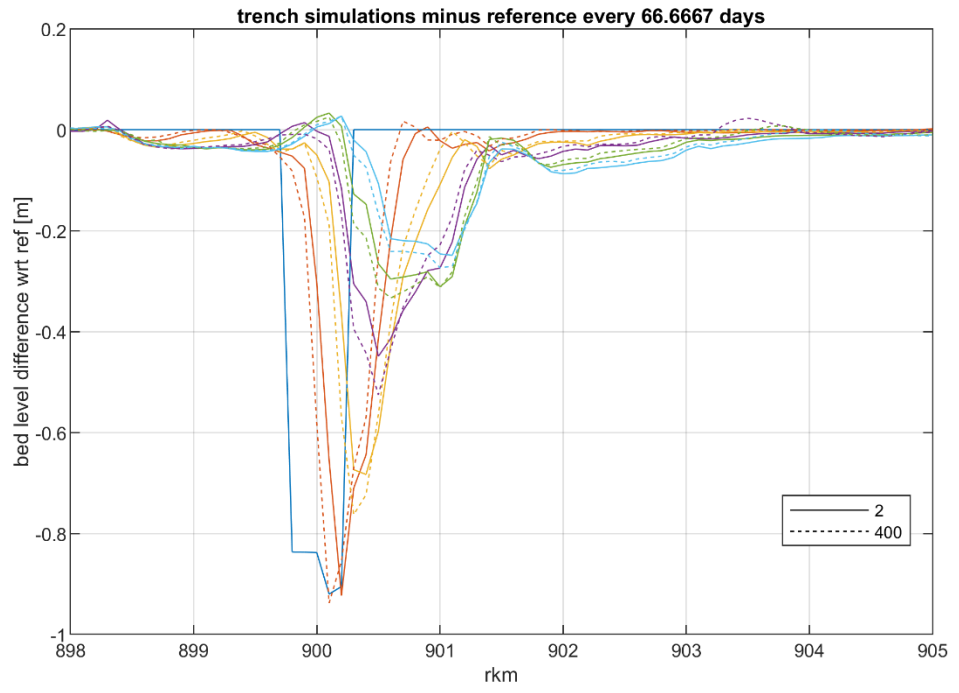
A.1.3.2. Morfac = 2, 100 and 200





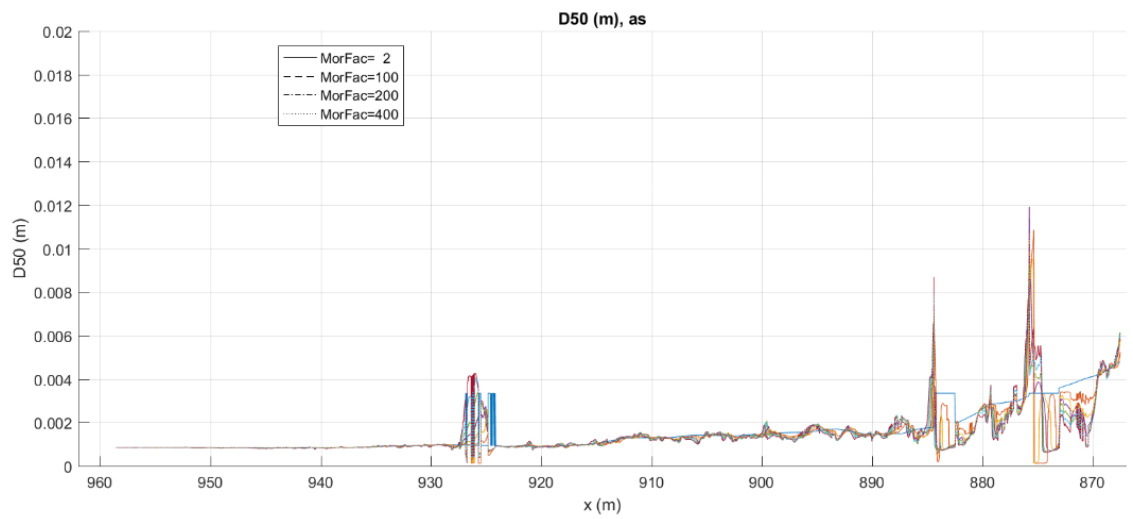
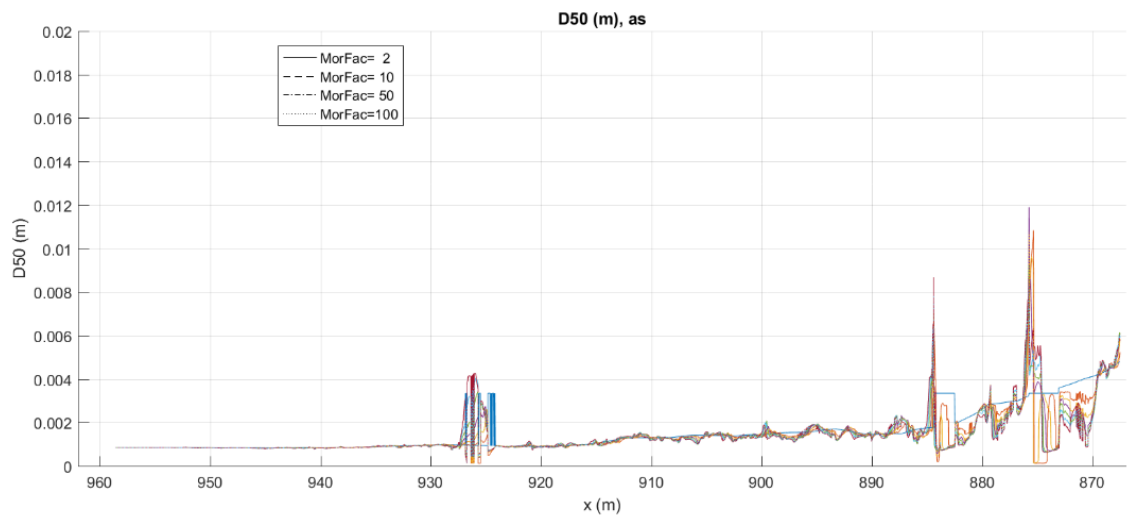
A.1.3.3. Morfac = 2 and 400



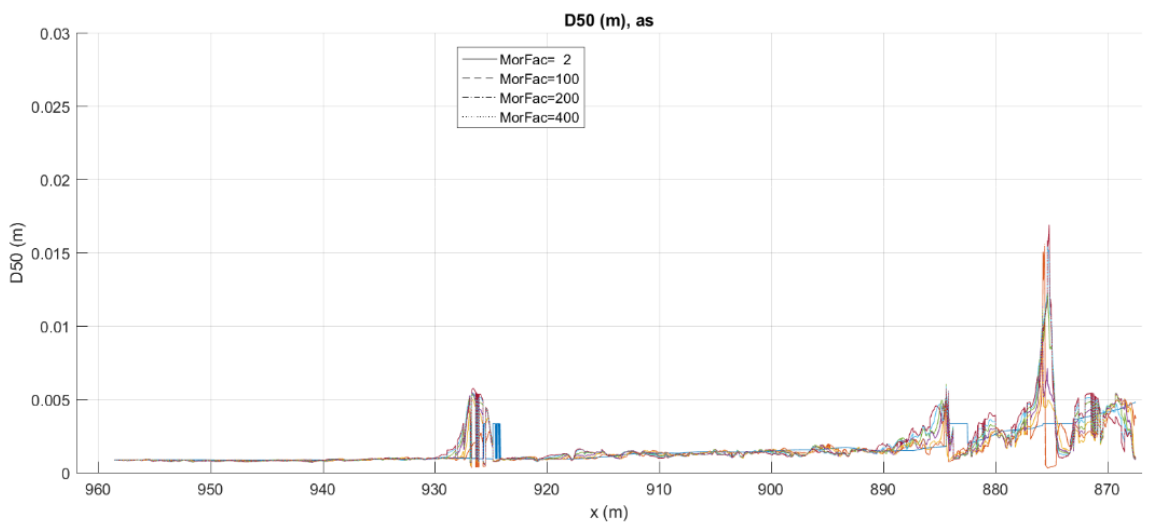
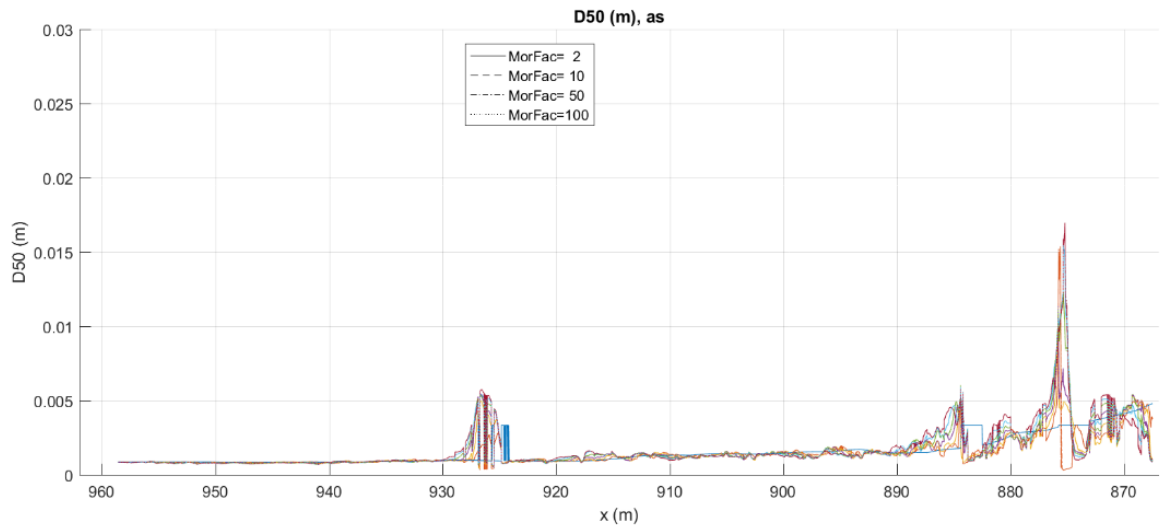


A.2 Sediment composition in trench simulations

A.2.1 $Q_{\text{Lobith}} = 1.635 \text{ m}^3/\text{s}$

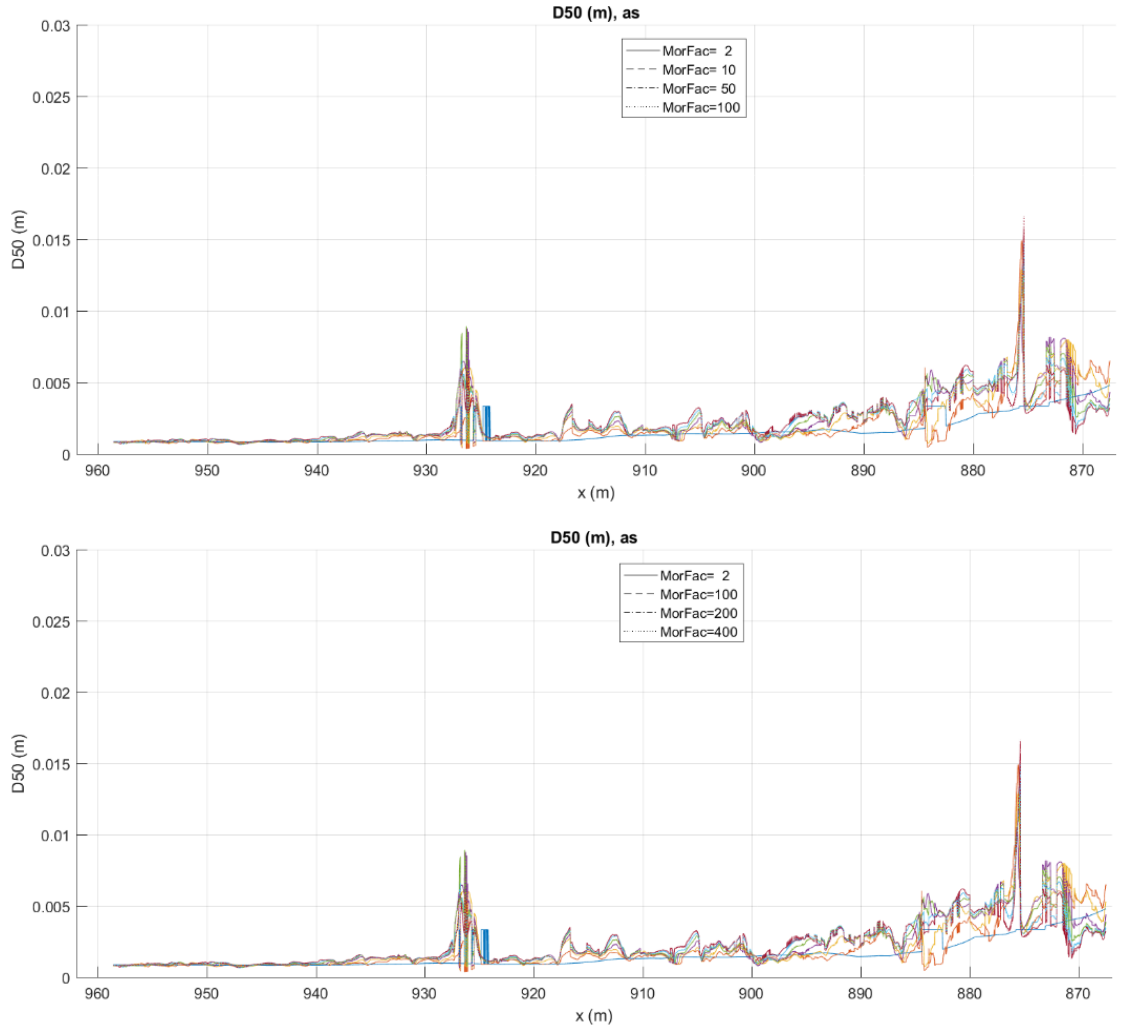


A.2.2 QLobith = 3.824 m³/s



A.2.3

$Q_{\text{Lobith}} = 8.592 \text{ m}^3/\text{s}$

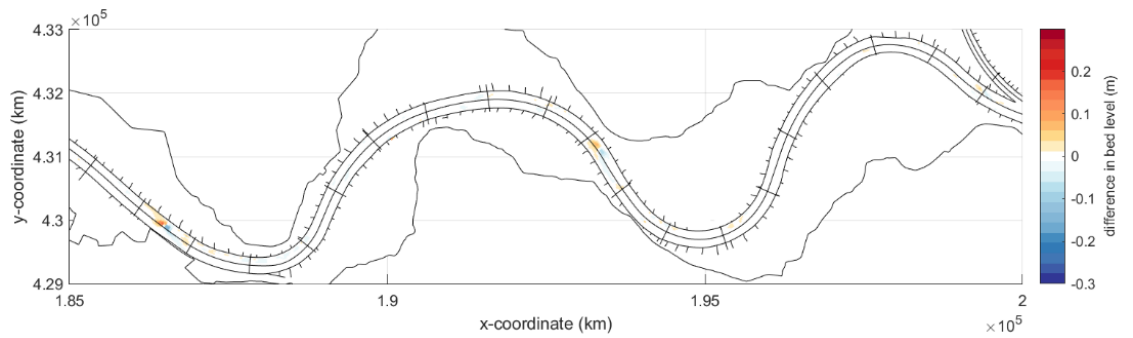


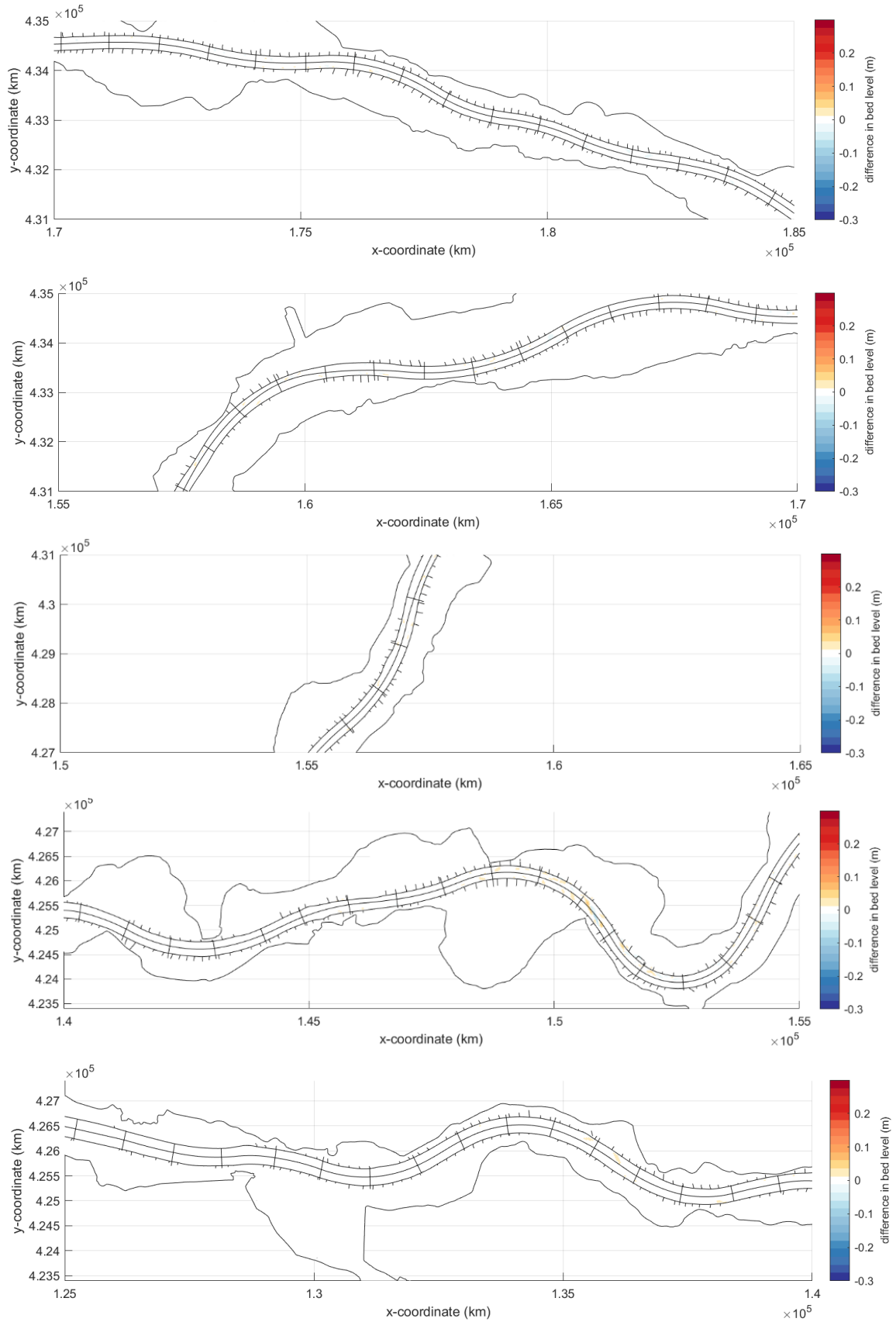
A.3

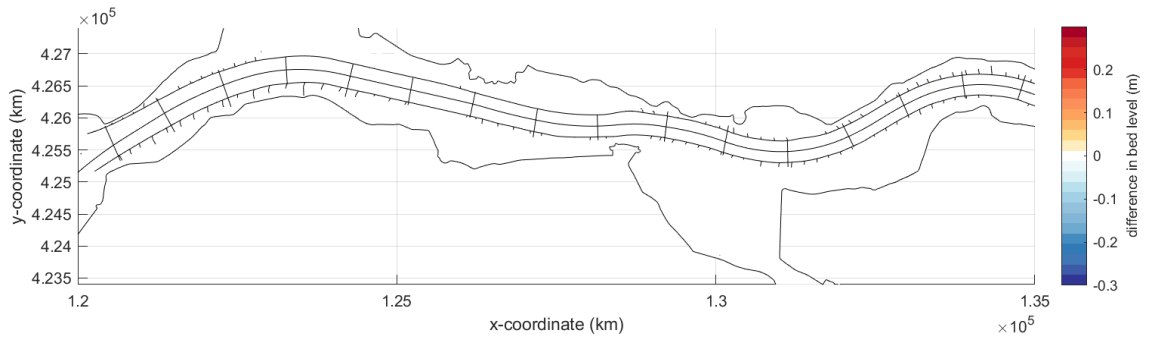
Bed level differences for hydrograph simulations

A.3.1

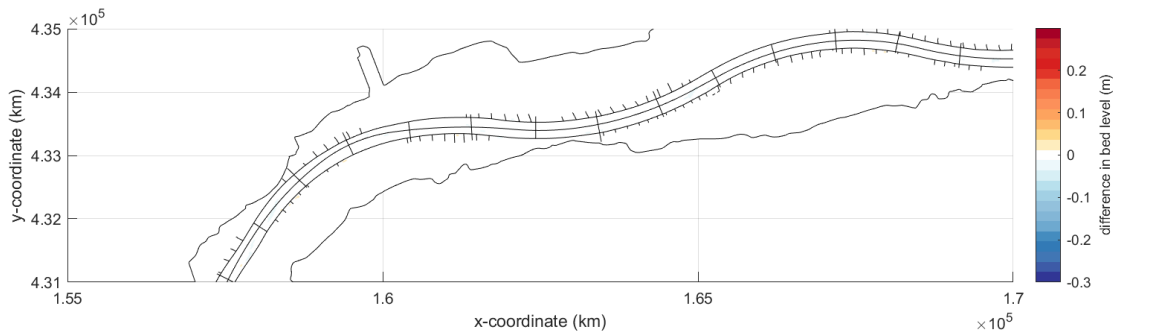
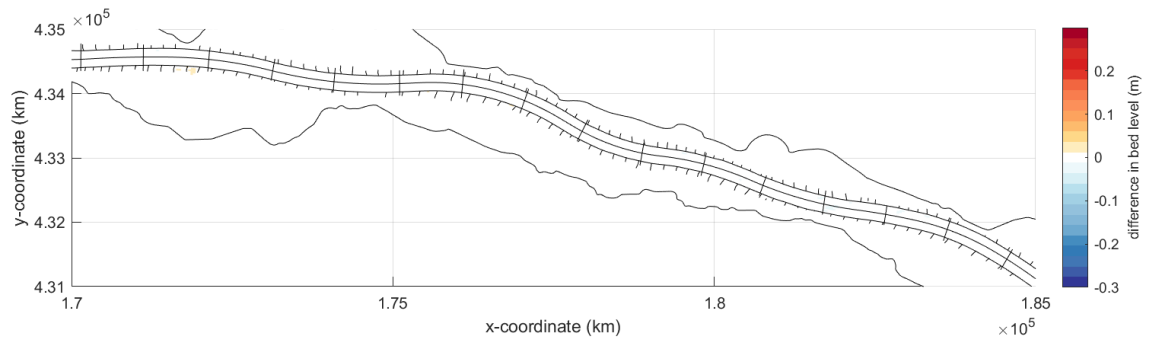
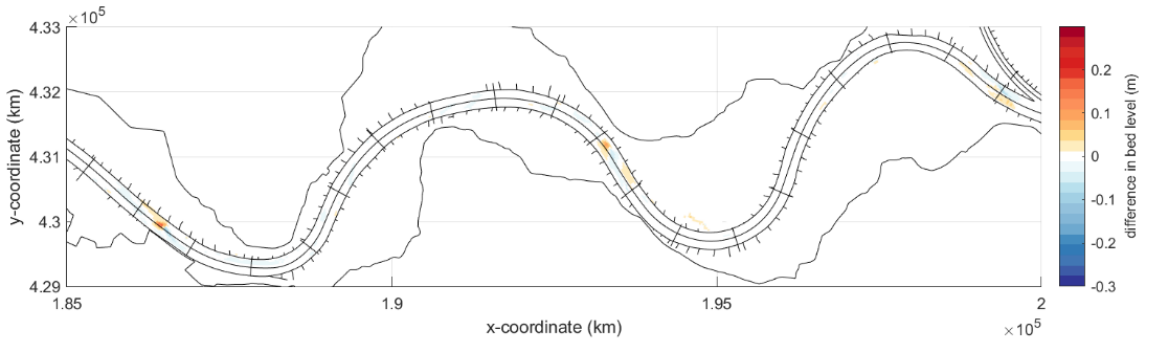
r068-r066

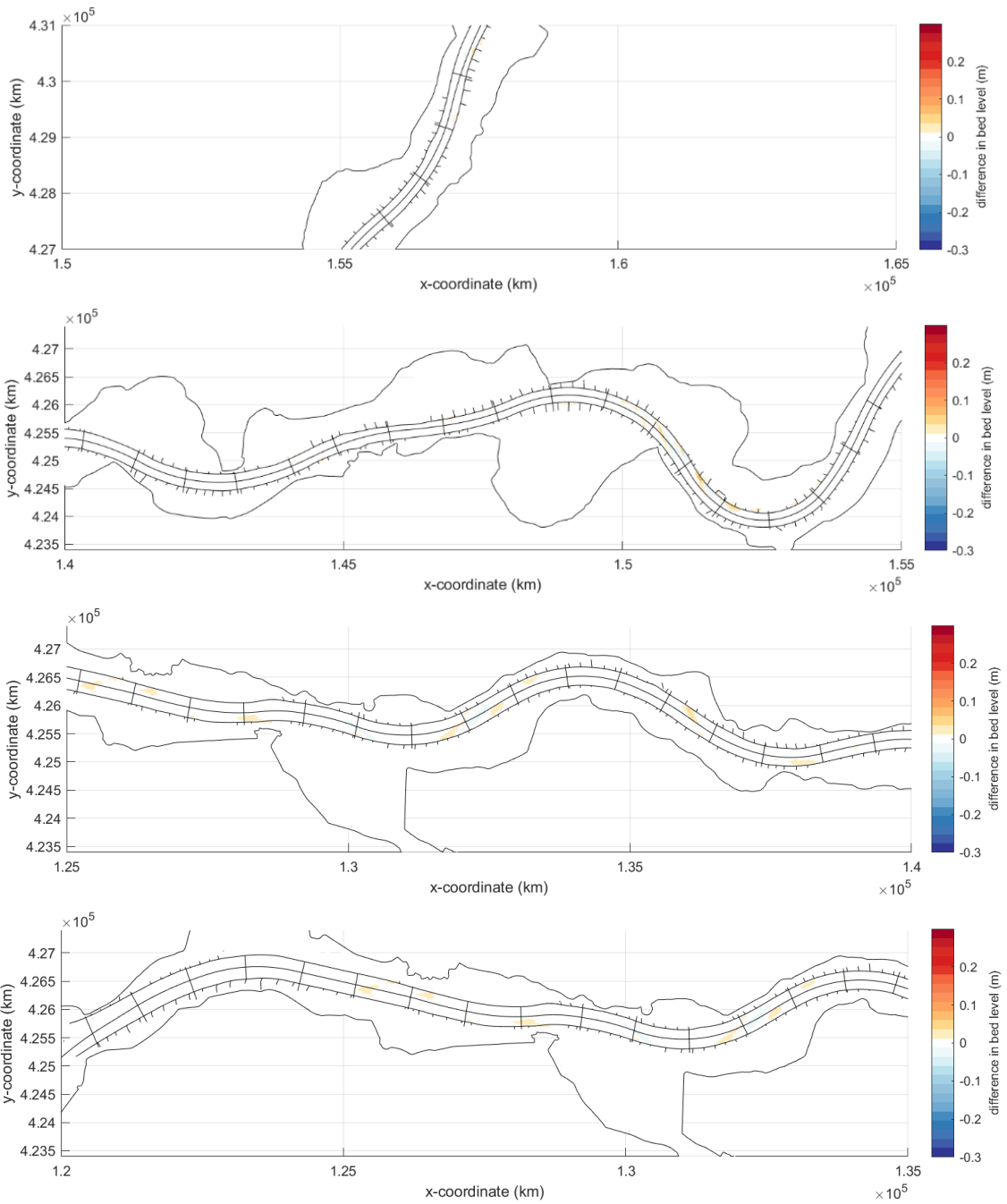


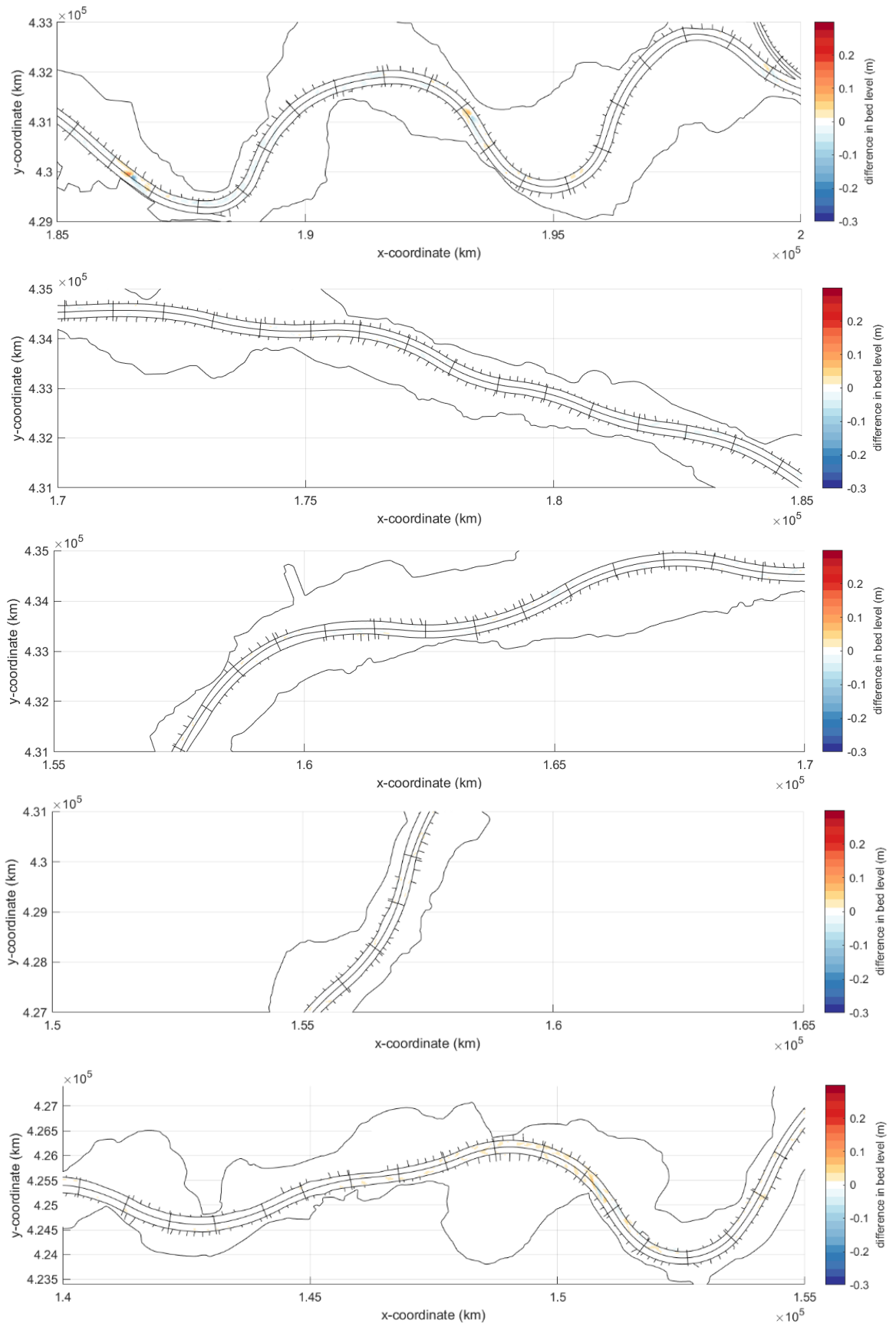


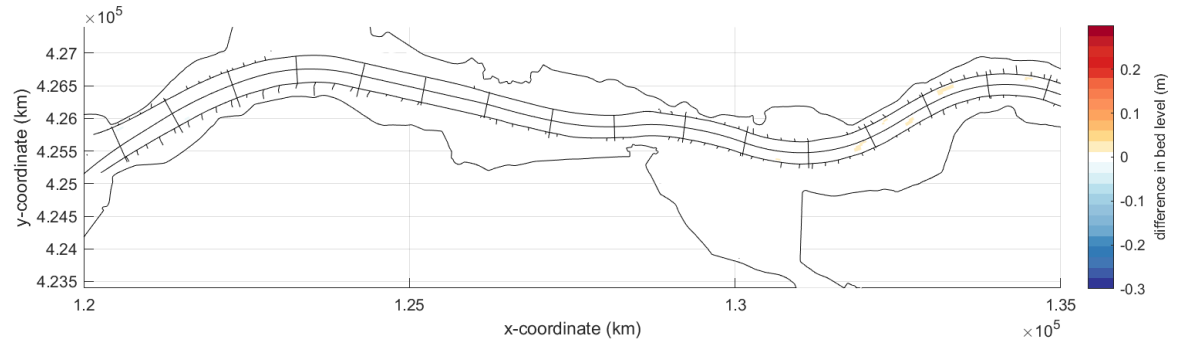
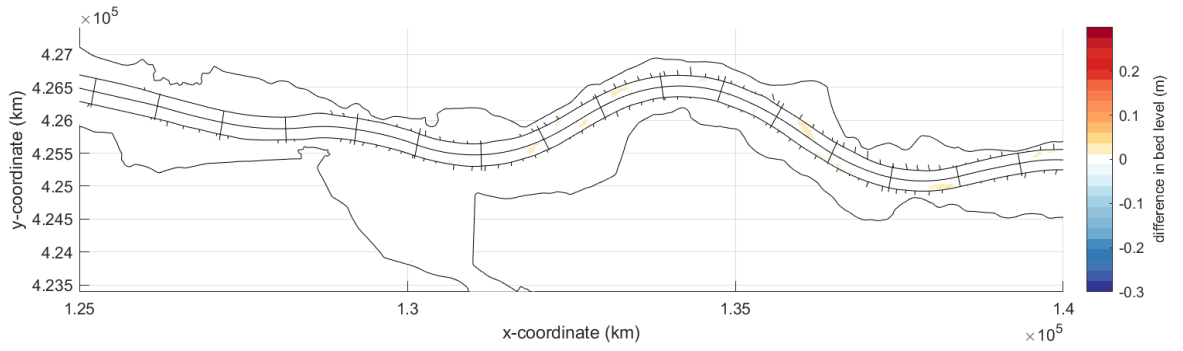


A.3.2 r067-r066

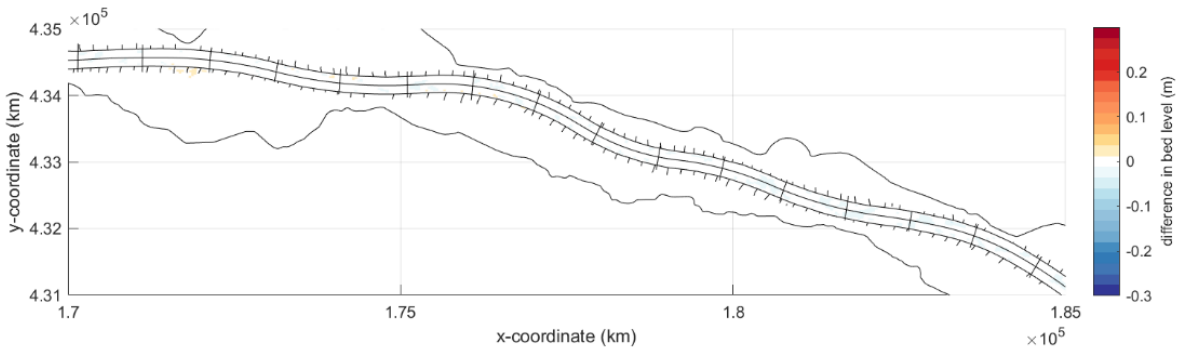
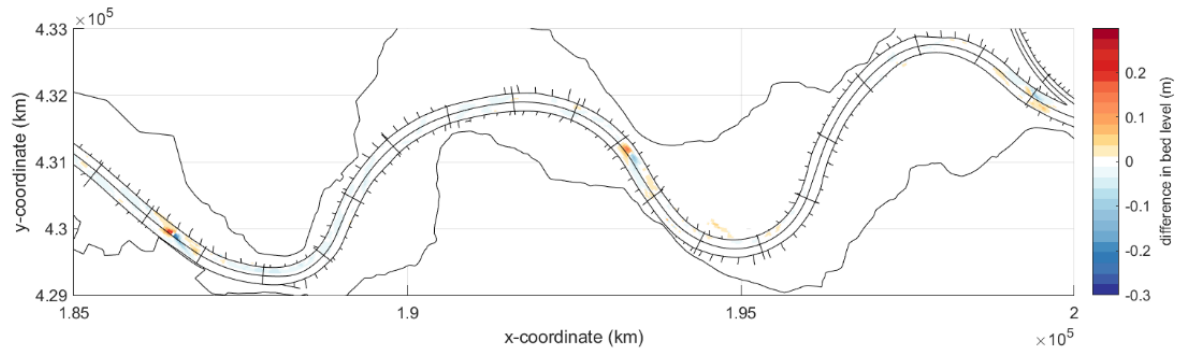


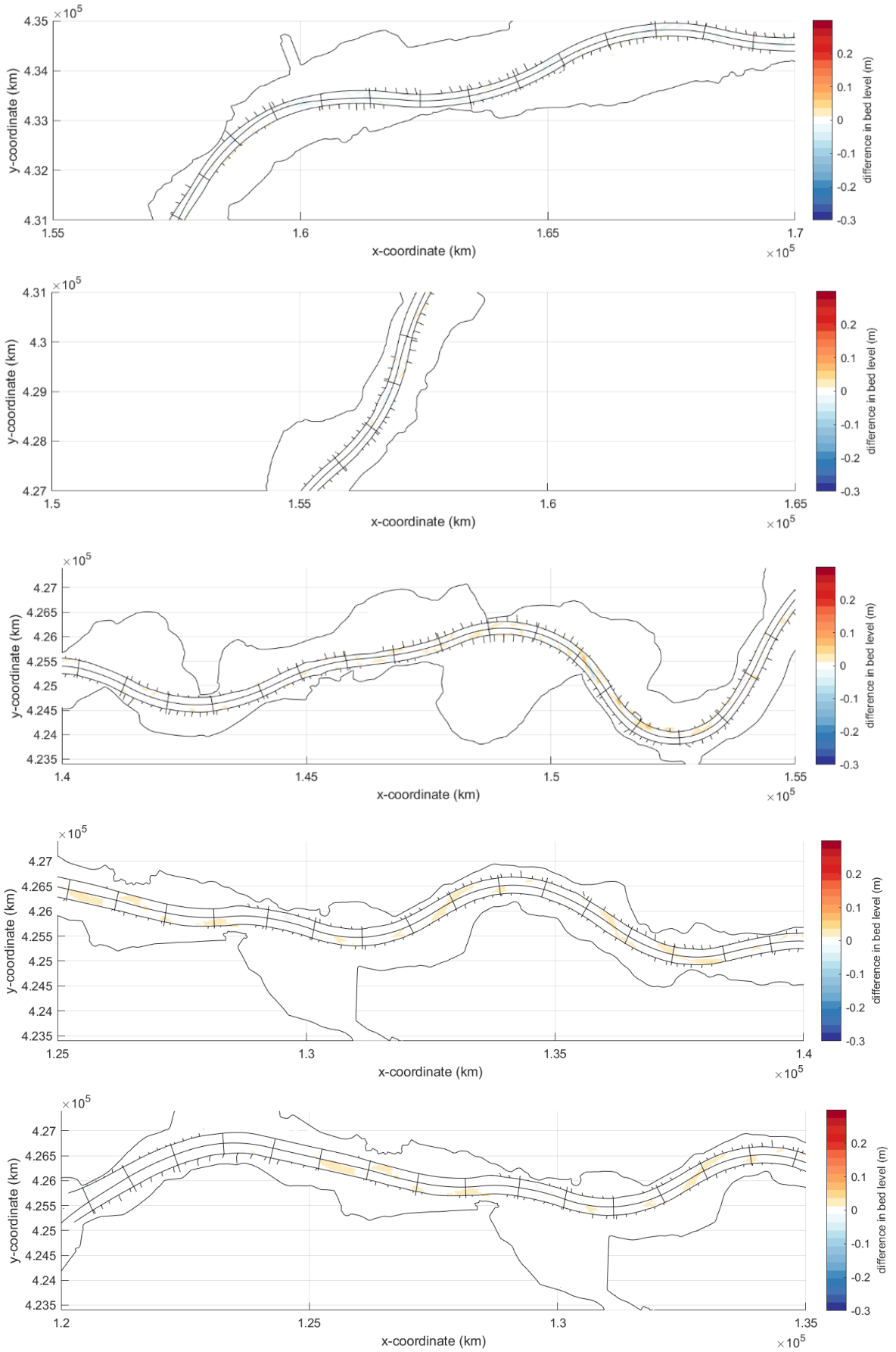


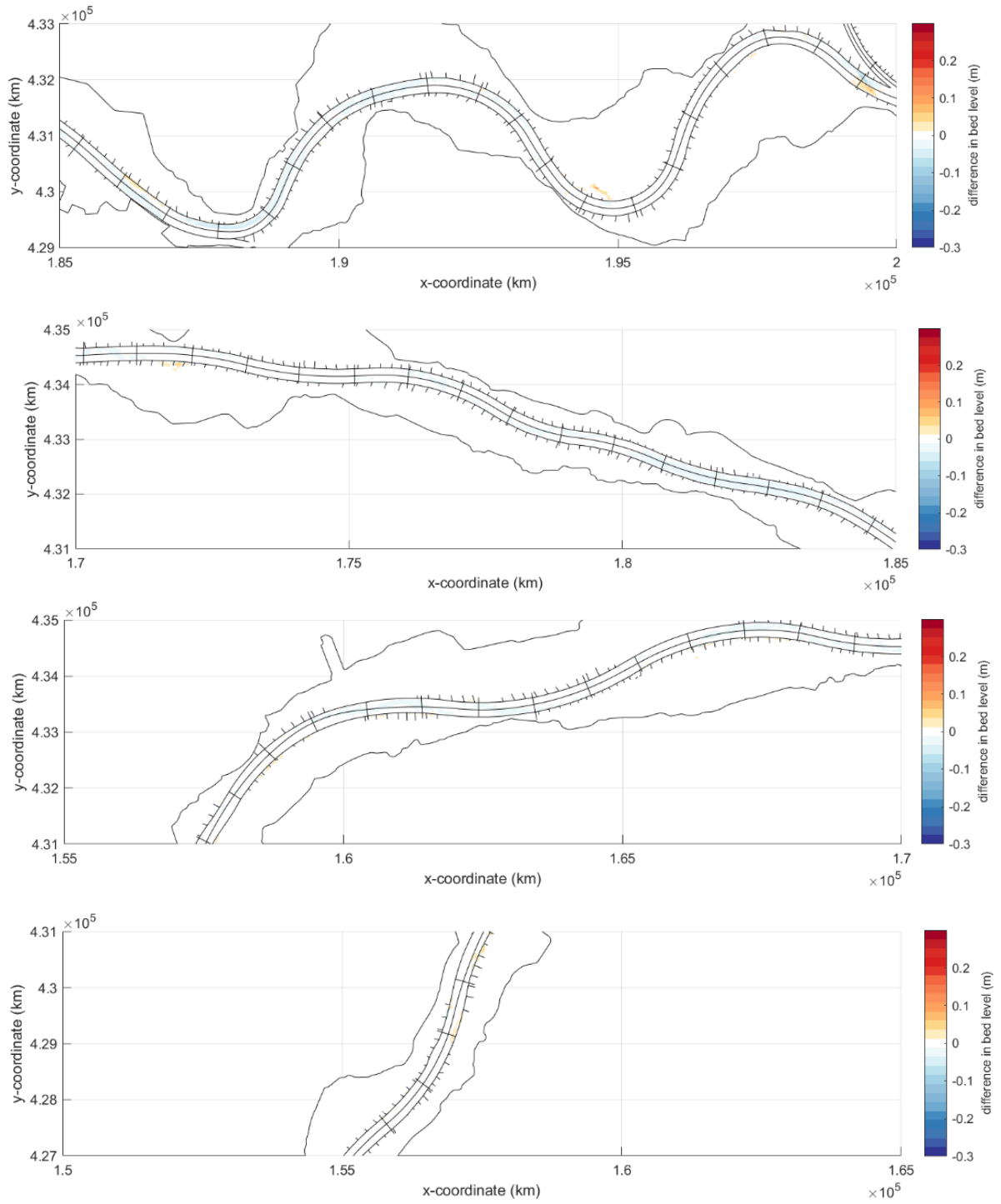


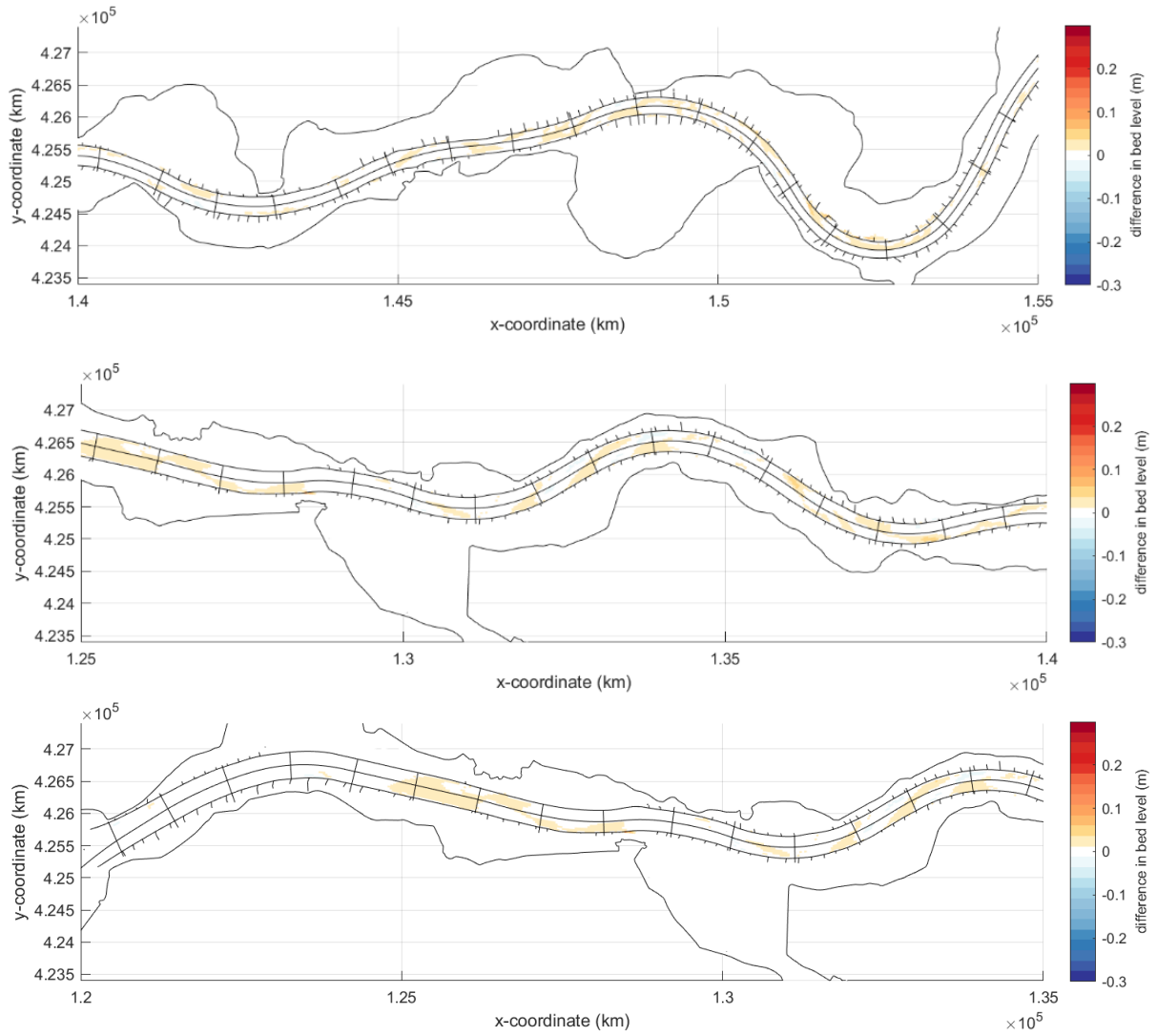


A.3.4 r072-r066



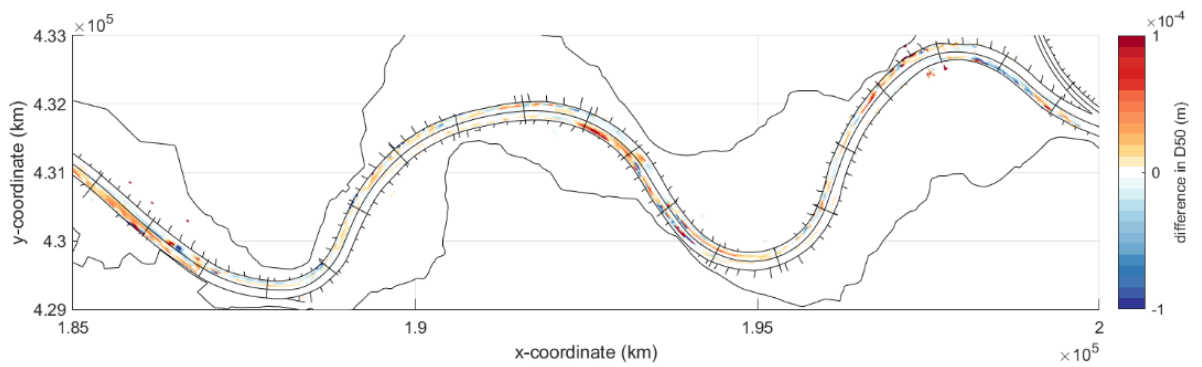


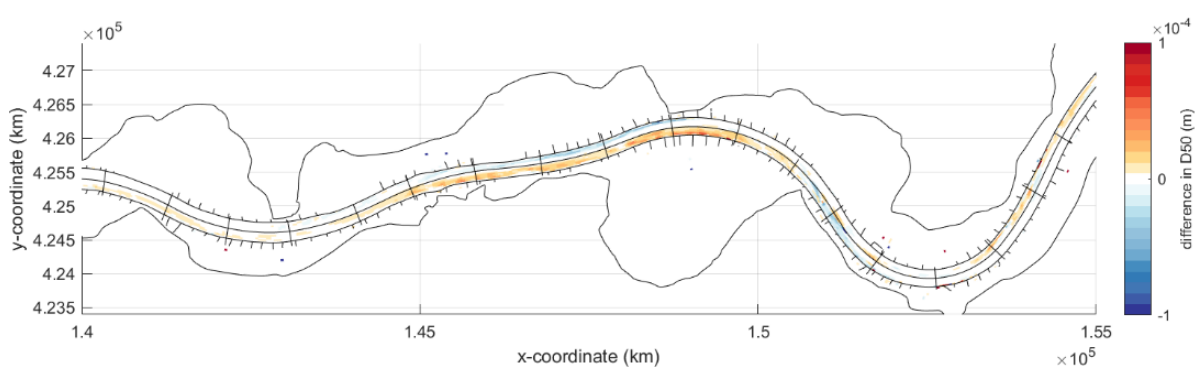
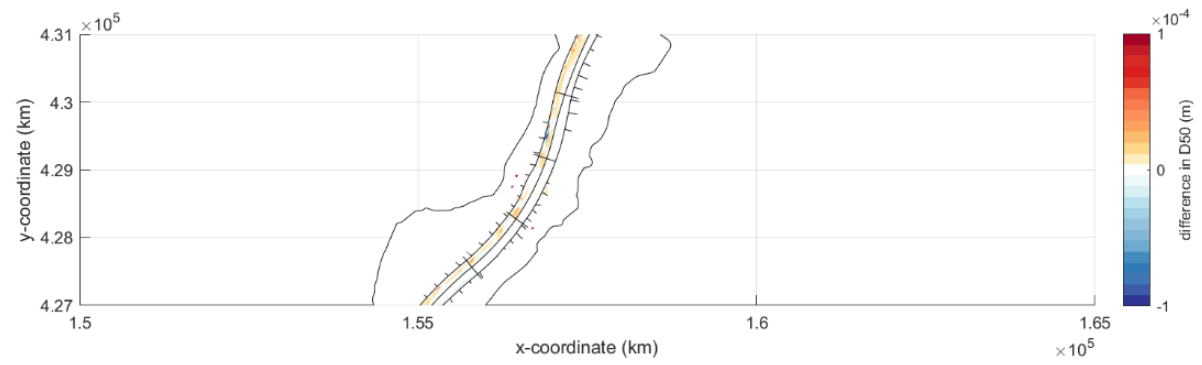
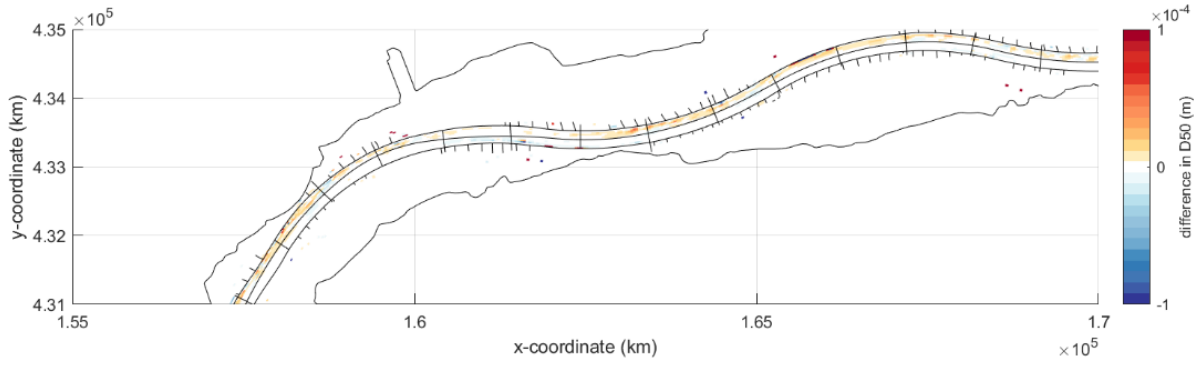
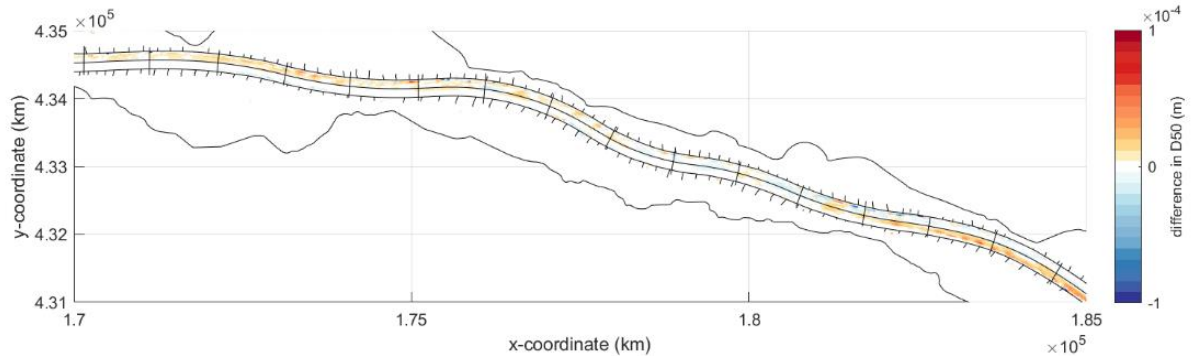


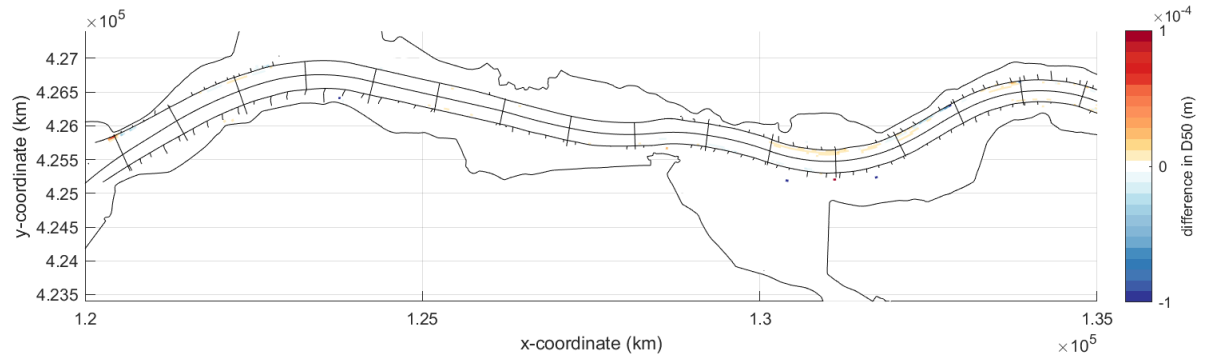
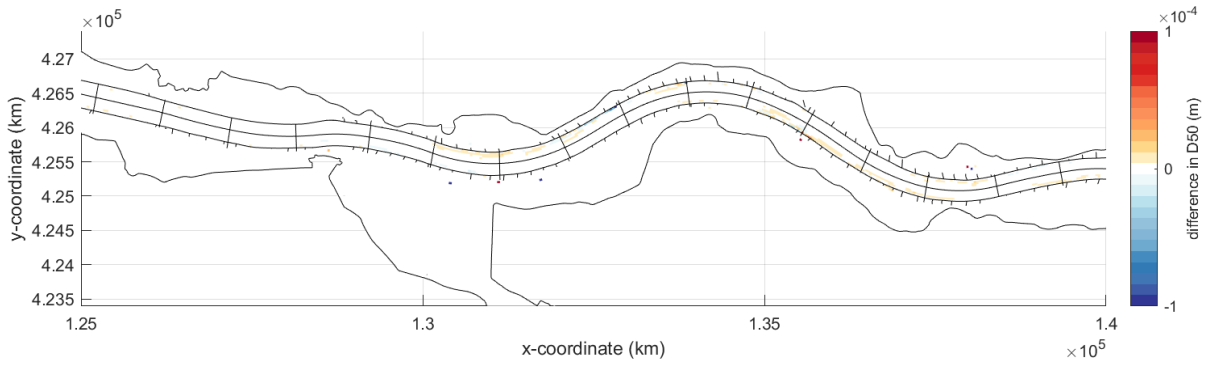


A.4 Differences in D_{50} for hydrograph simulations

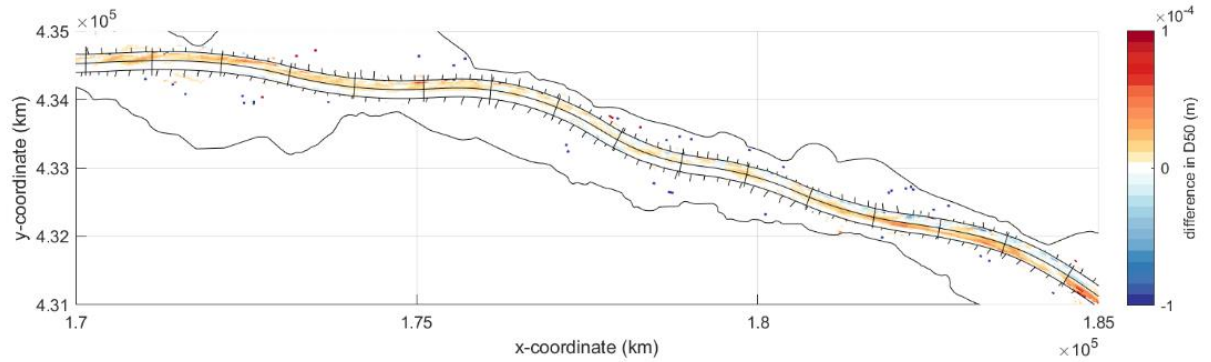
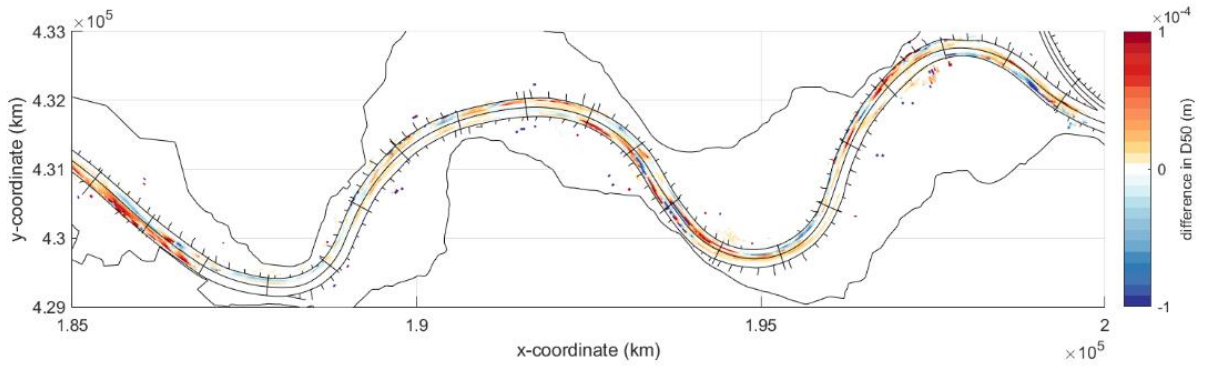
A.4.1 r068-r066

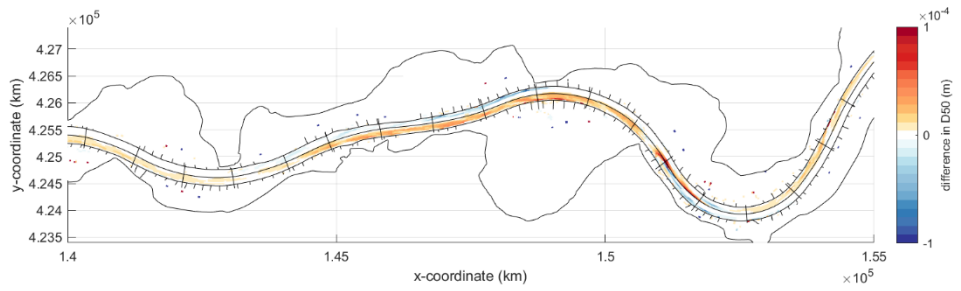
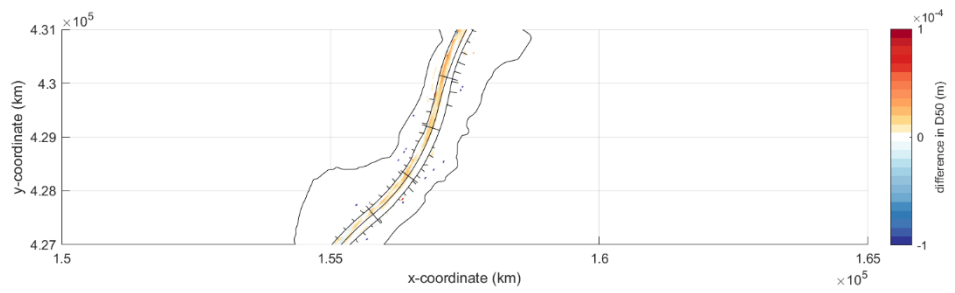
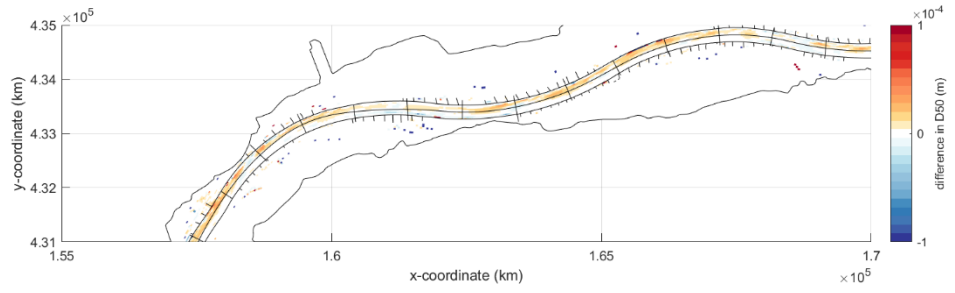


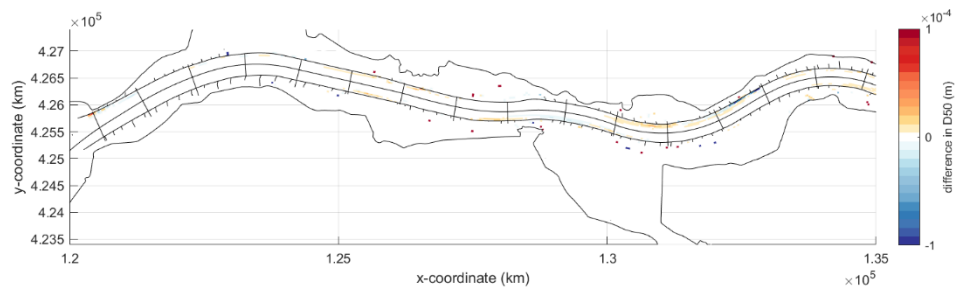
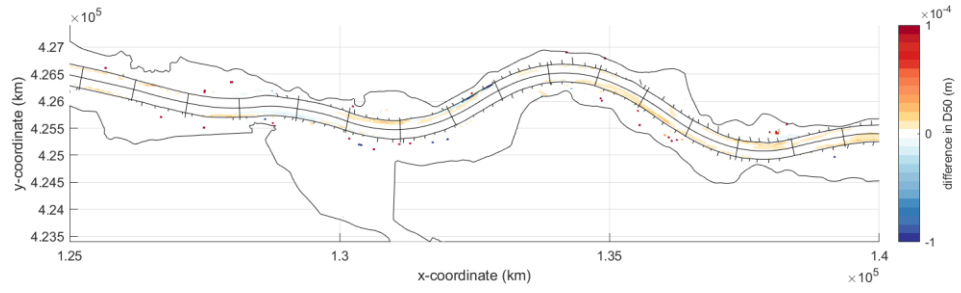




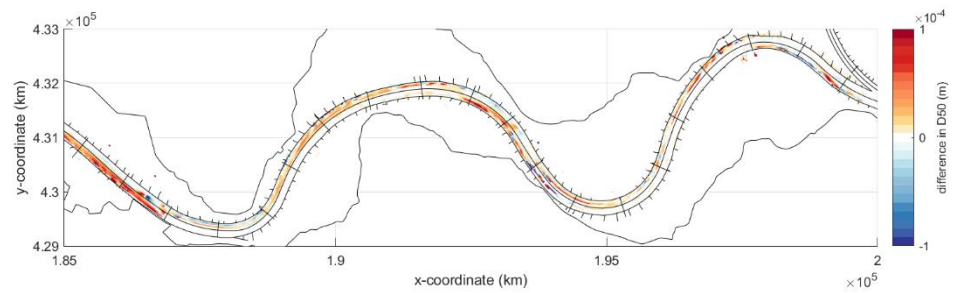
A.4.2 r067-r066

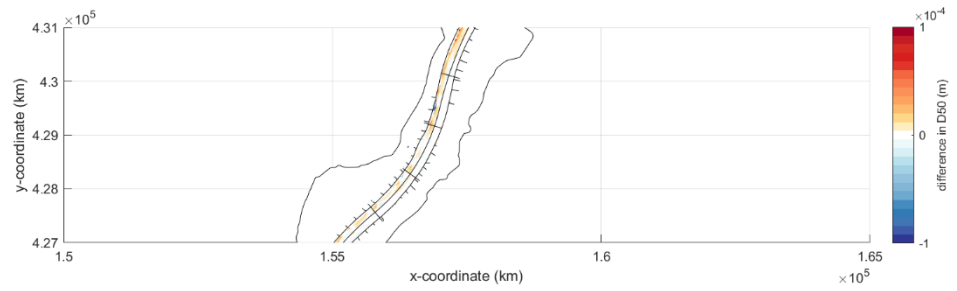
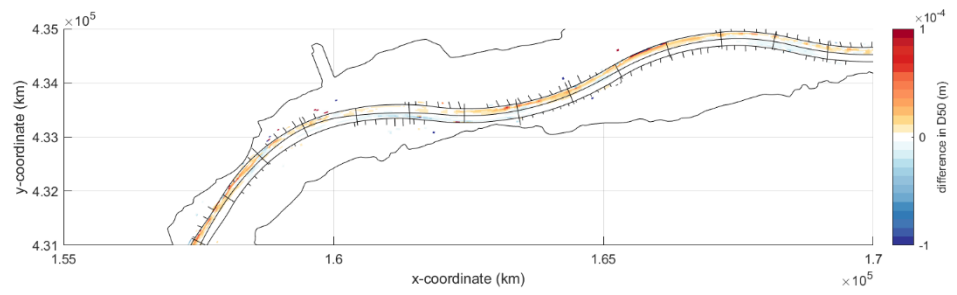
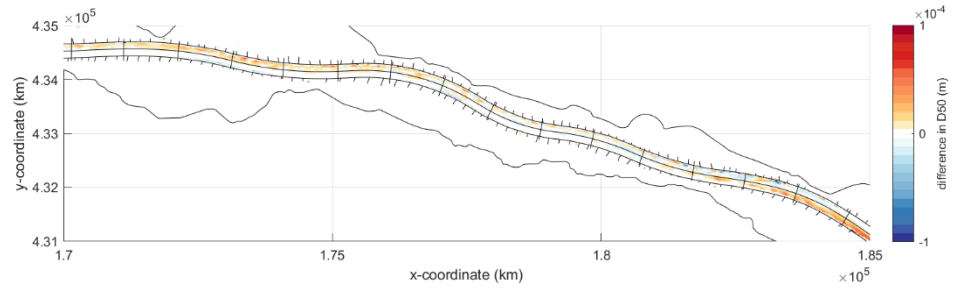


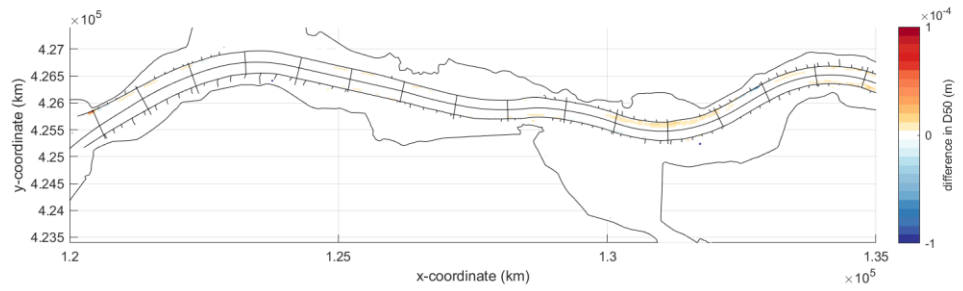
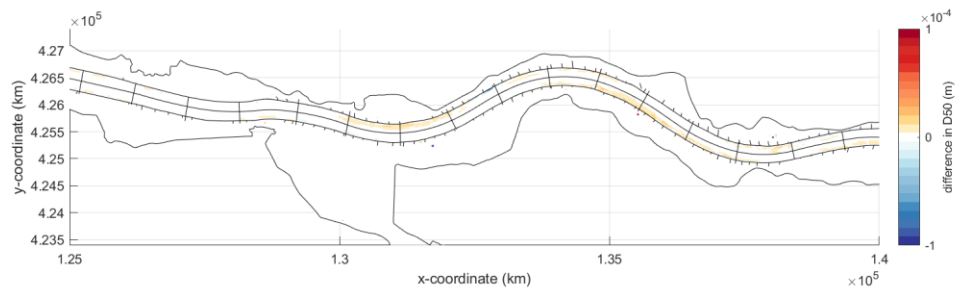
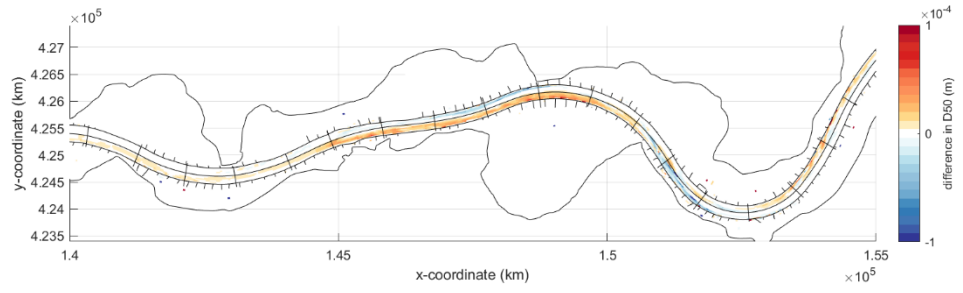


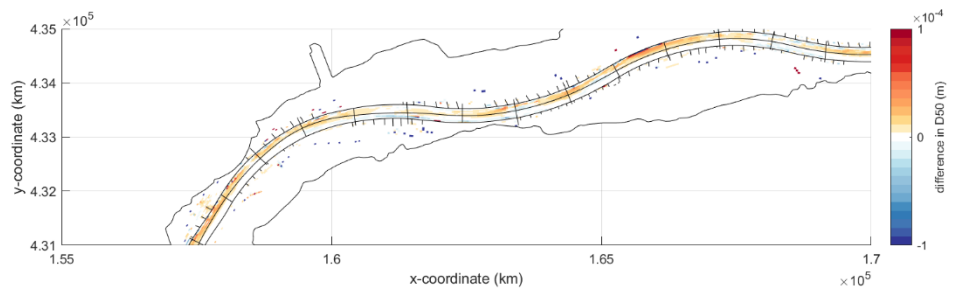
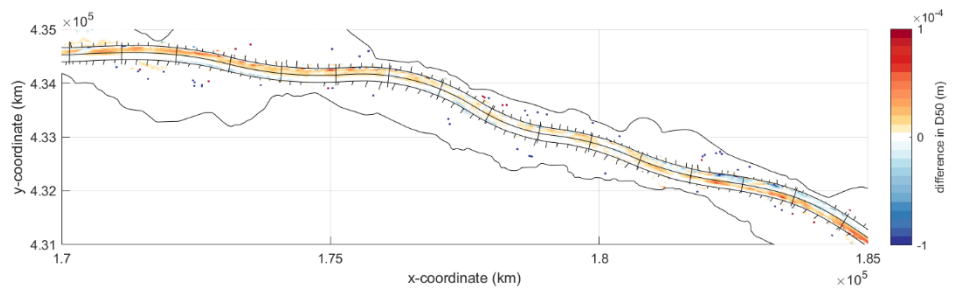
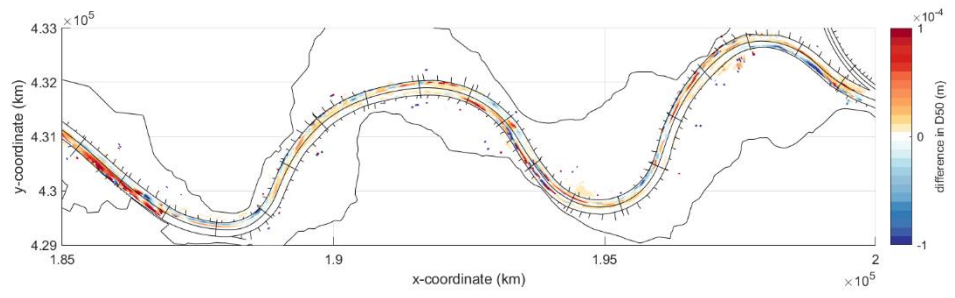


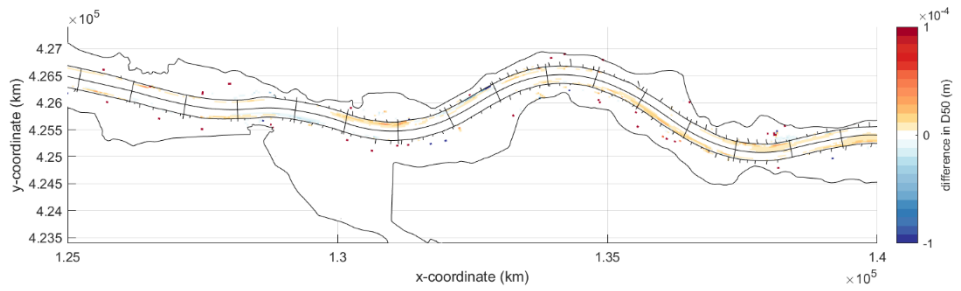
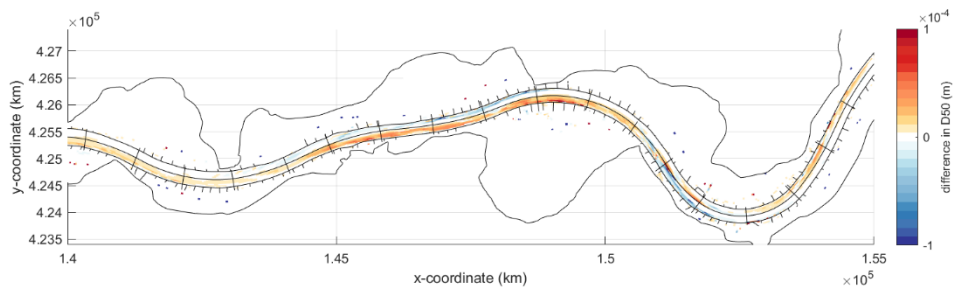
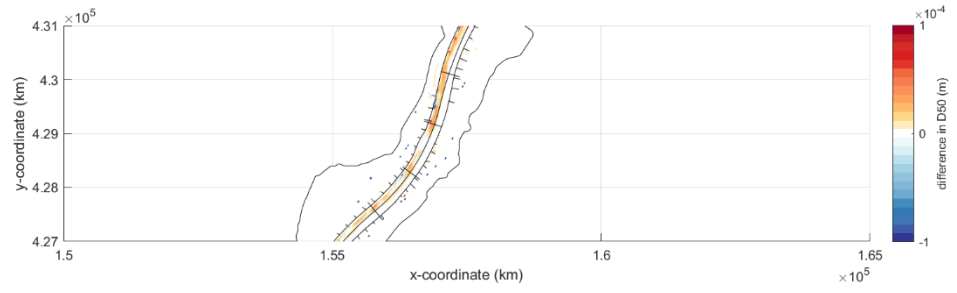
A.4.3 r070-r066

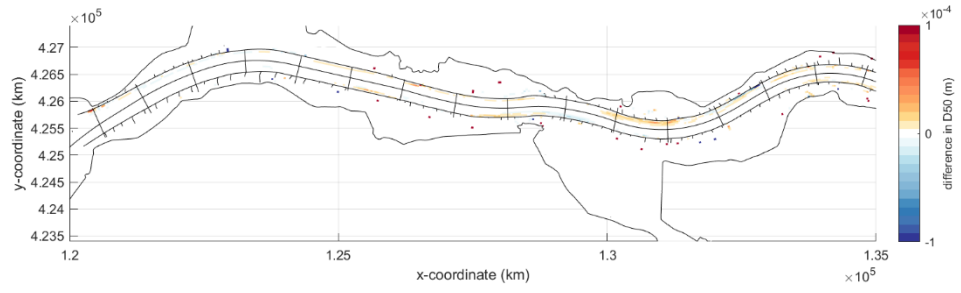




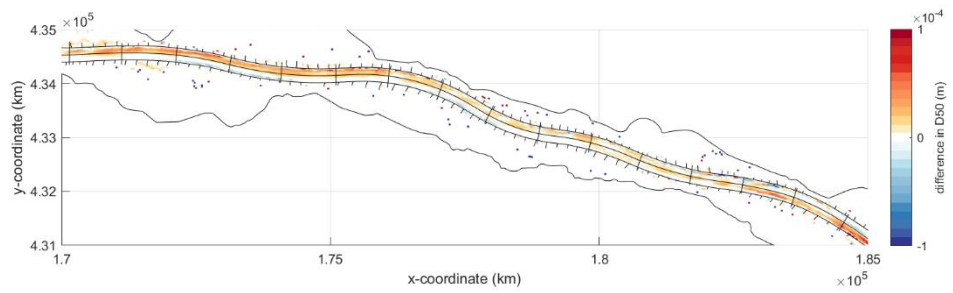
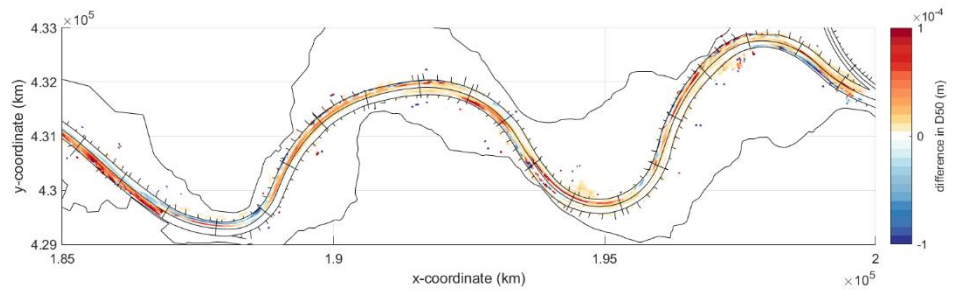


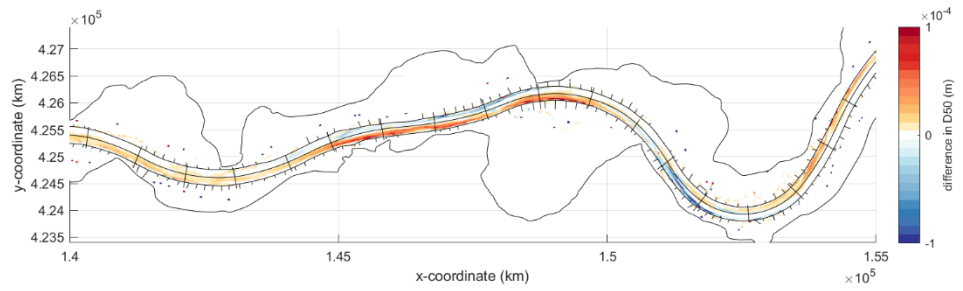
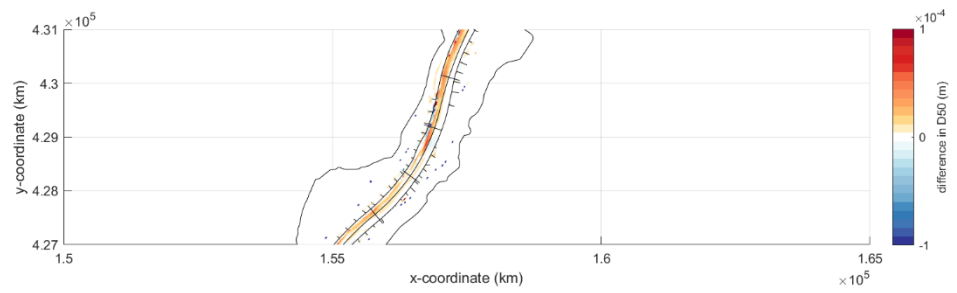
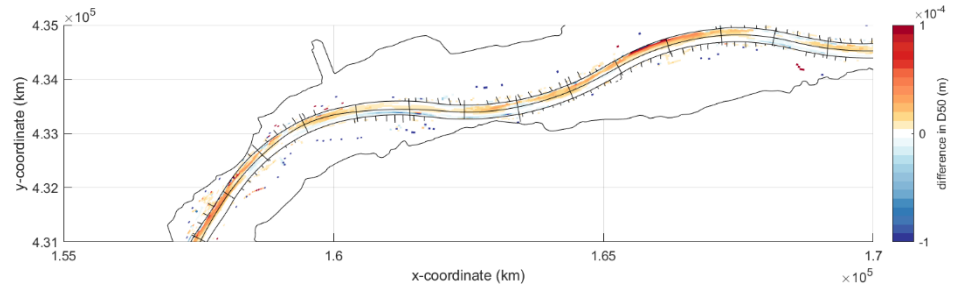


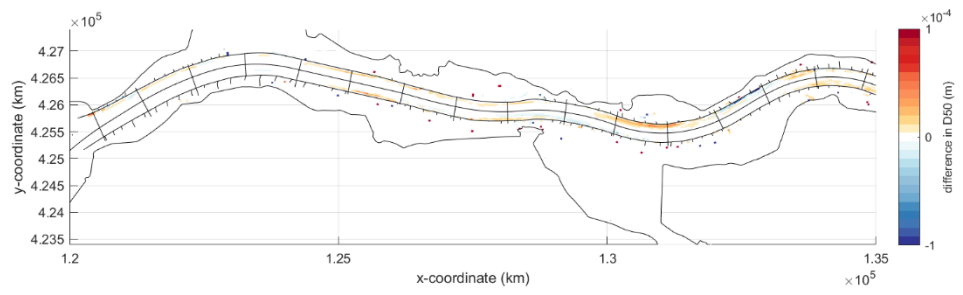
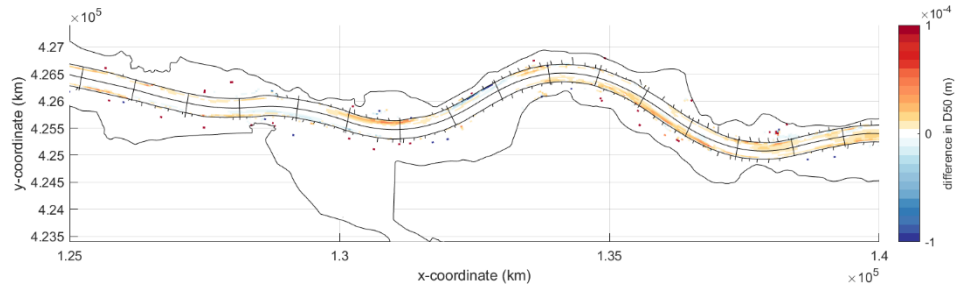




A.4.5 r071-r066







Deltares is an independent institute for applied research in the field of water and subsurface. Throughout the world, we work on smart solutions for people, environment and society.

Deltares

www.deltares.nl